ENV Report 17

Interim Report For The Upper Mississippi River - Illinois Waterway System Navigation Study

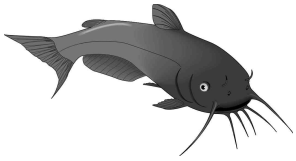

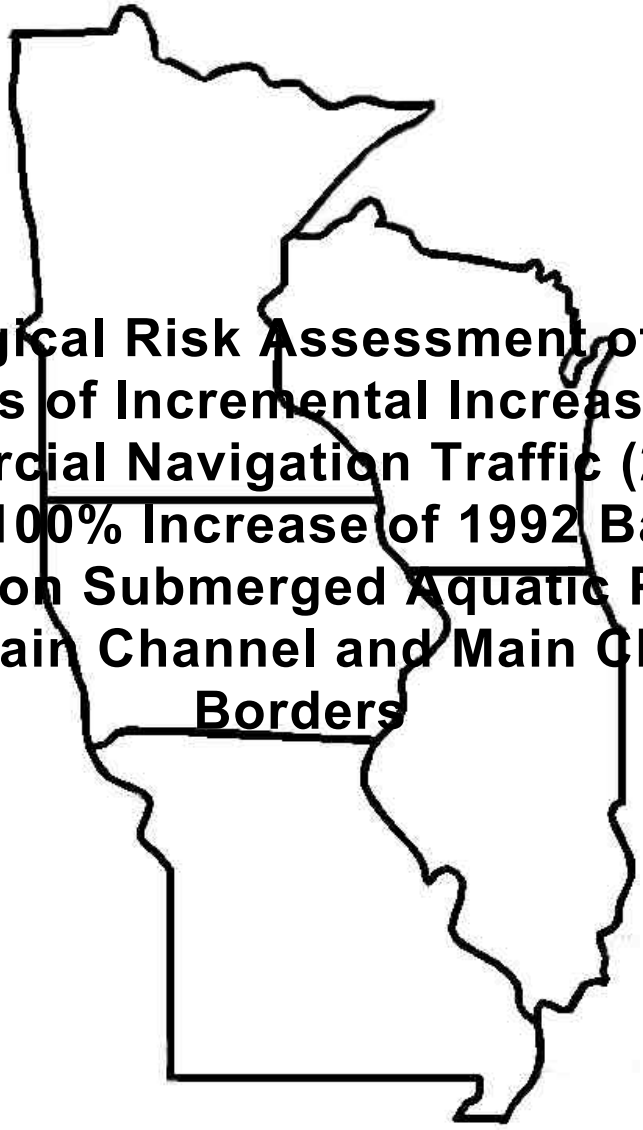

Ecological Risk Assessment of the Effects of Incremental Increase of Commercial Navigation Traffic (25, 50, 75, and 100% Increase of 1992 Baseline Traffic) on Submerged Aquatic Plants in the Main Channel and Main Channel Borders

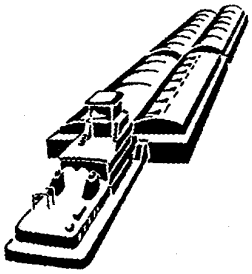

September 2000

US Army Corps of Engineers

Rock Island District
St. Louis District
St. Paul District

Upper Mississippi River - Illinois Waterway System Navigation Study

ENV Report 17
September 2000

Ecological Risk Assessment of the Effects of the Incremental Increase of Commercial Navigation Traffic (25, 50, 75, and 100% Increase of 1992 Baseline Traffic) on Submerged Aquatic Plants in the Main Channel and Main Channel Borders

by Steven M. Bartell, Kym Rouse Campbell

The Cadmus Group, Inc.
136 Mitchell Road
Oak Ridge, TN 37830

Elly P. H. Best, William A. Boyd

Environmental Laboratory
U.S. Army Engineer Research and Development Center
3909 Halls Ferry Road
Vicksburg, MS 39180-6199

Interim report

Prepared for U.S. Army Engineer District, Rock Island
Rock Island, IL 61204-2004
U.S. Army Engineer District, St. Louis
St. Louis, MO 63103-2833
U.S. Army Engineer District, St. Paul
St. Paul, MN 55101-1638

Engineer Research and Development Center Cataloging-in-Publication Data

Ecological risk assessment of the effects of the incremental increase of commercial navigation traffic (25, 50, 75, and 100% increase of 1992 baseline traffic) on submerged aquatic plants in the main channel and main channel borders / by Steven M. Bartell … [et al.] ; prepared for U.S. Army Engineer District, Rock Island, U.S. Army Engineer District, St. Louis, U.S. Army Engineer District, St. Paul.
109 p. : ill. ; 28 cm.
"ENV report 17"
Includes bibliographic references.
1. Ecological risk assessment — Mathematical models. 2. Aquatic plants — Mathematical models. 3. Navigation — Mississippi River — Environmental aspects — Mathematical models. 4. Illinois Waterway (Ill.) — Navigation. 5. Mississippi River — Navigation. I. Bartell, Steven M. II. United States. Army. Corps of Engineers. Rock Island District. III. United States. Army. Corps of Engineers. St. Louis District. IV. United States. Army. Corps of Engineers. St. Paul District. V. Engineer Research and Development Center (U.S.) VI. Upper Mississippi River-Illinois Waterway System Navigation Study. VII. Environmental Laboratory (U.S.) VIII. Title. IX. Title: Interim report for the Upper Mississippi River-Illinois Waterway System Navigation Study.
TA7 W3499 R5U7 ENV rept.17 2000

Contents

List of Figures

List of Tables

Preface

The work reported herein was conducted as part of the Upper Mississippi River - Illinois Waterway (UMR-IWW) System Navigation Study. The information generated for this interim effort will be considered as part of the plan formulation process for the System Navigation Study.

The UMR-IWW System Navigation Study is being conducted by the U.S. Army Engineer Districts of Rock Island, St. Louis, and St. Paul under the authority of Section 216 of the Flood Control Act of 1970. Commercial navigation traffic is increasing and, in consideration of existing system lock constraints, will result in traffic delays that will continue to grow in the future. The system navigation study scope is to examine the feasibility of navigation improvements to the Upper Mississippi River and Illinois Waterway to reduce delays to commercial navigation traffic. The study will determine the location and appropriate sequencing of potential navigation improvements on the system, prioritizing the improvements on the system, and prioritizing the improvements for the 50-year planning horizon from 2000 through 2050. The final product of the System Navigation Study is a Feasibility Report which is the decision document for processing to Congress.

This interim report was written by Steven M. Bartell and Kym Rouse Campbell of the Cadmus Group, Inc., Oakridge, TN, and Elly P. H. Best and William A. Boyd, Environmental Laboratory (EL) of the U.S. Army Engineer Research and Development Center (ERDC), Vicksburg, MS.

The authors appreciate the many helpful discussions and comments from John Barko (EL, ERDC), Dan Wilcox (U.S. Army Engineer District (USAED), St. Paul), Robert Doyle (Lewisville Aquatic Research Facility), Mike Stewart (EL, ERDC), Dave Schaeffer (EcoHealth Research, Inc.), and Sara Lubinski and Dave Soballe (Environmental Management Technical Center, U.S. Geological Survey (USGS)). Thanks also to Sandra Knight, Steve Maynord, Tom Pokrefke (Coastal and Hydraulics Laboratory (CHL, ERDC), Rose Kress, Salvador Rivera (EL, ERDC), Ron Copeland, Gary Brown, and Clay Lahatte (CHL, ERDC). Thanks to Dave Soballe also for providing data and model output.

The potential submerged aquatic plant coverage maps for Pools 4, 8, and 13 were provided by Sara Lubinski, USGS. The submerged aquatic plant model

review was performed by Cyndi Lovelock (The Cadmus Group, Inc.); in addition, she analyzed the results of the review using principal factor analysis and cluster analysis.

Project management support was provided by Ken Barr and Rich Fristik (USAED, Rock Island). Helpful comments were provided by Steve Carpenter and Anne Kimber during their reviews of an earlier draft of this report.

At the time of publication of this report, Director of ERDC was Dr. James R. Houston. Commander was COL James S. Weller, EN.

Summary

The Navigation Study Submerged Aquatic Plant Ecological Risk Assessment presents an initial assessment of the potential ecological risks posed by commercial traffic on submerged aquatic plants that grow in the main channel and main channel borders of the Upper Mississippi River-Illinois Waterway (UMR-IWW) System. Backwaters were not included in this risk assessment. This assessment addresses the possibility of plant breakage resulting from increases in current velocity or the momentum imparted by wake waves associated with the passing of commercial vessels. The assessment also examines the possibility that commercial vessel-induced increases in suspended sediments might diminish available underwater light enough to impair photosynthesis, growth, and vegetative reproduction of submerged aquatic plants.

Two species were selected to represent contrasting characteristic life forms of submerged aquatic vegetation in the UMR: American wild celery (*Vallisneria americana*) represents the submerged aquatic plant group with a rosette (i.e., having the majority of plant biomass resting on the sediments); in contrast, sago pondweed (*Potamogeton pectinatus*) exemplifies the canopy-forming plant group with elongated stems that reach up to and spread over the water surface. The potential and realized habitat for growth of these typical aquatic plant species was delineated based on the assumption that light availability limits submerged aquatic vegetation in the UMR-IWW System to areas where water depths are 1.5 m or less. Combined analysis of 1989 aerial imagery and application of this simple depth rule to bathymetry data for the Long Term Resource Monitoring Program (LTRMP) Trend Pools (UMR Pools 4, 8, 13, and 26 and IWW La Grange Pool) produced maps of existing and potential beds of submerged aquatic vegetation. This report describes the risk assessment of selected portions of UMR Pools 4, 8, and 13. Pool 13 has been suggested as a southern limit for maintaining viable populations of submerged aquatic plants in the main channel due to high turbidity in the lower pools. However, submerged aquatic vegetation does inhabit certain managed backwater areas in more southerly river segments (e.g., Pool 26).

The Navigation Study Submerged Aquatic Plant Ecological Risk Assessment was organized according to the fundamental components of the ecological risk

assessment process: problem formulation, analysis (characterization of exposure and characterization of ecological effects), and risk characterization (USEPA 1998). The risk assessment methodology described in this report is being developed to assess the potential ecological impacts associated with the anticipated growth of commercial traffic navigating the UMR-IWW System for the period 2000-2050. Assessments of potential impacts on early life stages of fish, adult fish, and fish spawning habitat, as well as impacts on the survival, growth, and reproduction of freshwater mussels, are concurrently being developed. In the absence of actual traffic projections, the present assessments are evaluating risks posed by hypothetical 25, 50, 75, and 100% increases in traffic intensity compared to traffic intensity determined from the 1992 lockage records. The hypothetical scenarios are presented as increases in the average daily number of vessels traversing each pool on the UMR-IWW System (i.e., tows/day).

The results of the screening for impacts on submerged aquatic plants due to direct physical forces suggested that less than 1.5% of the possible combinations of vessel type, location in relation to sailing line, and pool stage height would produce plant breakage for locations with a depth of 1.5 m or less. For all pool stage heights, the greatest physical impacts were associated with vessels located on the left edge of the navigation channel. More than 95% of the possible plant breakage resulted from secondary wave heights that exceeded the 0.2-m criteria.

A time series of light extinction coefficients was constructed for each location and traffic scenario using the suspended sediment concentrations derived from the traffic projections (e.g., tows/day) and the vessel characteristics (e.g., tow type). The values estimated for suspended sediments associated with the 1992 baseline traffic data resulted in monthly average extinction coefficients that ranged from 3.08 to 4.24 m^{-1} in Pool 4, 2.24 to 3.94 m^{-1} in Pool 8, and 2.96 to 3.42 m^{-1} in Pool 13. Using the average monthly ambient suspended sediment concentrations, the following ranges of light extinction coefficients were calculated: 2.62 to 3.00 m^{-1} for Pool 4, 3.30 to 3.84 m^{-1} for Pool 8, and 4.23 to 4.58 m^{-1} for Pool 13. The differences in the light extinction values based on simulated 1992 traffic and those calculated from ambient values result largely from different ambient suspended sediment concentrations reported for the particular cell within each pool in comparison to the reported monthly average value. The results of increased traffic on suspended sediments produced increases in light extinction coefficients in the order of 1 to 28%, depending on the combination of month, pool, and traffic scenario. The light extinction coefficient is an exponent, so a small increase in it actually means an exponentially greater decrease in light availability. In Pool 4, the greatest relative increase in light extinction occurred for the months of May and September. The greatest relative increase in light extinction occurred during the months of May and August in Pool 8. The greatest percentage increase in light extinction occurred for the months of June and July in Pool 13.

The plant growth models for American wild celery and sago pondweed were implemented for selected locations in Pools 4, 8, and 13. For wild celery, the

total annual biomass (living + non-living) decreased by as much as 27% for a 100% traffic increase in Pool 13; across the assessed scenarios, decreases in wild celery biomass ranged from 12-27% in Pool 13. The decreases in wild celery biomass due to the simulated traffic increases for Pools 4 and 8 were less and ranged from 1-8%. Gross production and living biomass (two other measures of plant growth) of wild celery decreased from ~10 to ~27% across the four increased traffic scenarios. Wild celery growth reductions were in the order of 0-4% in Pool 8, while corresponding impacts in Pool 4 range from ~3 to ~9% compared to the 1992 baseline simulations. The modeled impacts of increased traffic on the allocation of photosynthetically fixed carbon to the reproductive structures (i.e, tubers) of wild celery were minimal. The maximum values of wild celery tuber numbers and biomass were unchanged in Pools 8 and 13. The greatest impacts were in Pool 4, and the projected decreases were less than 3% for average tuber number and biomass; reductions in the maximum values ranged from 2-8% across the traffic scenarios in Pool 4.

As with wild celery, the largest impacts on sago pondweed from traffic increases were observed for Pool 13; however, the impact on sago pondweed growth was less than that on wild celery. The simulated values of sago pondweed biomass (living or total) were reduced by approximately 4-9% in Pool 13 compared with the 12-27% reductions simulated for wild celery in Pool 13. Modeled decreases in total sago pondweed biomass for Pools 4 and 8 were less than 3% of the 1992 baseline values across all increased traffic scenarios. For all four traffic increase scenarios, the modeled impacts were less than 10% of the 1992 baseline values for sago pondweed production and living biomass; the greatest impacts occurred in Pool 13, with correspondingly lesser impacts in Pools 4 and 8, respectively. No changes in average or maximum sago pondweed tuber numbers or biomass occurred in Pool 4. In both Pools 8 and 13, the average number and biomass of sago pondweed tubers increased slightly with increased traffic; however, the corresponding maximum values decreased by as much as 6% for the 100% traffic increase scenario in Pool 13.

The next phase in assessing traffic impacts on submerged aquatic plants will be to incorporate the current methodology into a framework that characterizes risk in probabilistic terms. More detailed, probabilistic assessments will be performed for selected locations and traffic scenarios identified by the preliminary analyses. Parameters used in the calculations (e.g., suspended sediment concentrations produced by the NAVSED model (Copeland et al. 1999), light extinction coefficients based on the regression equations developed by Soballe (Environmental Management Technical Center (EMTC)), plant growth model coefficients) that are imprecisely known will be defined as statistical distributions. Monte Carlo simulation methods will be used to propagate these uncertainties through the model calculations to produce distributions of impacts on growth and vegetative reproduction in relation to specific traffic scenarios. These distributions of results can be used to estimate the probability of different magnitudes of impact in a manner consistent with probabilistic risk estimation.

1 Introduction

Background

The Mississippi River is an integral part of American heritage, a unique resource, and the best example of a multipurpose river in the U.S. The Mississippi River, with a drainage basin of nearly 4 million km^2, is one of the largest and most productive ecosystems in the world (Holland-Bartels et al. 1990b). The river above the confluence of the Ohio River is commonly called the UMR (Figure 1) and includes nearly 500,000 km^2 of watershed (Holland-Bartels et al. 1990b). The UMR, including the IWW and several important tributaries (Figure 1), is designated both a nationally significant ecosystem and a nationally significant navigation system; it is the only inland river in the U.S. to have such a designation. Many national wildlife refuges exist along the river corridor. In addition, the Mississippi Flyway is the migration corridor for 40% of North America's waterfowl and shorebirds, as well as an important flyway for raptors and neotropical songbirds.

The history of navigation on the UMR-IWW System began in the 1820s, when Congress authorized navigation improvements by the Corps of Engineers; these improvements included the removal of snags and other obstructions in several locations of the Mississippi River and the construction of a canal connecting Lake Michigan to the Illinois River (Fremling and Claflin 1984). Several navigation improvement projects, such as the excavation of rocks, closing off sloughs, construction of the 4.5-foot navigation channel, and construction of the 6-foot navigation channel, continued throughout the early 1900s (Fremling and Claflin 1984). Projects creating the current 9-foot navigation channel were authorized in the 1930s, and by 1940, most had been completed by the U.S. Army Corps of Engineers (USACOE) (Fremling and Claflin 1984). Twenty-nine locks and dams on the Mississippi and eight on the Illinois replaced rapids and falls with a series of terraced pools for commercial and recreational traffic (Figure 1). Habitats in a typical pool include a braided channel in the upper pool, a lotic area at the head of the pool, and a lentic environment above the impounding lock and dam (Van Vooren 1983). Barge traffic transports a wide variety of essential goods on the UMR-IWW System. Agricultural commodities, petroleum products, and coal are the leading cargoes, with farm products accounting for approximately half of the total tonnage shipped.

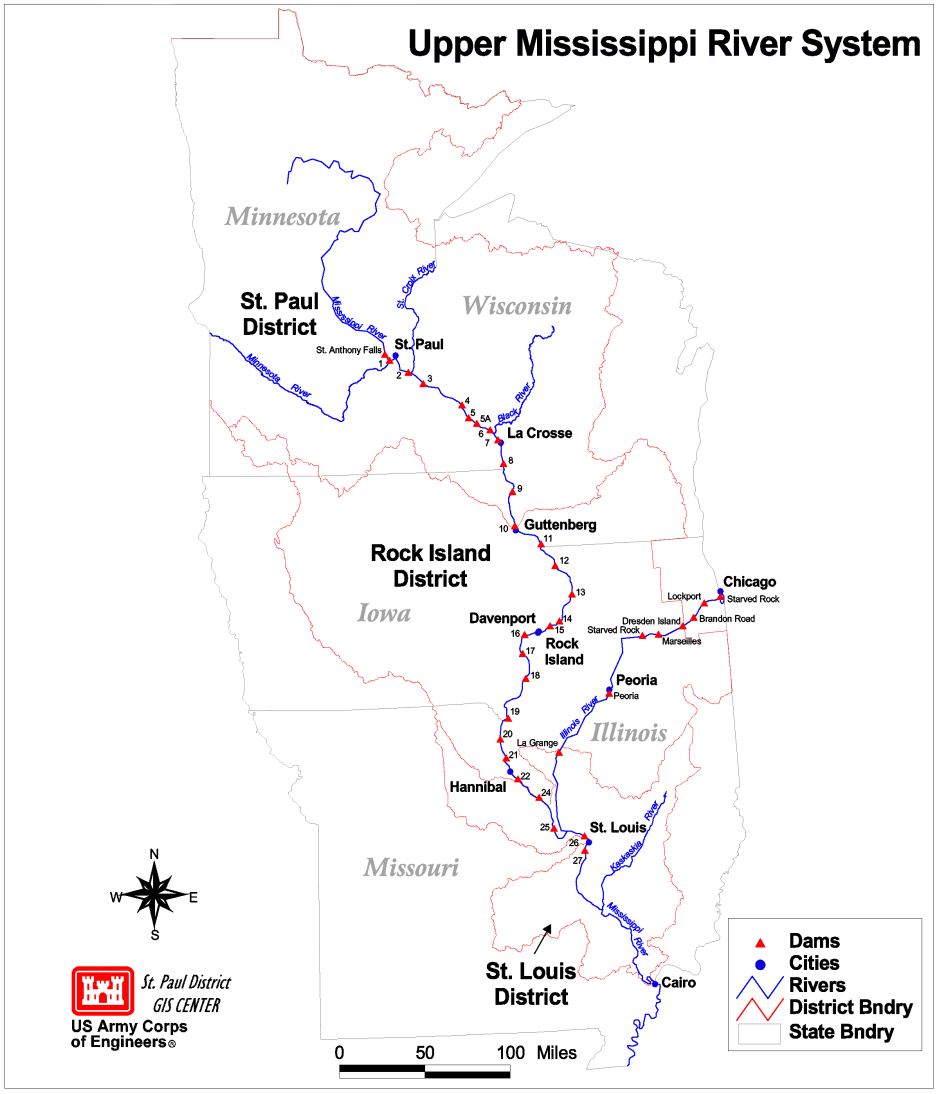

Figure 1. The Upper Mississippi River-Illinois Waterway (UMR-IWW) System, the pool upstream from the dam has the same number or name as the dam

Estimates indicate that the transport of commodities (commercial navigation traffic) on the river system could significantly increase in the future (Holland 1986, Holland-Bartels et al. 1990a). In the UMR-IWW System, a typical commercial "tow" consists of a towboat and 15 barges with the configuration of 3 barges wide by 5 barges long (Holland 1986). Direct impacts on submerged aquatic plants that could result from a passing tow include breakage or uprooting of plants from the changes in current velocity and waves produced by the commercial tows as they pass. Possible indirect impacts include the reduction in plant growth and/or vegetative reproduction caused by the decrease in available underwater light because of resuspension of nearshore sediments caused by tows passing throughout the growing season.

The purpose of the Navigation Study Submerged Aquatic Plant Ecological Risk Assessment is to assess the incremental impact of increased commercial navigation traffic from 2000 to 2050 (in 10-year increments) on submerged aquatic plants in the main channel and main channel borders of the UMR-IWW System. Backwaters were not included in this risk assessment primarily due to the absence of ambient suspended sediment data in backwaters and the difficulty of translating traffic increases to changes in suspended sediment in backwaters. As of the writing of this initial risk assessment, commercial traffic projections are being developed by the USACOE economists; therefore, to characterize commercial traffic intensity, a baseline number of vessels passing through each pool for each month was developed using 1992 lockage data. For this initial risk assessment, four hypothetical future traffic scenarios were constructed assuming 25, 50, 75, and 100% increases over the 1992 baseline data. Existing fleet data were also analyzed to construct a data set that describes, by pool and by month, the relative distribution of vessels across categories of vessel direction, size, speed, load, and whether or not the vessel had a Kort nozzle (a type of propeller jet). This classification scheme produced 108 possible configurations for commercial vessels operating on the UMR-IWW System. In developing and assessing the future traffic scenarios, it was assumed that the current fleet configuration will apply through the year 2050.

A rule-based model was developed to assess the direct physical impacts on submerged aquatic plants caused by currents and waves resulting from commercial navigation. Physical forces resulting from a passing commercial tow were calculated using a physical forces model, NAVEFF (Maynord 1999). These calculations have been integrated with the potential submerged aquatic plant coverage in the UMR-IWW System to determine areas in the river system where rules are exceeded and where physical forces resulting from a passing commercial tow would pose an ecological risk to submerged aquatic plants. Maps of the geographic information system (GIS) coverages of the existing and potential beds of submerged aquatic vegetation for UMR Pools 4, 8, and 13 are located in Appendix A. The estimated incremental impacts of increased commercial navigation traffic on submerged aquatic plant growth and vegetative reproduction were calculated using a physiological process model developed for hydrilla (*Hydrilla verticillata*) (Best and Boyd 1996, Boyd and Best 1996) that was modified for sago pondweed and American wild celery (also commonly referred to as eelgrass), two representative species of submerged aquatic plants common to the UMR-IWW System.

The U.S. Environmental Protection Agency (USEPA) Framework for Ecological Risk Assessment

The assessment of potential environmental impacts caused by commercial tows on submerged aquatic plants in the UMR-IWW System will meet the technical requirements of the National Environmental Policy Act (NEPA), but will be conducted and organized in a manner consistent with the framework for ecological risk assessment recommended in the Guidelines for Ecological Risk

Assessment developed by the USEPA (USEPA 1998). The framework was developed to promote consistent approaches to ecological risk assessment, identify key issues, and define the terminology (Bartell 1996). The framework represents a step toward developing guidelines for incorporating ecological principles into USEPA decisions (USEPA 1998). The framework developed by the USEPA includes three components: problem formulation, analysis (characterization of exposure and characterization of ecological effects), and risk characterization (USEPA 1998).

In the problem formulation component, the disturbance or stressor is identified, the subject or ecological effects (commonly referred to endpoints) of the risk assessment are defined, and the scope and scale of the ecological risk assessment is presented. In the characterization of exposure, the frequency, magnitude, extent, and duration of the disturbance is described. The ecological effects consistent with the objectives of the assessment are defined and the exposure-response relationships used to translate the exposure profile into risk estimates are presented in the characterization of ecological effects phase of the assessment process. In the risk characterization section, the available information and data are integrated, the risks are estimated, and the uncertainties and their assessment implications are identified and estimated. (USEPA 1998)

2 Problem Formulation

The disturbances or stressors in the Navigation Study Submerged Aquatic Plant Ecological Risk Assessment are the physical forces associated with the incremental increase in commercial navigation traffic, specifically a commercial tow passing through the river system. The ecological effects that are the focus of this risk assessment are (1) submerged aquatic plant breakage resulting from physical forces caused by the increase in commercial navigation traffic, and (2) the decrease in submerged aquatic plant growth and vegetative reproduction due to the decrease in underwater light availability because of increased suspended sediment concentrations resulting from increased commercial navigation traffic.

Traffic projections are being developed by USACOE economists for the future (2000, 2010, 2020, 2030, 2040, and 2050) for the conditions that would occur without any major improvements to the UMR-IWW System, referred to as the "without-project" conditions. Future traffic projections also are being developed for the selected National Economic Development (NED) Plan for the years 2000-2050 (every 10 years). Traffic that actually occurred on the river system in 1992 is used as the baseline for comparison. As of the writing of this report, traffic projections are still under development; therefore, four future traffic scenarios were constructed assuming 25, 50, 75, and 100% increases over the 1992 baseline data for this initial risk assessment.

For the purposes of this ecological risk assessment, traffic projections were broken down into tows per day by month for each pool. The physical forces (i.e., current, wave height, shear stress) resulting from all possible configurations (108) of a passing commercial tow were calculated for the main channel of the LTRMP "trend pools" using the NAVEFF model (Maynord 1999). The characteristics that define a particular vessel configuration include the direction of travel (upbound, downbound), vessel speed (slow, medium, fast), vessel size (small, medium, big), barge loads (empty, mixed, loaded), and propeller type (Kort nozzle, open wheel). These classifications result in 108 different vessel configurations; each vessel configuration is assigned a code value (1-108) that identifies its particular combination of attributes. These fleet characteristics that have been developed by the USACOE economists are presumed not to change over the study period. The NAVEFF model estimates the far-field changes in the main channel river current velocity in relation to tow characteristics and traffic intensity. NAVEFF calculates the change in velocity integrated over

depth (i.e., one-dimensional) at distances greater than one tow-width from the moving tow, between this distance, and the shorelines. In addition, the NAVEFF model was used to estimate areas of the river (main channel/main channel border) where current velocity and wave height thresholds (minimum values at which effects on submerged aquatic plants occur) were exceeded as a result of the incremental increase in commercial navigation traffic. Output from the NAVEFF model is also being used to calculate the magnitude and duration of sediment resuspension resulting from a passing commercial tow in the sediment modeling effort (NAVSED (Copeland et al. 1999)).

A GIS coverage of potential submerged aquatic plant habitat was developed by the EMTC for UMR Pools 4, 8, and 13 using the 1989 aerial coverage of submerged aquatic plants in the UMR-IWW System and bathymetry data from the U.S. Army Engineer Research and Development Center (ERDC) (Appendix A). Discussions during meetings and workshops with aquatic plant experts concluded that the spatial distribution of submerged aquatic plants in 1989 for Pool 8 was indicative of an extensive spatial distribution within this pool in comparison with previous years. Submerged aquatic plants are generally considered not to grow below Pool 13 in the UMR or in the IWW due to excessive suspended sediment concentrations and current velocities. Exceptions include an area in UMR Pool 19 and managed backwater areas in the UMR (e.g., Pool 26) and the IWW.

A rule-based model for submerged aquatic plants was developed to determine current velocity and wave values that cause submerged aquatic plant breakage based on field and laboratory studies and literature (Figure 2). Displacement of submerged aquatic plant tubers via uprooting was not included in this risk assessment. Field studies have indicated that physical forces resulting from commercial traffic do not normally uproot plants and displace tubers (Korschgen et al. 1988). Though wave forces sufficient for uprooting plants can be generated by navigation traffic in nearshore areas, plants typically have been previously excluded from these locations by current levels of navigation traffic. The effects of waves on submerged aquatic plant colonization and distribution are not included in this ecological risk assessment.

The rule-based model for physical breakage was used to evaluate all cells (defined as 10 m wide by 0.5 mile long parallel to the sailing line) with mean depths of 1.5 m or less for the GIS data file for UMR Pools 4, 8, and 13. Each cell references a 3-dimensional location with a GIS data file that describes the bathymetry of the pool and was assigned a unique identification code in relation to its pool location in river miles and distance of its center point left or right of the sailing line (e.g., 135R5250, 135 m right of the sailing line at River Mile 525.0). Evaluations were performed for three Pool 4, 8, and 13 stage heights (low, medium, high); for each stage height, three sailing line scenarios (centered on the sailing line, located on the left edge of the navigation channel, or located on the right edge of the navigation channel) were evaluated. For all nine conditions, the impacts of 108 different vessel types on plant breakage were assessed. The values of current velocity and wave height for each vessel and location were calculated using the NAVEFF model (Maynord 1999). All cell

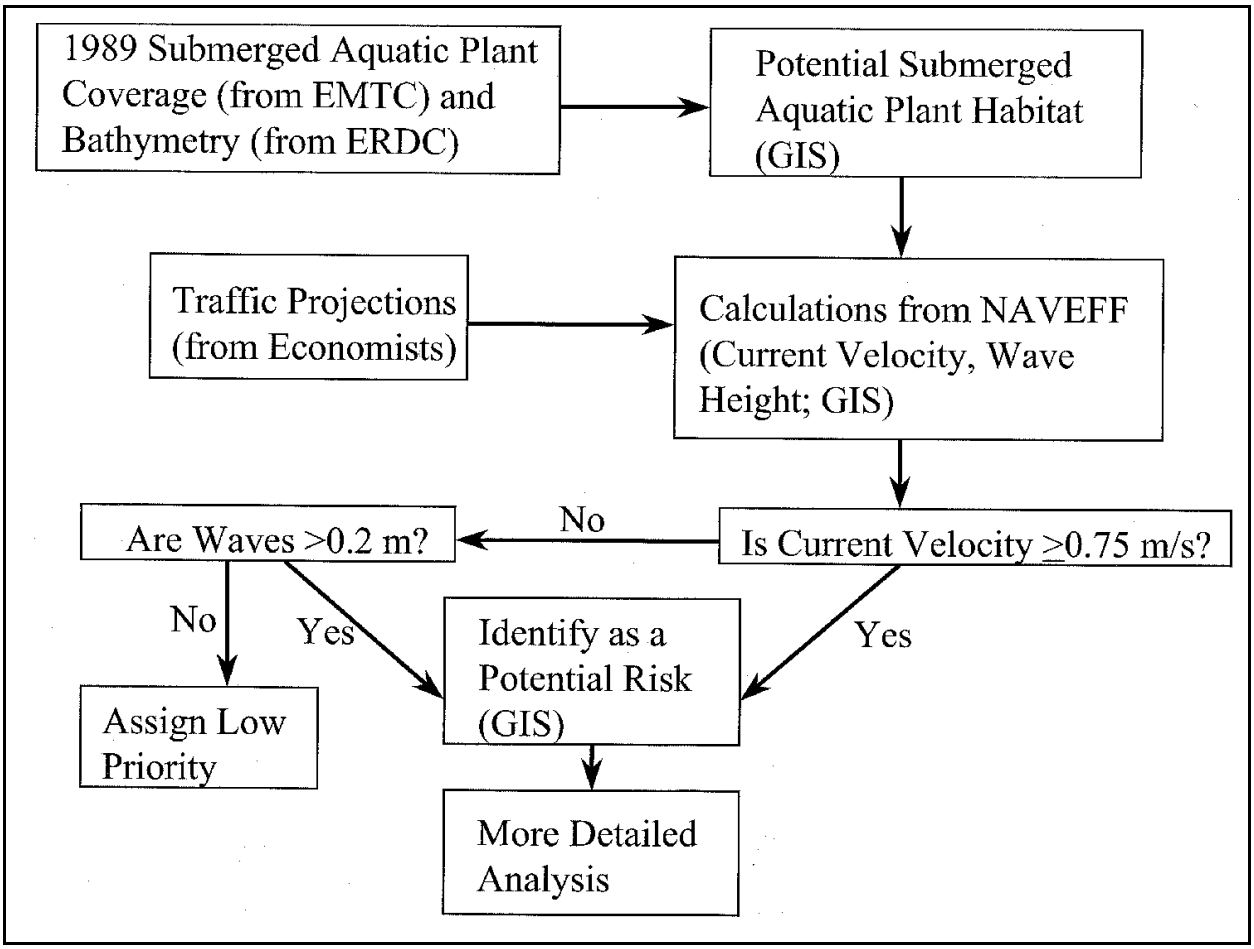

Figure 2. The rule-based model developed to assess the ecological effect of breakage of submerged aquatic plants due to the incremental increase in commercial navigation traffic

and vessel type combinations that failed the screening criteria for change in current velocity, wave height, or both were identified and tallied.

Plant growth models were used to evaluate the potential impacts of increased commercial traffic in UMR Pools 4, 8, and 13. Suspended sediment concentrations associated with the 108 vessel types for selected cells (<1.5-m depth) in Pools 4, 8, and 13 were estimated using a combination of the NAVEFF and NAVSED (a modification of NAVEFF) models (Copeland et al. 1999). For this initial risk assessment, one cell was selected in each pool. Using calculations of current velocities, bed shear stresses, and wave heights produced by the NAVEFF, the NAVSED model calculated a time series of suspended sediment concentrations for each vessel type and location within a pool. These suspended sediment concentrations were used to develop correspondingly increased light extinction coefficients that were used as input to the plant growth models (Figure 3). These models estimated the magnitude of reduced growth and vegetative reproduction for the scenarios of 25, 50, 75, and 100% increases in commercial traffic.

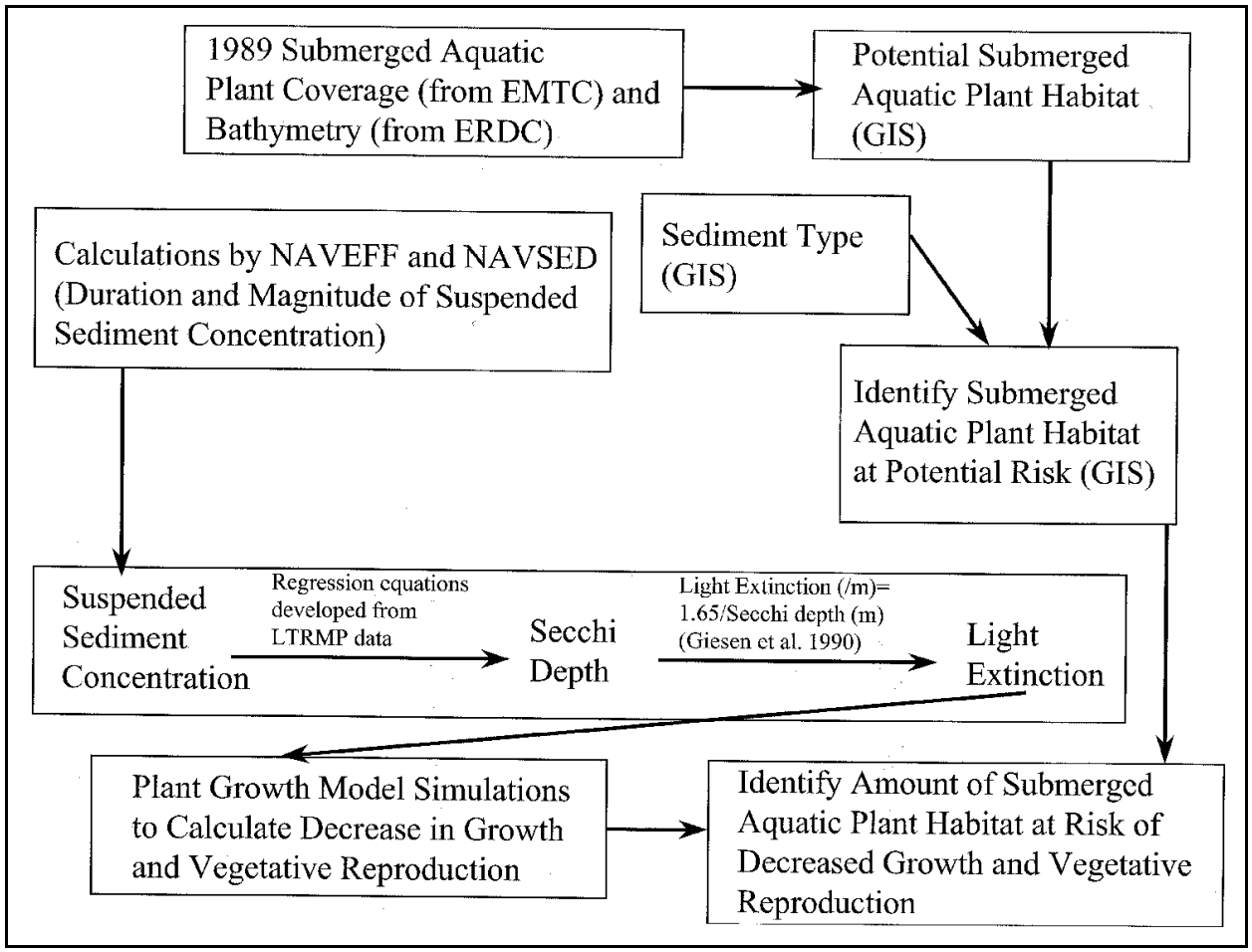

Figure 3. The methodology to assess the ecological effect of decreased growth and vegetative reproduction of submerged aquatic plants resulting from the incremental increase in commercial navigation traffic

3 Analysis-Characterization of Exposure

In order to perform this ecological risk assessment, the important initial step was to characterize the nature of the environmental stress. This step in assessing ecological risks posed to submerged aquatic plants by commercial traffic describes and quantifies the nature, magnitude, and extent of physical forces produced by commercial vessels navigating on the UMR-IWW System.

In this ecological risk assessment, the analysis of potential impacts on submerged aquatic plants is limited (1) spatially, to the main channel and main channel borders of the UMR-IWW System, using the UMR Pools 4, 8, and 13 as typical examples, and (2) temporally, to the typical growing season that extends approximately from May through September on the UMR-IWW System. It is noted that submerged aquatic plants appear to be confined to a few managed backwater areas in some pools such as in UMR Pool 26 and in the IWW La Grange Pool, but these areas have not been included in the current risk assessment.

Commercial Traffic Scenarios

Commercial traffic scenarios that define the average number of vessels which traverse each pool each day were addressed in this risk assessment. Table 1 lists the number of tows per day for each month of the growing season for each scenario in Pool 4. The baseline values of tows/day range from between 4.7 tows/day in September to 5.9 tows/day in July. These values translate into approximately 141 tows in September to 183 tows for July. The corresponding values for the traffic scenarios for Pools 8 and 13 are listed in Tables 2 and 3, respectively. These data indicate the general trend for increased traffic in more southerly pools; for example, the September and July traffic baseline values were 207 and 285 tows/day, respectively, for Pool 13.

Table 1
Traffic Scenarios Used in the Risk Assessment of Commercial Traffic Impacts on Submerged Aquatic Vegetation in the UMR Pool 4[1]

Month		Baseline 1992	Percent Increase			
			25%	50%	75%	100%
May	Tows/day	5.7	7.1	8.6	10.0	11.4
	Total	177	221	265	309	353
	IAT (h)	4.2	3.4	2.8	2.4	2.1
June	Tows/day	5.4	6.8	8.1	9.5	10.8
	Total	162	203	243	284	324
	IAT (h)	4.4	3.6	3.0	2.5	2.2
July	Tows/day	5.9	7.4	8.9	10.3	11.8
	Total	183	229	274	320	366
	IAT (h)	4.1	3.3	2.7	2.3	2.0
August	Tows/day	5.8	7.3	8.7	10.2	11.6
	Total	180	225	270	315	360
	IAT (h)	4.1	3.3	2.8	2.4	2.1
September	Tows/day	4.7	5.9	7.1	8.2	9.4
	Total	141	176	212	247	282
	IAT (h)	5.1	4.1	3.4	2.9	2.6
Seasonal Values	Tows/day	5.5	6.9	8.3	9.6	11.0
	Total	843	1,054	1,264	1,475	1,685
	IAT (h)	4.4	3.5	2.9	2.5	2.2

[1] IAT = Interarrival Time.

Table 2
Traffic Scenarios Used in the Risk Assessment of Commercial Traffic Impacts on Submerged Aquatic Vegetation in the UMR Pool 8[1]

Month		Baseline 1992	Percent Increase			
			25%	50%	75%	100%
May	Tows/day	6.2	7.8	9.3	10.9	12.4
	Total	192	240	288	336	384
	IAT (h)	3.9	3.1	2.6	2.2	1.9
June	Tows/day	6.1	7.6	9.2	10.7	12.2
	Total	183	229	275	320	366
	IAT (h)	3.9	3.1	2.6	2.2	2.0
July	Tows/day	6.7	8.4	10.1	11.7	13.4
	Total	208	260	312	363	415
	IAT (h)	3.6	2.9	2.4	2.0	1.8
August	Tows/day	6.4	8.0	9.6	11.2	12.8
	Total	198	248	298	347	397
	IAT (h)	3.8	3.0	2.5	2.1	1.9
September	Tows/day	5.2	6.5	7.8	9.1	10.4
	Total	156	195	234	273	312
	IAT (h)	4.6	3.7	3.1	2.6	2.3
Seasonal Values	Tows/day	6.1	7.7	9.2	10.7	12.3
	Total	937	1,172	1,407	1,639	1,874
	IAT (h)	3.9	3.1	2.6	2.2	2.0

[1] IAT = Interarrival Time.

Table 3
Traffic Scenarios Used in the Risk Assessment of Commercial Traffic Impacts on Submerged Aquatic Vegetation in the UMR Pool 13[1]

Month		Baseline 1992	Percent Increase			
			25%	50%	75%	100%
May	Tows/day	8.9	11.1	13.4	15.6	17.8
	Total	276	345	414	483	552
	IAT (h)	2.7	2.2	1.8	1.5	1.3
June	Tows/day	8.3	10.4	12.5	14.5	16.6
	Total	249	311	374	436	498
	IAT (h)	2.9	2.3	1.9	1.7	1.4
July	Tows/day	9.2	11.5	13.8	16.1	18.4
	Total	285	357	428	499	570
	IAT (h)	2.6	2.1	1.7	1.5	1.3
August	Tows/day	8.3	10.4	12.5	14.5	16.6
	Total	257	322	386	450	515
	IAT (h)	2.9	2.3	1.9	1.7	1.4
September	Tows/day	6.9	8.6	10.4	12.1	13.8
	Total	207	259	311	362	414
	IAT (h)	3.5	2.8	2.3	2.0	1.7
Seasonal Values	Tows/day	8.3	10.4	12.5	14.6	16.7
	Total	1,274	1,594	1,913	2,230	2,549
	IAT (h)	2.9	2.3	1.9	1.6	1.4

[1] IAT = Interarrival Time

Interarrival times

The assessment of potential impacts examines the implications of increased traffic on plant growth on a tow-by-tow basis. As the number of tows/day increases, the average time between successive tows passing any reference location within a pool decreases. For Pool 4, the average time expected between baseline tow passages was 5.1 hours in September and 4.1 hours in July. The corresponding interarrival times for Pool 13 were 3.5 hours in September and 2.6 hours in July. These September and July interarrival times decrease to 1.7 hours and 1.3 hours, respectively, for the 100% traffic increase scenario for Pool 13. Tables 1-3 summarize these interarrival values for the May through September growing season for Pools 4, 8, and 13. These data were fundamental to characterizing the potential ecological stresses imposed by commercial navigation on the UMR-IWW System.

For this risk assessment, hypothetical time series of tow passages were defined for Pools 4, 8, and 13 for each traffic scenario. A sequence of tow events describes a series of points in time (hour) that a commercial vessel passes an arbitrary point in the pool of interest during an average day in the month of interest. A sequence of tow events equal to the number of vessels expected each day was constructed separately for each pool and month. This was done by sampling the total number of expected events (i.e., Tables 1-3) randomly from an exponential distribution defined by the inverse of the corresponding interarrival time. The resulting series of interarrival times were summed to construct the time line of tow passages by any location in the pool, assuming all vessels navigated the entire pool on the day they were selected. Interarrival times were adjusted to whole hours (e.g., tow events at 1.25 and 1.75 hours would both be classified as having occurred in Hour 2).

Vessel characteristics

The next step in characterizing exposure for the commercial traffic scenarios entailed assigning a vessel type to each of the events in the time series of tow passages described previously. The characteristics that define vessel type include the direction of travel (upbound, downbound), vessel speed (slow, medium, fast), vessel size (small, medium, big), barge loads (empty, mixed, loaded), and propeller type (Kort nozzle, open wheel). These classifications result in 108 different vessel configurations; each vessel configuration was assigned a code value (1-108) that identified its particular combination of attributes.

The distributions of these possible vessel configurations were developed for each month and pool using the 1992 lockage records. Figure 4 illustrates the cumulative frequency functions for vessel configuration calculated for May through September for UMR Pool 13. Similar distributions were also developed for Pools 4 and 8 using their respective traffic data. The distributions are similar for these months, with perhaps the exception of September. Though illustrated as a continuous variable, the cumulative frequency functions for the discrete vessel types demonstrate essentially three clusters of vessel configuration: small, slow vessels; medium size vessels; and the big, fast vessels.

An equal number of vessel types was selected randomly from the corresponding month and traffic scenarios to match the time series of events selected on the basis of interarrival time. The combined result of sampling was a time line of the hours in each month in which a tow passed, plus an identification of each event as one of the 108 possible vessel configurations. Each vessel type has associated current velocities and secondary wave heights in relation to its particular characteristics.

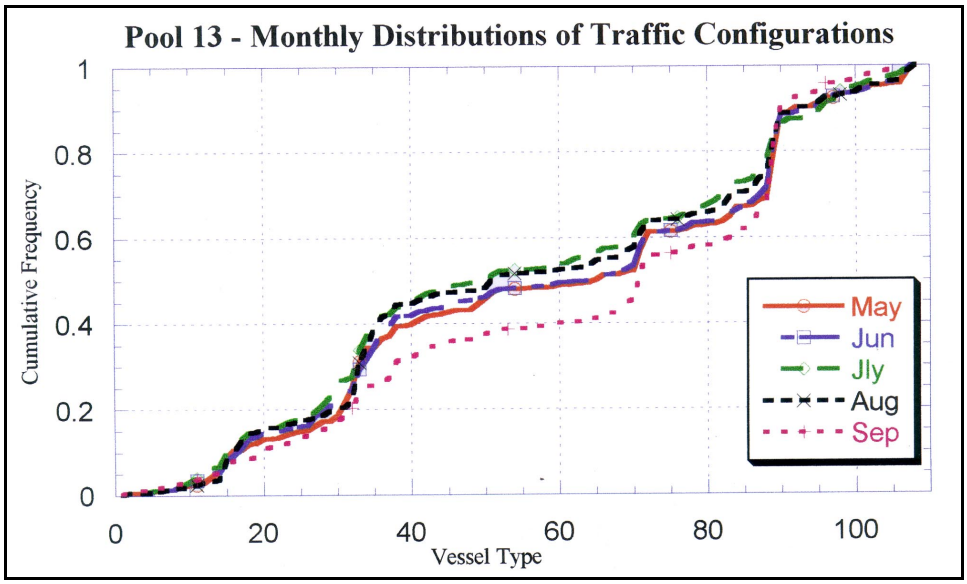

Figure 4. The cumulative frequency functions for vessel configuration for May through September for UMR Pool 13

Physical Forces

The main direct physical forces of interest in this risk assessment are changes in current velocity and the generation of secondary waves that might be of sufficient magnitude to physically damage submerged aquatic plants.

Current velocities

Current velocities (m/s) were estimated for Pools 4, 8, and 13 using the NAVEFF model (Maynord 1999). This model uses input values of vessel size, vessel speed, distance from left/right bank, and pool bathymetry to calculate the far-field (i.e., >1.5 boat widths from the vessel) physical forces including a depth-averaged current velocity.

Wake waves

The NAVEFF model also estimates the height of secondary waves (m) as a function of distance from the vessel that are generated by the moving tow. Using detailed bathymetry data, the NAVEFF model was implemented for cross sections located at each river mile in Pools 4, 8, and 13. For each cross section, all 108 vessel configurations were simulated for three different stage heights (low, medium, or high) and three assumptions of vessel location in relation to the sailing line identified on the available navigation chart (centered on the sailing line, located on the left edge of the navigation channel, or located on the right edge of the navigation channel). The results for each simulation were recorded for spatial cells (10 m wide by 0.5 mile long) parallel to the sailing line. Each cell was assigned a unique identification code in relation to its pool location in

river miles and distance of its center point left or right of the sailing line (e.g., 135R5250, 135 m right of the sailing line at River Mile 525.0).

Sediment Resuspension

Sediment resuspension by vessels passing in the vicinity of plant beds is the second focus of the exposure analysis. The NAVEFF model was modified (modification called NAVSED) (Copeland et al. 1999) to include the estimation of bed shear stresses; these stresses were used in combination with spatial distribution of sediment types (e.g., cohesive, noncohesive) and sediment characteristics (e.g., particle size, bulk density) to estimate sediment resuspension by passing vessels. The difference in physical forces generated by upbound vs. downbound vessels is considered in the NAVEFF model calculations. A time series of suspended sediments was calculated for each combination of pool stage, vessel type, and vessel location in relation to the sailing line. The temporal scale of each time series was -1800 to 8000 seconds (i.e., 0.5 hour before tow passage to 2.22 hours after tow passage) with a variable time step that averaged approximately 1 minute.

For each spatial cell of existing or potential submerged aquatic plant habitat within a pool (i.e., cells <1.5-m depth), a time series of daily suspended sediment concentrations can be constructed by adding the suspended sediment time series for the selected vessel to the portion of the monthly time line of events defined by the selected interarrival times. To construct this time series, the 1.5-m values were used to calculate hourly time-averaged concentrations for a 2-hour duration for each vessel configuration. An hourly time step for this aggregation was determined as a useful scaling between the 1-minute time scale of the suspended sediment computations and the daily time step of the plant growth model.

Example suspended sediment results are presented for the month of July, which is the month during the growing season with the greatest traffic intensities for Pools 4, 8, and 13. Figures 5-7 illustrate example time series of suspended sediments constructed for the first 48 hours of July in selected cells of ~1.5 m in depth for Pools 4, 8, and 13. The time series indicate a trend toward increased suspended sediments in relation to increased traffic. The results also demonstrate the different ambient suspended sediment concentrations that are input to the assessment. These ambient values are assumed to be constant for the month, but change from month to month for each pool. When expanded to the entire month (i.e., 744 hours), the sediment time series begins to demonstrate an increase in the average suspended sediment concentrations for selected cells and traffic scenarios with constant percentage increases (Figures 8-10). The magnitude of the projected concentrations for July increases from Pool 4 to 13. The corresponding time series were developed for each pool for the remaining months in the May through September period of assessment.

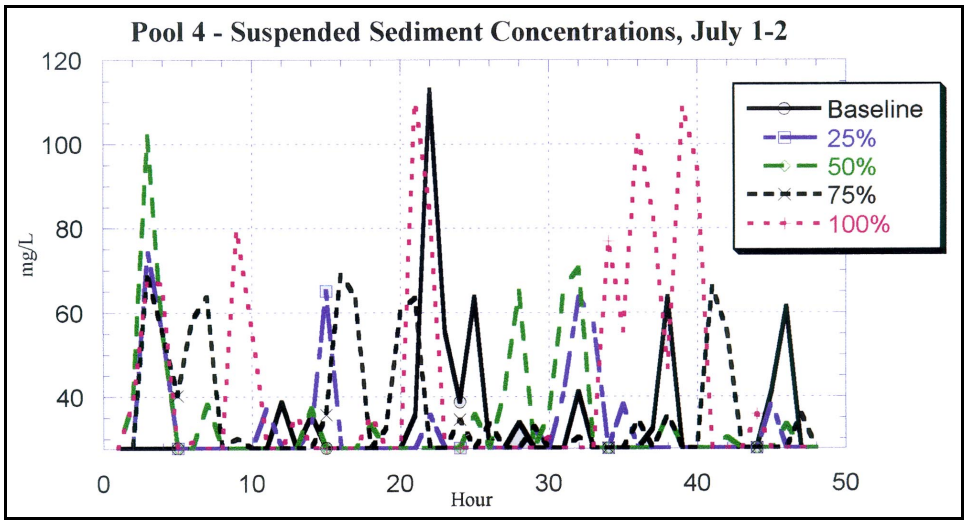

Figure 5. A time series of suspended sediment concentrations constructed for July 1 and 2 in selected cells of approximately 1.5 m in depth for UMR Pool 4

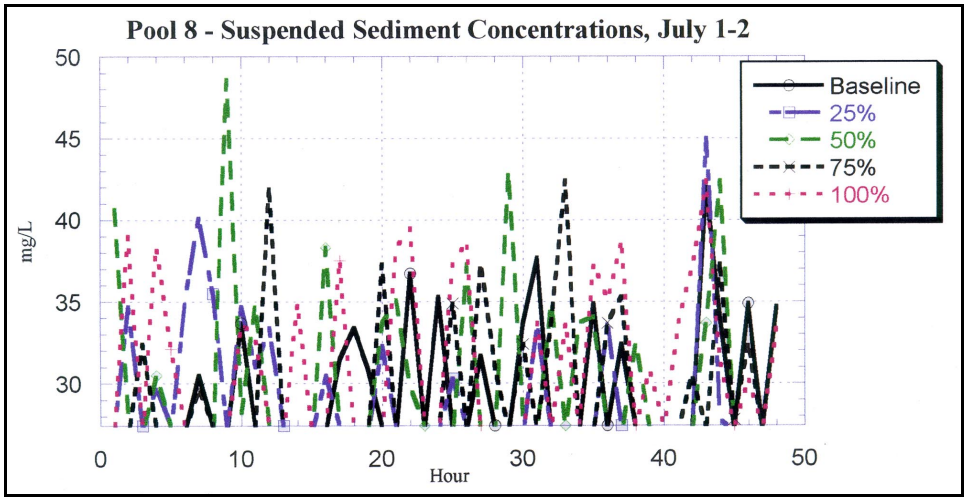

Figure 6. A time series of suspended sediment concentrations constructed for July 1 and 2 in selected cells of approximately 1.5 m in depth for UMR Pool 8

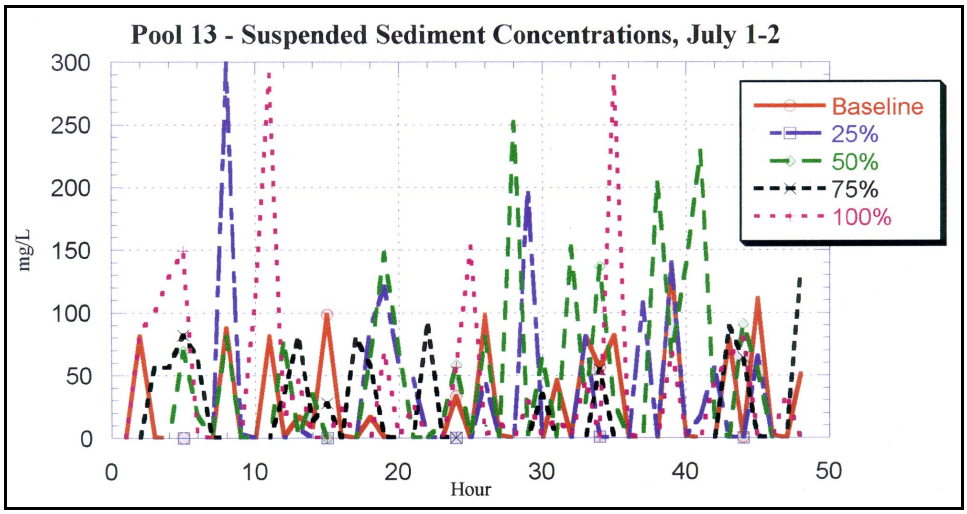

Figure 7. A time series of suspended sediment concentrations constructed for July 1 and 2 in selected cells of approximately 1.5 m in depth for UMR Pool 13

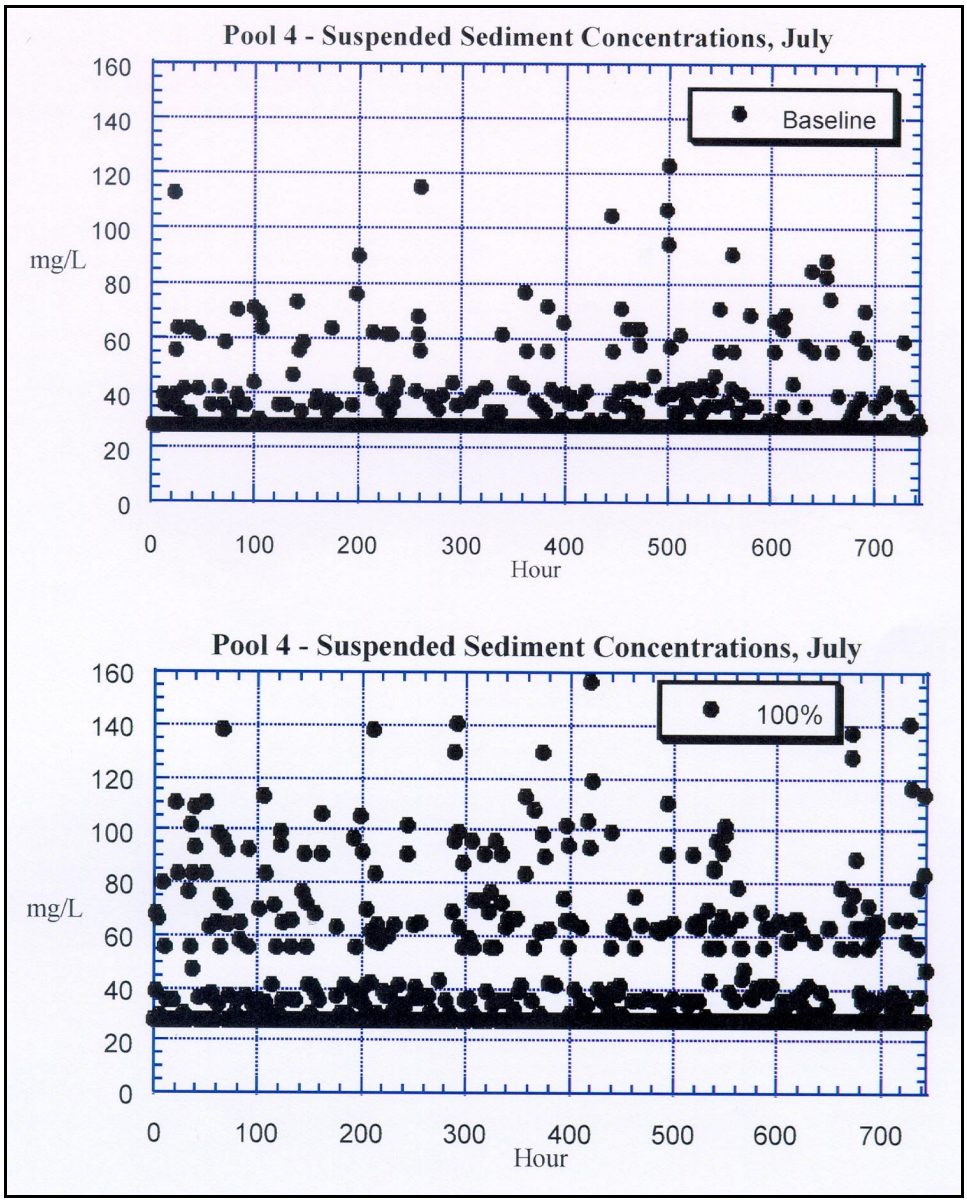

Figure 8. A time series of suspended sediment concentrations constructed for July in selected cells of approximately 1.5 m in depth for UMR Pool 4 for the baseline and 100% increase in traffic scenarios

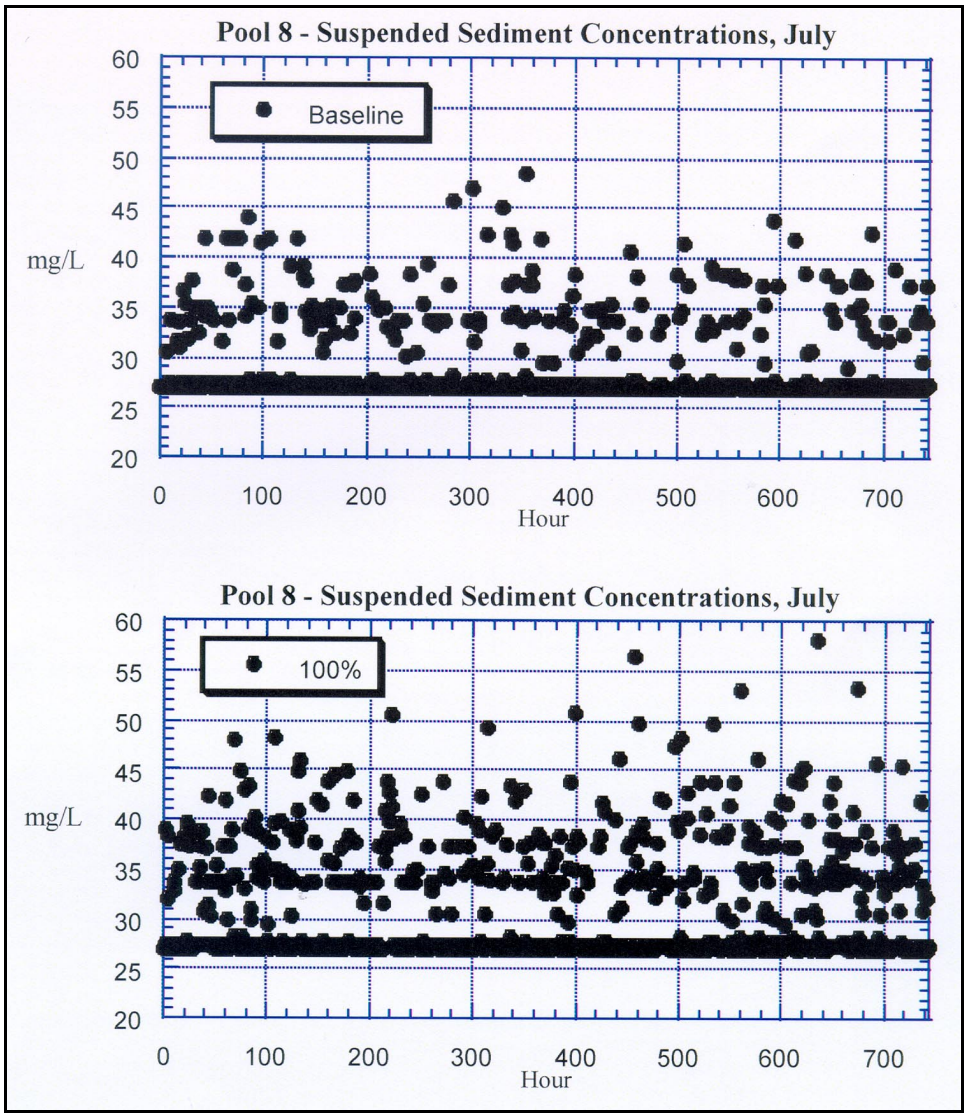

Figure 9. A time series of suspended sediment concentrations constructed for July in selected cells of approximately 1.5 m in depth for UMR Pool 8 for the baseline and 100% increase in traffic scenarios

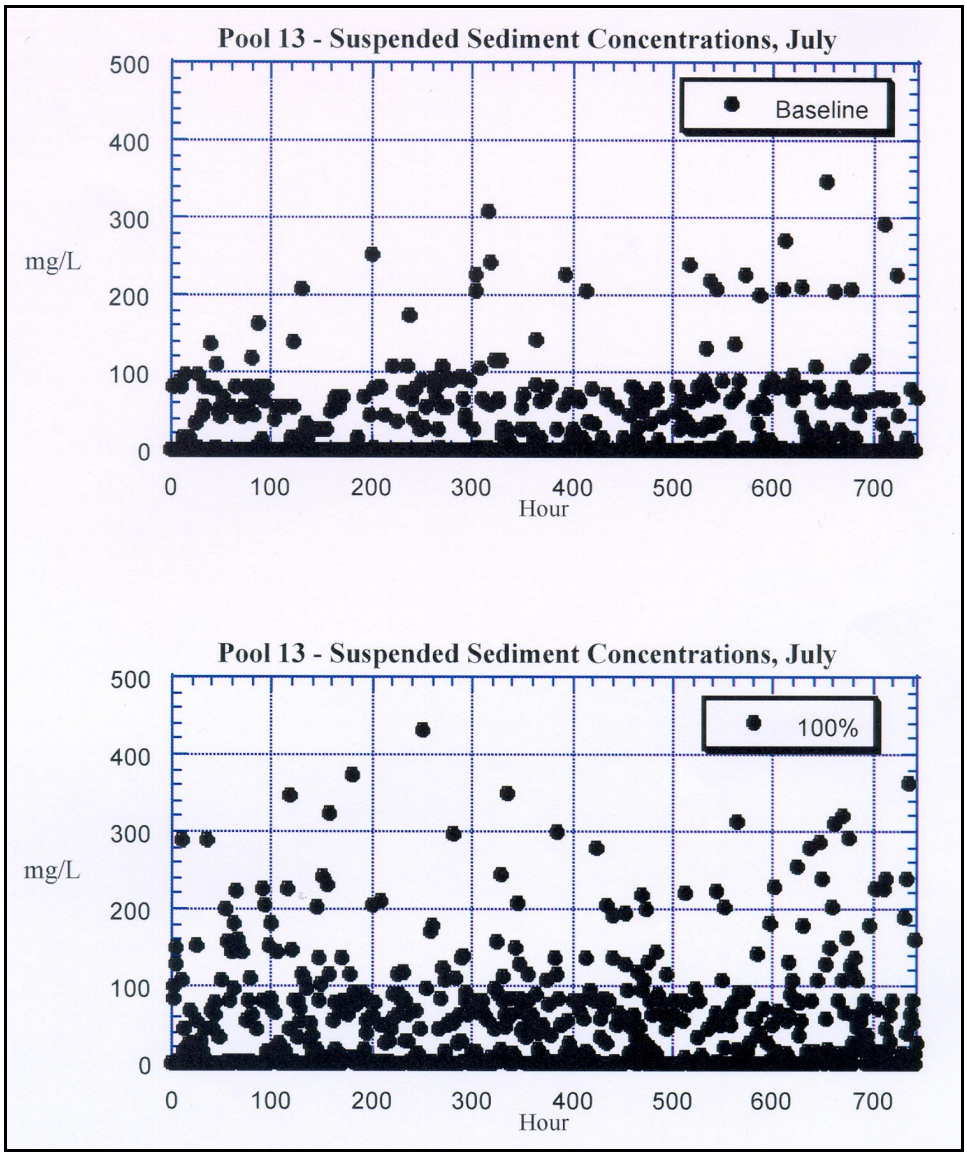

Figure 10. A time series of suspended sediment concentrations constructed for July in selected cells of approximately 1.5 m in depth for UMR Pool 13 for the baseline and 100% increase in traffic scenarios

The time series of hourly suspended sediment concentrations, which are not influenced by daylight or darkness, for each month and pool were subsequently "filtered" to remove the night time hours from potentially impacting the photosynthetic response of wild celery and sago pondweed. Daily average times of sunrise and sunset were determined for each month and pool, and these values were used to set the "effective" suspended sediment concentrations to zero for the night time hours. An effective concentration equals the suspended sediment concentration multiplied by 1.0 for a daylight hour and zero for a night time hour.

Exposure Profile

The exposure profile resulting from the characterization of exposure to passing commercial vessels consisted of two components: (1) values of current velocity and wave heights for assessing physical breakage of plants, and (2) a time series of effective suspended sediment concentrations used to estimate increased light attenuation as a function of traffic intensity.

The values of current velocity and wave height were collated for all combinations of vessel types and cells of <1.5-m depth for Pools 4, 8, and 13. For each pool, these values were collated as nine separate data sets for the combinations of three stage heights and vessel locations in relation to the sailing line (left, center, or right).

A time series of daily effective suspended sediment concentrations for each selected cell of interest was constructed for the duration of the growing season. In this preliminary assessment, the series was constructed using Pool 4, 8, and 13 sediment model outputs for the combination of high stage and tow location on the left edge of the navigation channel. Based on the results of the NAVEFF model calculations, these conditions of stage height and vessel sailing line produced the greatest direct physical impacts on plants, and it was assumed that these conditions would also lead to the most severe impacts concerning sediment resuspension and reduced plant growth and vegetative reproduction.

Other studies have found that greater physical damage occurs at low stage height (Simons et al. 1981, 1988, Spence 1982). However, the NAVSED results for nearshore (i.e., <1.5 m) environments demonstrated that the highest values of sediment resuspension did not always occur at low-flow conditions. The relationship between low-flow conditions and high sediment resuspension was more consistently demonstrated in the vicinity of the vessel, at depths >1.5 m.

4 Analysis-Characterization of Ecological Effects

Quantitative relationships between the physical forces and effects of commercial tows on submerged aquatic plants must be established in order to estimate the ecological risks. These "stress-response" relationships, which emphasize the uncertainties inherent to their development, implementation, and interpretation, provide the scientific basis for ecological risk assessment. A rule-based model was developed as a result of field and laboratory studies and, in conjunction with a physical forces model [NAVEFF (Maynord 1999)], quantitative relationships were established between waves and currents resulting from commercial traffic and their effects on submerged aquatic plants (Figure 2). Decreased growth and vegetative reproduction of submerged aquatic plants due to the increase in suspended sediment concentrations resulting from commercial traffic were quantified using two modifications of a submerged aquatic plant growth model (Figure 3).

Breakage of Submerged Aquatic Plants

The threshold for plant breakage was set at a current velocity of $\geq$0.75 m/s for the rule-based model (Figure 2). This value is somewhat lower than a velocity of 1.0 m/s, above which submerged aquatic plants rarely grow (Chambers et al. 1991, Biggs 1996), but higher than 0.25 m/s found as the breakage threshold for American wild celery and water milfoil (*Myriophyllum spicatum*) by Stewart et al. (1997). Limitations associated with the study by Stewart et al. (1997) included the exclusive use of unidirectional waves and currents, a limitation imposed by the test flume capabilities, and the use of greenhouse-cultured plants, which were documented to be weaker and less resistant to tensile breakage than field-collected plants. Because of the limitations associated with the Stewart et al. (1997) study, the authors of this report felt that the value of 0.25 m/s was too low to use as the threshold value in the rule-based model. Therefore, the value of $\geq$0.75 m/s was selected in an attempt to consistently bias the assumptions toward over-estimating impacts and risks.

A wave height threshold of 0.2 m, at a current velocity <0.75 m/s, was set for the rule-based model (Figure 2). This value was chosen because, at current velocities <0.75 m/s, waves higher than 0.2 m caused plant breakage resulting from entanglement due to current reversals in the passing wave series (Stewart et al. 1997). This value is consistent with observations that vegetation density and height is reduced at a wave height of 0.23 m (Coops and Van der Velde 1996). Both thresholds may be modified in a future version of this risk assessment if results using the initial version of the rule-based model indicate that the thresholds should be modified.

Thresholds for current velocity and wave height were used as criteria for the rule-based model used to evaluate the cells within UMR Pools 4, 8, and 13, characterized by a mean depth of $\leq$1.5 m (each cell references a three-dimensional location with a GIS data file that describes the bathymetry of the pool). These cells defined the area of existing (i.e., 1989) submerged aquatic plant beds, previously recorded plant beds, or areas that offer habitat for future plant beds. The number of these cells varied across the three stage heights that were examined.

Decreased Growth and Vegetative Reproduction of Submerged Aquatic Plants

A decrease in growth and vegetative reproduction of submerged aquatic plants resulting from increased commercial traffic may occur due to a decrease in light availability within the water column as a consequence of increased suspended sediment concentrations. The frequency, duration, and magnitude of the increase in the suspended sediment concentration above the background, ambient concentration is important, because all of these factors decrease the daily light available to submerged aquatic plants. The GIS coverage of potential submerged aquatic plant habitat (i.e., Appendix A) was compared with a GIS coverage of sediment types to determine areas of the river system where submerged aquatic plants may be at risk of decreased growth and vegetative reproduction resulting from increased suspended sediment concentrations due to a passing commercial tow (Figure 3).

To calculate an increase in the light extinction coefficient resulting from the increase in the suspended sediment concentration, suspended sediment concentrations are converted into Secchi depth (m) measurements using regressions (pool and month specific) fitted to LTRMP data from Pools 4, 8, and 13 of the UMR (by Soballe, EMTC)[1] (Table 4). Mean initial or ambient suspended sediment concentrations and Secchi depth (m) measurements were obtained from the LTRMP of the UMR Trend Pools where submerged aquatic plants are known to occur (Pools 4, 8, and 13). Monthly data (1991 through 1996) from main

[1] D. Soballe, U.S. Geological Survey. Environmental Management Technical Center (EMTC), Onalaska, WI, collects and analyzes LTRMP water quality data (in addition to other job duties).

Table 4
Regression Equations for the LTRMP Trend Pools That Characterize the Relationship Between Secchi Depth and Total Suspended Sediment Concentration[1]

Month	Regression Equation
UMR Pool 4	
May	Log_{10}(Secchi depth in cm) = 2.33 - 0.401[Log_{10}(total suspended sediment conc. in mg/l)]
June	Log_{10}(Secchi depth in cm) = 2.48 - 0.539[Log_{10}(total suspended sediment conc. in mg/l)]
July	Log_{10}(Secchi depth in cm) = 2.44 - 0.535[Log_{10}(total suspended sediment conc. in mg/l)]
August	Log_{10}(Secchi depth in cm) = 2.45 - 0.541[Log_{10}(total suspended sediment conc. in mg/l)]
September	Log_{10}(Secchi depth in cm) = 2.46 - 0.566[Log_{10}(total suspended sediment conc. in mg/l)]
UMR Pool 8	
May	Log_{10}(Secchi depth in cm) = 2.26 - 0.358[Log_{10}(total suspended sediment conc. in mg/l)]
June	Log_{10}(Secchi depth in cm) = 2.65 - 0.706[Log_{10}(total suspended sediment conc. in mg/l)]
July	Log_{10}(Secchi depth in cm) = 2.43 - 0.558[Log_{10}(total suspended sediment conc. in mg/l)]
August	Log_{10}(Secchi depth in cm) = 2.32 - 0.456[Log_{10}(total suspended sediment conc. in mg/l)]
September	Log_{10}(Secchi depth in cm) = 2.43 - 0.541[Log_{10}(total suspended sediment conc. in mg/l)]
UMR Pool 13	
May	Log_{10}(Secchi depth in cm) = 2.75 - 0.659[Log_{10}(total suspended sediment conc. in mg/l)]
June	Log_{10}(Secchi depth in cm) = 2.37 - 0.497[Log_{10}(total suspended sediment conc. in mg/l)]
July	Log_{10}(Secchi depth in cm) = 2.38 - 0.497[Log_{10}(total suspended sediment conc. in mg/l)]
August	Log_{10}(Secchi depth in cm) = 2.46 - 0.538[Log_{10}(total suspended sediment conc. in mg/l)]
September	Log_{10}(Secchi depth in cm) = 2.39 - 0.498[Log_{10}(total suspended sediment conc. in mg/l)]

[1] These equations form the first step in calculating the change in light extinction caused by increased suspended sediment concentrations resulting from increased commercial traffic (see Figure 3)

channel sites in Pools 4, 8, and 13 were summarized by Soballe (Table 5). Ambient conditions were summarized for the entire year for use as input into the plant growth models (Table 5). The plant growth models simulate each day for

Table 5
Initial, Ambient Conditions in the LTRMP Trend Pools and Light Extinction Coefficients Derived from Monthly Secchi Depth Measurements for Main Channel Sites from 1991-1996

Month	Mean Suspended Sediment Concentration (mg/l)	Mean Secchi Depth (m)	Light Extinction Coefficient (/m) [1.65/Secchi Depth (m), Giesen et al. 1990]
UMR Pool 4			
May	27.0	0.63	2.619
June	31.0	0.59	2.796
July	32.0	0.55	3.000
August	29.0	0.57	2.895
September	30.0	0.52	3.173
UMR Pool 8			
May	20.0	0.50	3.300
June	30.0	0.46	3.587
July	27.0	0.43	3.837
August	19.0	0.45	3.667
September	20.0	0.49	3.367
UMR Pool 13			
May	76.0	0.37	4.459
June	56.0	0.36	4.583
July	53.0	0.37	4.459
August	47.0	0.39	4.231
September	46.0	0.39	4.231

an entire year; however, the impacts on plant growth and vegetative reproduction are only simulated for the growing season (May 1 through September 30) during this annual time period.

In each case, Secchi depth was converted into a light extinction coefficient using the relationship developed by Giesen et al. (1990) (Figure 3). This relationship, light extinction (m^{-1}) = 1.65/Secchi depth (m), was chosen since it appears valid for turbid, shallow water with a Secchi depth range of 0.5-2.0 m, similar to conditions found in the UMR-IWW System.

Initial simulations using the plant growth models selected for this risk assessment were performed for Pools 4, 8, and 13 of the UMR. Ambient light extinction coefficients calculated from the LTRMP data (Table 4) and weather

data from the Minneapolis/St. Paul, Minnesota, airport (10-year average, 1985-1994) for Pool 4, from the La Crosse, Wisconsin, airport (30-year daily average, 1961-1990) for Pool 8, and from the Moline, Illinois, airport (30-year daily average, 1961-1990) for Pool 13 were used to quantify submerged aquatic plant growth and vegetative reproduction under ambient conditions. Output variables that best describe submerged aquatic plant growth and vegetative reproduction for this ecological risk assessment include the total live plant dry weight (excluding tubers, TGW), the total biomass (living + dead plant dry weight excluding tubers, TW), the number of dormant tubers (NDTUB), and the biomass or total dry weight of dormant tubers (TWTUB) (Table B1 in Appendix B).

Submerged aquatic plant growth model review

Available submerged aquatic plant simulation models were reviewed for use in this ecological risk assessment (Table 6). Additional plant models, not included in Table 6, were reviewed and found not to be appropriate for this risk assessment; consequently, these were not included in the statistical analyses (Ikusima 1970, Ondok and Gloser 1978, Weber et al. 1981, Laing and Browse 1985, Madsen and Adams 1989, Knight 1992). A statistical cluster analysis and principal factor analysis were performed to determine the similarities and differences between the submerged aquatic plant models. These analyses helped identify models that could be used in this ecological risk assessment. The state variables and model components used to classify these models for the cluster analysis and principal factor analysis are presented in Table 7. A state variable with the value of "0" indicates that the model does not contain that particular model attribute, while a variable with the value of "1" indicates that the model includes it. All state variables were used in both analyses.

Results of the cluster analysis are depicted by the dendrogram presented in Figure 11. The results indicate that Models 2 and 6, Models 1 and 5, and Models 4 and 10 are the most closely related, respectively. Models 1, 5, 2, 6, 12, 4, and 10, Models 3 and 13, and Models 7 and 8 fall out into similar groups. Models 9 and 11 are most dissimilar to the other models.

Results of the principal factor analysis are presented in Table 8 and illustrated in Figure 12. In the figure, distant points have rays which are displayed in grey while points that are near have rays which appear in black. The results of the principal factor analysis suggest that Models 1, 6, and 12, Models 2 and 3, and Models 4 and 10 are closely related. Models 7 and 8 also appear to be related. Model 9 is the most different from the other models.

Based on the results of these analyses and many discussions during workshops and meetings, the submerged aquatic plant growth model developed by Best and Boyd (1996) and Boyd and Best (1996) (Model 2) was selected to serve as the prototype in the Navigation Study Submerged Aquatic Plant Ecological Risk Assessment. The model, originally developed for hydrilla, was

modified for sago pondweed and American wild celery, respectively. Both models are summarized in the sections below.

Table 6
Summary of Reviewed Submerged Aquatic Plant Growth Models

Model Output	Species	Reference	Number Assigned for Statistical Analysis
Biomass, carbon flow	*Ceratophyllum demersum*	Best 1981	1
Biomass, carbon flow	*Hydrilla verticillata*	Best and Boyd 1996, Boyd and Best 1996	2
Biomass, carbon flow	Generic	Best and Jacobs 1990	3
Biomass, nutrient (C, N, P) flow	*Hydrilla verticillata, Myriophyllum spicatum*	Collins et al. 1985, Collins and Wlosinski 1989	4
Biomass, carbon flow	*Potamogeton pectinatus*	Hootsmans 1991	5
Biomass, carbon flow	*Hydrilla verticillata*	Lips 1985	6
Carbon flow, oxygen, CO_2, and HCO_3^- exchange	*Elodea canadensis*	Ondok et al. 1984	7
Oxygen flow	*Egeria densa, Lagorosiphon major*	Rutherford 1977	8
Biomass	Generic	Scheffer et al. 1993	9
Biomass, carbon flow	*Myriophyllum spicatum*	Titus et al. 1975	10
Oxygen exchange	*Potamogeton pectinatus*	Westlake 1966	11
Biomass, carbon flow	Submerged phases of *Juncus bulbosus, Littorella uniflora*	Wortelboer 1990	12
Biomass, oxygen flow	Generic	Wright and McDonnell 1986	13

Table 7
State Variables and Model Components Used in the Submerged Aquatic Plant Model Cluster Analysis and Principal Factor Analysis

Model	1	2	3	4	5	6	7	8	9	10	11	12	13
Plant Growth													
Whole plant	1	1	1	1	1	1	1	0	1	1	0	1	1
Leaves	0	1	1	0	0	1	0	0	0	1	0	1	0
Stems	0	1	1	0	0	1	0	0	0	1	0	0	0
Shoot/root ratio	1	1	1	0	1	1	0	0	1	0	0	0	0
Roots/tubers	0	1	1	0	1	1	0	0	1	1	0	1	0
Photosynthesis	1	1	1	1	1	1	1	1	1	1	1	1	1
Development phase	0	1	1	0	0	0	0	0	0	0	0	0	0
Biomass	1	1	1	1	1	1	0	1	1	1	0	1	1
Plant Reproduction													
Sexual	0	0	0	0	0	0	0	0	0	0	0	0	0
Asexual	0	1	1	0	0	1	0	0	1	0	0	0	0
Wintering strategy	0	1	0	0	0	0	0	0	1	0	0	0	0
Maintenance Costs													
Respiration	1	1	1	1	1	1	1	1	1	1	1	1	1
Photorespiration	0	0	0	1	0	0	0	0	0	1	0	0	0
Excretion/leaching	0	0	0	1	0	1	0	0	0	1	0	0	0
Nonpredatory mortality	1	1	1	1	1	1	1	0	1	1	0	1	1
Photoinhibition	0	0	0	1	0	0	0	0	0	0	0	0	0
Environmental Data													
Surface light intensity	1	1	1	1	1	1	1	1	1	1	1	1	1
Self-shading	1	1	1	1	1	1	0	0	1	1	1	1	1
Other light field data	0	1	1	1	1	1	0	0	1	1	1	1	1
Latitude, day length, etc.	0	1	1	0	1	1	1	1	0	0	0	1	1
Nutrients (other than carbon)	0	0	0	1	0	0	0	0	0	0	0	1	1
Carbon supply	1	1	1	1	0	1	1	0	0	1	0	1	0
Water and/or air temperature	1	1	1	1	1	1	1	1	1	1	1	1	1
Turbidity	1	1	1	1	1	0	0	0	1	1	1	0	1
Current velocity/wave action	0	0	0	0	1	0	0	1	1	0	0	0	1

Note: “0" indicates model does not contain that particular model attribute. “I” indicates model includes it.

Table 7 (Continued)													
Model	**1**	**2**	**3**	**4**	**5**	**6**	**7**	**8**	**9**	**10**	**11**	**12**	**13**
Spatial Scale													
Specified area	0	0	0	0	0	1	0	1	0	1	0	1	1
Spatially explicit	1	1	1	1	1	1	1	1	1	1	1	0	1
Temporal Scale-Duration													
Day	0	0	0	0	0	0	1	1	1	0	1	0	0
Week	0	0	0	0	0	0	1	0	0	0	0	0	0
Month	0	0	0	0	0	0	1	0	0	1	0	0	1
Annual	1	1	1	1	1	1	0	0	1	1	0	1	1
>Annual	0	1	0	0	1	0	0	0	1	0	0	1	0
Temporal Scale-Resolution													
Minute	0	0	0	0	0	0	0	0	0	0	1	0	0
Hour	0	0	0	1	0	0	1	1	0	0	1	0	0
Day	1	1	1	1	1	1	0	0	1	1	0	1	1
>Day	1	1	1	1	1	1	0	0	1	1	0	1	0
Previous Application-Systems													
Lakes	1	1	1	1	1	1	0	0	1	1	0	1	0
Larger rivers	0	0	0	0	0	0	0	1	0	0	0	0	0
Streams	0	0	1	0	0	0	0	0	0	0	1	0	1
Previous Application-Plant Species													
Generic	0	0	1	0	0	0	0	0	1	0	0	0	1
Species-specific	1	1	0	1	1	1	1	1	1	1	1	1	0
Sago Pondweed	0	0	0	0	1	0	0	0	1	0	1	0	0
Wild Celery	0	0	0	0	0	0	0	0	0	0	0	0	0
Previous Model Testing													
Calibrated	1	1	1	1	1	1	1	1	1	1	1	1	1
Model:data comparisons	1	1	0	1	1	1	1	1	1	1	1	1	1
Sensitivity/uncertainty analysis	0	1	0	0	1	1	0	1	1	0	0	0	1
Model Type													
Deterministic	1	1	1	1	1	1	0	1	0	1	1	1	1
Statistical/regression type	0	0	0	0	0	0	1	1	0	0	0	0	0
Stochastic	0	0	0	0	0	0	0	0	1	0	0	0	0
Process/mechanistic	1	1	1	1	1	1	1	1	1	1	1	1	1

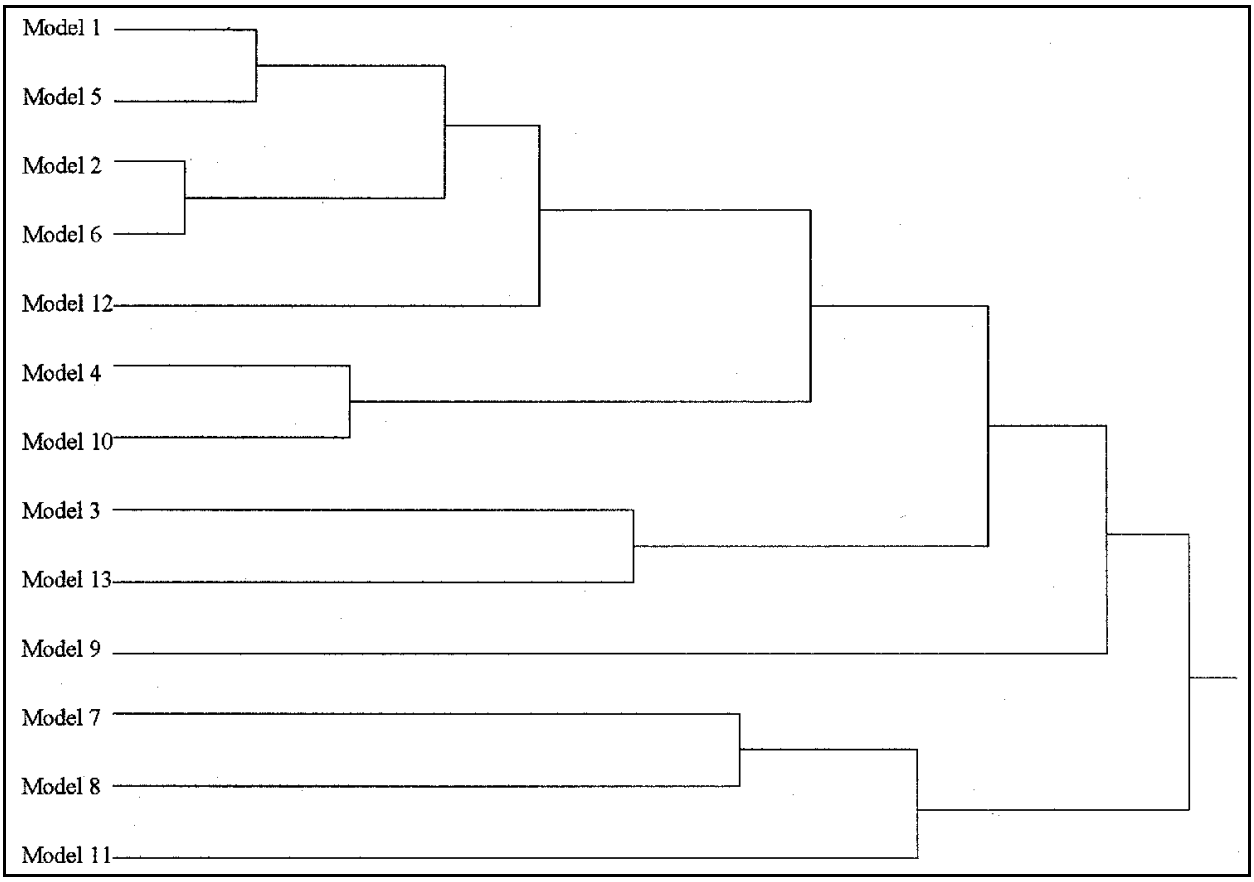

Figure 11. The dendrogram that summarizes the results of the submerged aquatic plant model cluster analysis

Table 8
Results of the Submerged Aquatic Plant Model Principal Factor Analysis

Model	Rotated Factor Pattern			Communalities
1	0.3644318	-0.151082	0.1958219	0.19398
2	0.3340455	0.0332848	0.2672137	0.18410
3	0.3401582	0.0759461	0.1961758	0.15996
4	0.3704532	-0.191447	0.0134951	0.17407
5	0.2305636	-0.120852	0.3842616	0.21542
6	0.4016443	-0.02568	0.1511217	0.18482
7	0.0751550	-0.374849	-0.088486	0.15399
8	0.0022896	-0.397053	0.0785064	0.16382
9	0.0837724	-0.045675	0.4320853	0.19580
10	0.4401282	-0.0716	0.0233599	0.19939
11	0.0454178	-0.342629	0.1252170	0.13514
12	0.3915137	-0.071878	0.1140348	0.17145
13	0.1758623	-0.206988	0.2006968	0.11405
Rotation Matrix				
0.80870	-0.31421	0.49727		
-0.27782	-0.94917	-0.14795		
-0.51848	0.01850	0.85489		

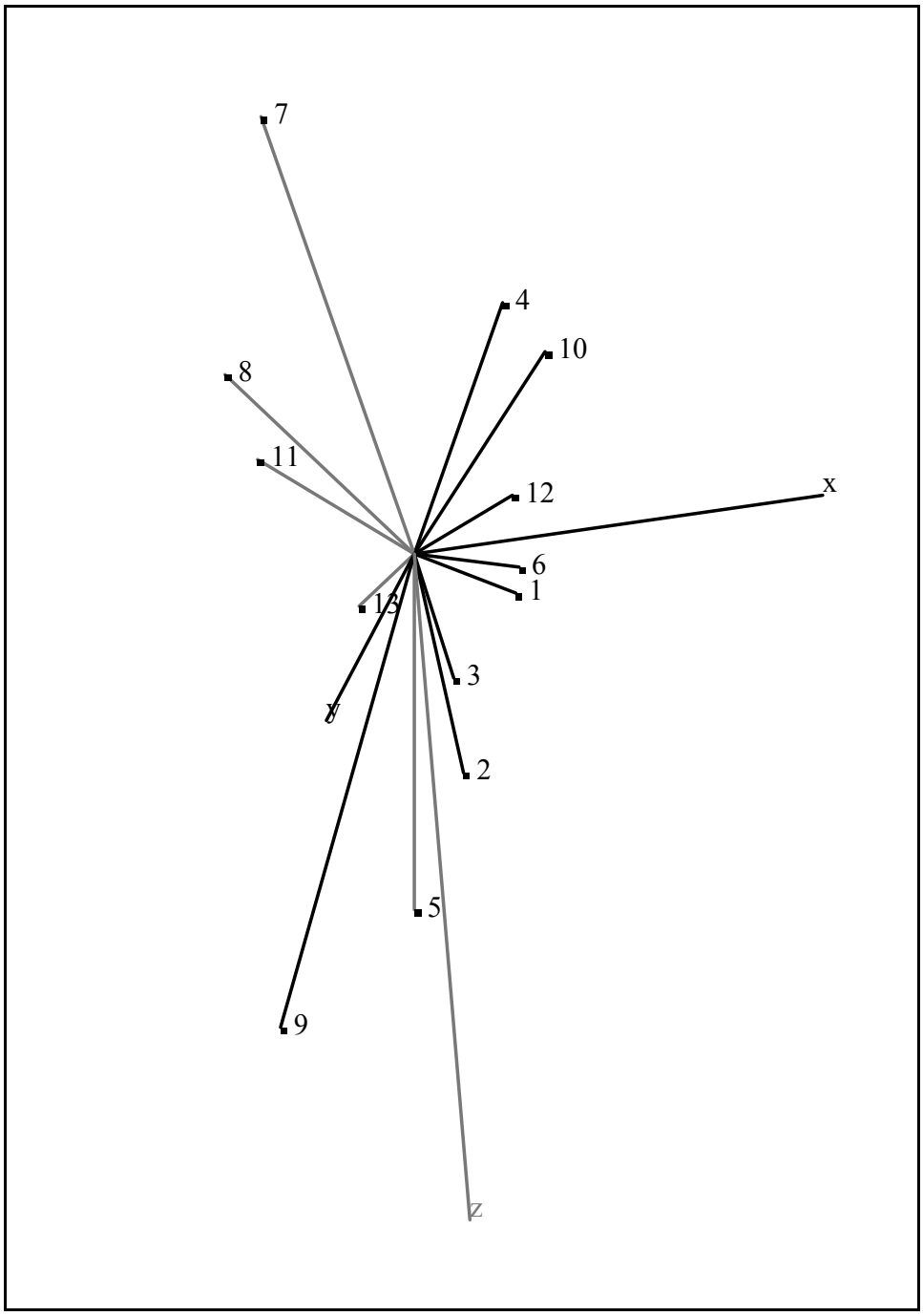

Figure 12. Results of a principal factor analysis of the submerged aquatic plant models

Plant growth model descriptions

Two simulation models, developed for sago pondweed and American wild celery, both representative submerged aquatic plant species common in the UMR, are summarized below. The model for American wild celery is referred to as "VALLA" and the model for sago pondweed as "POTAM." Both models have been developed after a published prototype pertaining to hydrilla and focus on processes of carbon transfer between the plants and their environment. Nutrient relations have not yet been incorporated into these models due to lack of evidence for nutrient limitation in the water bodies concerned (Best and Boyd 1996, Boyd and Best 1996). These models are published elsewhere (Best and Boyd 2000a, 2000b, 2000c, 2000d); their parameters are listed in Tables B4 and B5.

Both species are rooted, tuber-forming, submerged aquatic plants native to the U.S. and have similar, important phases in their phenological cycles. However, they differ greatly in their geographical distribution and in their growth habits in terms of the vertical distribution of biomass within the water column. American wild celery occurs typically in relatively clear and cool, fresh, alkaline, or brackish waters of ponds, rivers, and estuaries. It occurs from Nova Scotia to northern parts of Mexico. Sago pondweed is common in fresh, alkaline, or saline waters of ponds, rivers, marshes, and ocean shores. It occurs from Newfoundland to South America, in Africa, and in parts of Asia. Sago pondweed can have over 60% of its biomass located in the upper third of the water column, where it forms a canopy-like cover near or at the water surface. In contrast to sago pondweed, wild celery has a basal rosette of leaves which may extend to the water surface but does not form a canopy. Canopy formation can be viewed as an optimum growth form for submerged aquatic plants on the basis of maximizing carbon gain in relation to light availability.

The models can be used to quantify the impacts of changes in important environmental factors on the dynamics of populations of submerged aquatic plant species, distinguished on the basis of their phenology and morphology. The effects on the following environmental factors can be tested: climate (site irradiance and air temperature), water depth, transparency, temperature, and wave action (removal of shoot biomass from water surface to a given water depth). Each model is equipped with input files containing plant characteristics and environmental conditions that can be changed by the user. Numeric model output is provided and can be easily viewed within a user-friendly shell, which provides graphical output. The models are currently in the process of being published, and executable programs of the FORTRAN files and user manuals are available (Best and Boyd 2000a, 2000b, 2000c, 2000d).

The models simulate growth of a monotypic (single species) submerged aquatic plant community, including roots and tubers. The modeled rate of dry matter accumulation is a function of irradiance, temperature, CO_2 availability, and plant characteristics. The rate of CO_2 assimilation (photosynthesis) of the plant community depends on the radiant energy absorbed by the shoots, which is a function of incident radiation, reflection at the water surface, attenuation by the

water column, attenuation by the plant material, and leaf area of the community. The daily rate of gross CO_2 assimilation of the plant community is calculated as a function of the absorbed radiation, the photosynthetic characteristics of individual shoot tips, and the pH-determined CO_2 availability.

A fraction of the carbohydrates assimilated is allocated to maintain the existing plant biomass. The remaining carbohydrates are converted into structural dry matter (e.g., plant organs). In the process of conversion, part of the mass is lost in respiration. The dry matter produced is partitioned among the various plant organs using partitioning factors defined as a function of the phenological cycle of the species. The dry mass of the plant organs is obtained by integration of their growth rates over time. The plant species winter either as a system composed of rooted plants and subterranean tubers, or as tubers alone. Environmental factors and plant growth characteristics vary with depth; therefore, the model partitions the water column and the associated growth-related processes into 0.1-m depth classes. All calculations are performed on a m^2 basis.

The models are equipped with input files in which standard physiological properties, initial plant and tuber biomass, and water temperature are given. These input files can easily be changed by the user to apply to the study site. The models run at daily time steps for periods of one to five years.

Development and Phenological Cycle. The phenology of the plant community is an ordered sequence of processes which take place over a period of time, punctuated by more or less discrete phenological events. The rate of phenological development is modeled as a function of temperature based on the degree-day hypothesis (Thornley and Johnson 1990a). Calibration according to this hypothesis allows for use of the model for the same plant species at other sites differing in temperature regimes. The relationships between the development phase, the day-of-year, and the 3 °C temperature sum for a temperate climate are presented in Table B2 for wild celery and in Table B3 for sago pondweed.

Wintering, Sprouting of Tubers, and Growth of Sprouts to the Water Surface. Plant growth is initiated at a certain developmental phase, and a fixed number of plants develop through conversion of carbohydrates from hibernating tubers into plant material. The developmental phase and the plant density are species-specific (Tables B2 and B3). Plant density is presumed to be constant throughout the year. This presumption is based on estimates of density of adolescent plants in the field, which indicate narrow density ranges for both species (Titus and Stephens 1983, Doyle 1999, Sher Kaul et al. 1995). It is possible that late in the growing season density increases somewhat through emergence of rosettes or shoots from stolons, but the role of these organs in biomass production and population survival is deemed negligible due to their low carbon gain (shaded by neighbor plants) and absence or low production of small-sized tubers. Small-sized tubers have low survival value for both species. The dormant period of the tubers appears to be far shorter in sago pondweed

than in wild celery, providing a relatively longer period for new plant establishment for sago pondweed. Plant density for both species is 30 plants m^{-2} (Tables B4 and B5). Remobilization proceeds until a lower biomass limit is reached, equaling 10% of dry mass per tuber. Given the initial tuber mass, sprouts can only elongate a certain distance on these reserves. If net photosynthesis after this elongation period is negative for 23 days in wild celery or for 27 consecutive days in sago pondweed , the sprouts are presumed to die. The next tuber class can sprout subsequently, provided floral initiation has not yet been reached and temperature is within a range of 5-25 °C in wild celery and 5-28 °C in sago pondweed. In the elongation phase, shoot biomass is distributed equally over the successive 0.1-m depth layers, with each layer growing after the preceding layer achieves a minimum shoot biomass. After reaching maximum shoot height [water surface or $\leq$1.2 m for wild celery, water surface for sago pondweed (Best and Boyd 1996, 2000a, 2000c)], biomass is distributed following the species-specific spatial distribution (pyramid-type in wild celery, umbrella-type in sago pondweed). A relational diagram illustrating wintering and sprouting of tubers is presented in Figure 13.

Light, Photosynthesis, and Growth. The measured daily total irradiance (wavelengths of 300-3000 nm) and the maximum/minimum temperatures of the site are used as input for the model in the form of a separate weather data file. Only half of the irradiance reaching the water surface is presumed to be photosynthetically active radiation (PAR), and 6% of the remaining PAR is presumed to be reflected by the water surface (Best and Boyd 1996, Boyd and Best 1996).

In the models, daily irradiance within the water column is attenuated following the Lambert-Beer law. Although subsurface irradiance is attenuated by both color and particles within the water column, no distinction between either of these factors has been made, and one site-specific light extinction coefficient accounts for subsurface attenuation. The vertical profiles of light within the vegetation layers also are characterized, and the light absorbed by each horizontal vegetation layer is derived using these profiles. The plant community-specific extinction coefficient, *K*, is assumed to be constant throughout the year and is 0.0235 m^2 g DW^{-1} for wild celery (Titus and Adams 1979a) and 0.095 m^2 g DW^{-1} for sago pondweed (Best 1987).

Instantaneous gross photosynthesis (*FGL* expressed in g CO_2 m^{-2} h^{-1}) in the models depends on the standing crop per depth layer *i* (SC_i in g DW m^{-2} layer $^{-1}$), the photosynthesis light response of individual shoot apices at ambient temperature (*AMAX* in g CO_2 g DW^{-1} h^{-1}), the initial light use efficiency (*EE* in g CO_2 J^{-1} absorbed), the absorbed light energy (*IABSL* in J m^{-2} s^{-1}), and temperature (*AMTMPT*). The photosynthesis light response of leaves is described by the following exponential function.

$$FGL = SC_i \; AMAX \; (1 - exp \; [- EE \; IABSL_i \; 3600 / AMAX \; SC_i]) \qquad (1)$$

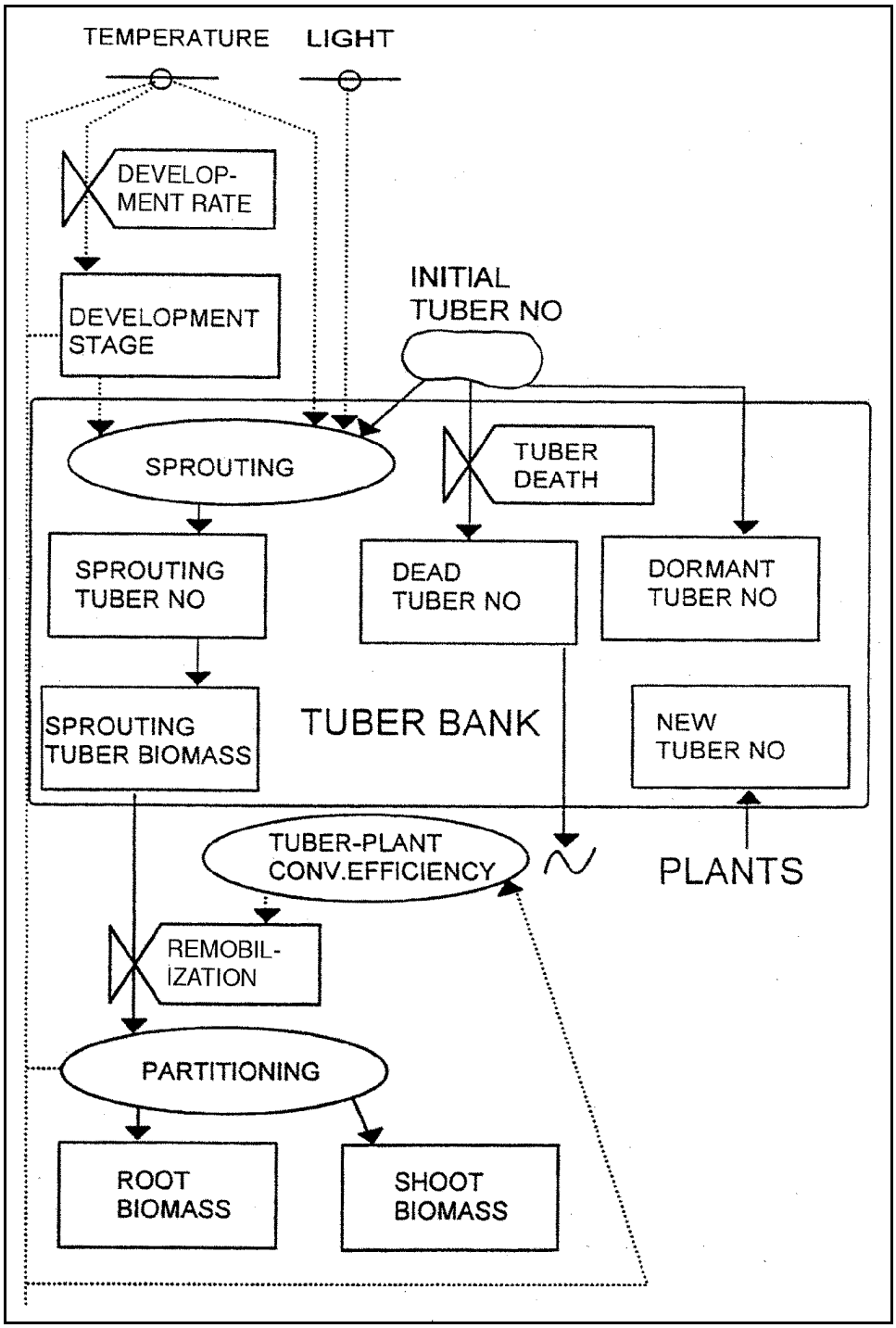

Figure 13. A relational diagram illustrating wintering and sprouting of tubers in the tuber bank

For photosynthetic activity at light saturation and optimum temperature (*AMX*), the values of 0.0165 g CO_2 g DW^{-1} h^{-1} for wild celery (Titus and Adams 1979a) and 0.019 g CO_2 g DW^{-1} h^{-1} for sago pondweed (Van der Bijl et al. 1989) were used. The photosynthetic activity at ambient temperature (*AMAX*) is calculated proportionally from that at optimum temperature using a relative function fitted to data for wild celery (Titus and Adams 1979a) and sago pondweed (Best 1987). For photosynthetic light use efficiency (*EE*), a value of 11 x 10^{-6} g CO_2 J^{-1}, typical for C_3 plants, is used (Penning de Vries and Van Laar 1982a). Substituting the appropriate value for the absorbed PAR yields the assimilation rate for each specific shoot layer.

The instantaneous rate of gross assimilation over the height of the vegetation is calculated by relating the assimilation rate per layer to the community-specific biomass distribution and by subsequent integration of all 0.1-m-high vegetation layers. The daily rate of gross assimilation is calculated by using a 3-point Gaussian integration method (Goudriaan 1986, Spitters 1986).

Maintenance costs are calculated based on the chemical composition characteristic for the plant organs, ranging from 0.010 to 0.016 g CH_2O g $AFDW^{-1}$ (Penning de Vries and Van Laar 1982b). Maintenance costs for the dormant tubers are negligible. A temperature increase of 10 ^oC is assumed to increase maintenance respiration by a factor of about 2 (with a reference temperature of 30 ^oC) (Penning de Vries and Van Laar 1982b).

Assimilates in excess of maintenance costs are converted into structural plant material. Growth efficiency and concomitant CO_2 evolution (=growth respiration) are accounted for using the assimilate requirement for growth. The assimilates required to produce one unit weight of plant organ are calculated from its chemical composition, and typical values are 1.46 g CH_2O g DW^{-1} for leaves, 1.51 for stems, and 1.44 for roots (Penning de Vries and Van Laar 1982b, Griffin 1994).

As summarized in Equation 2 below, plant growth (*GTW* expressed as g DW m^{-2} d^{-1}) equals remobilized carbohydrates (*REMOB* in g DW m^{-2} d^{-1}, converted to g CH_2O m^{-2} d^{-1} by multiplication with *CVT,* a conversion factor of translocated dry matter into glucose) augmented with gross photosynthesis (*GPHOT*) and decreased by downward translocation (*TRANS1*) and maintenance respiration (*MAINT*), all expressed as g CH_2O m^{-2} d^{-1}, divided by the assimilate requirement for plant biomass production (*ASRQ*, expressed as g CH_2O g DW^{-1}).

$$GTW = ((REMOB \,.\, CVT) + (GPHOT - TRANS1 - MAINT) / ASRQ \qquad (2)$$

The assimilate allocation pattern in plants (excluding tubers) is proportional to the biomass distribution pattern and depends on the physiological age. The typical patterns are followed when shoots have reached their maximum height and are 72% to leaves, 16% to stems, and 12% to roots in wild celery (Haller

1974, Titus and Stephens 1983), and 73% of the total to leaves, 18% to stems, and 9% to roots in sago pondweed (Best 1987).

The vertical shoot biomass distribution within the water column follows typical patterns, being pyramid-shaped in wild celery with 78% of the shoot biomass in the lower 0.5 m of the water column (Titus and Adams 1979a), and umbrella-shaped in sago pondweed with 78% of the shoot biomass in the upper 0.5 m of the water column (Best 1987). This entails the distribution of shoot biomass in the upper (sago pondweed) or lower (wild celery) five 0.1-m vegetation layers according to a specific fitted function (*DMPC*) based on the respective species-specific shapes, followed by equal distribution of the remaining biomass over the remaining 0.1-m layers up to a total biomass share of 5% per layer and proportional distribution of the then-remaining biomass over all 0.1-m vegetation layers. A species-specific share of total biomass is allocated to the roots presumed to be situated in the upper 0.1 m of the sediment layer. The vertical biomass distribution pattern is recalculated and redistributed by the models when a rooting (= water) depth other than the nominal one is chosen. A relational diagram illustrating photosynthesis, respiration, and biomass formation is presented in Figure 14.

Flowering, Translocation, Tuber Formation, and Senescence. Flowering affects metabolic activity of the modeled plants by initiating substantial downward translocation of assimilates to form tubers in both sago pondweed and wild celery. Translocation and tuber formation have been formulated similarly for both species, but the parameter values are species-specific. In wild celery, translocation occurs after flowering is initiated, at a day length <14.7 hours (Titus and Stephens 1983, Donnermeyer and Smart 1985), and at a temperature between 5 and 25 ^{o}C (Donnermeyer and Smart 1985). Wild celery tubers grow with a maximal rate of 24.7% of net production per day (Donnermeyer and Smart 1985). Translocation continues as long as plant biomass is greater than 0. In sago pondweed, translocation occurs after flowering is initiated, at a day length <16 hours (Best 1987), and at a temperature between 5 and 28 ^{0}C (Van Vierssen et al. 1994). Sago pondweed tubers grow at a maximal rate of 19% of net production per day (Wetzel and Neckles 1986, Best 1987), with remaining assimilates available for other processes.

Tuber production is based on the hypothesis that plants produce the largest possible tubers at their ambient light levels, because large tubers have the largest potential to survive future adverse low temperatures, low irradiance, and a short growth season. This hypothesis is supported by field data on sago pondweed (Van Dijk et al. 1992) and experimental data on sago pondweed and wild celery (Doyle 1999). The variation in tuber size found in the field is attributed to the inability of the plants to complete the last tuber class with such a large tuber size of the season. In the models, after reaching a given tuber size, all concurrently initiated tubers of that "class" are added to the tuber bank, and a new tuber class is initiated. A fixed, linear relationship was found in both species, indicating that the tuber number concurrently initiated increases with tuber size, with a larger range for sago pondweed than for wild celery (Figure 15).

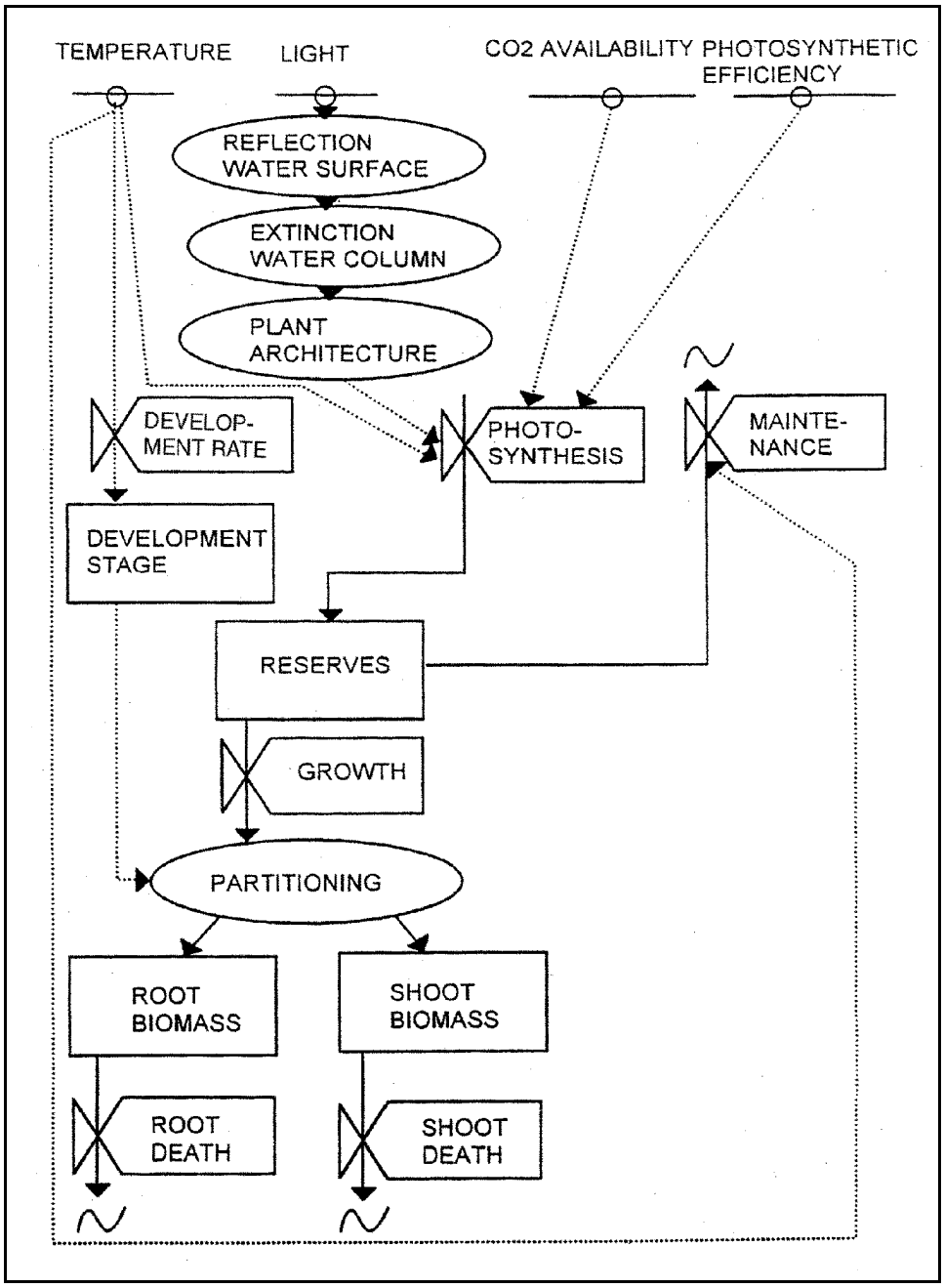

Figure 14. A relational diagram illustrating photosynthesis, respiration, and biomass formation

Senescence is modeled by defining a death rate as a certain fraction of plant biomass per day when the conditions for growth deteriorate. The timing and the values of relative death rates for plants have been derived from field observations on shoot biomass for wild celery by Titus and Stephens (1983) and for sago pondweed by Best (1987). The timing was found by running the model repeatedly with different development rates and different base and reference

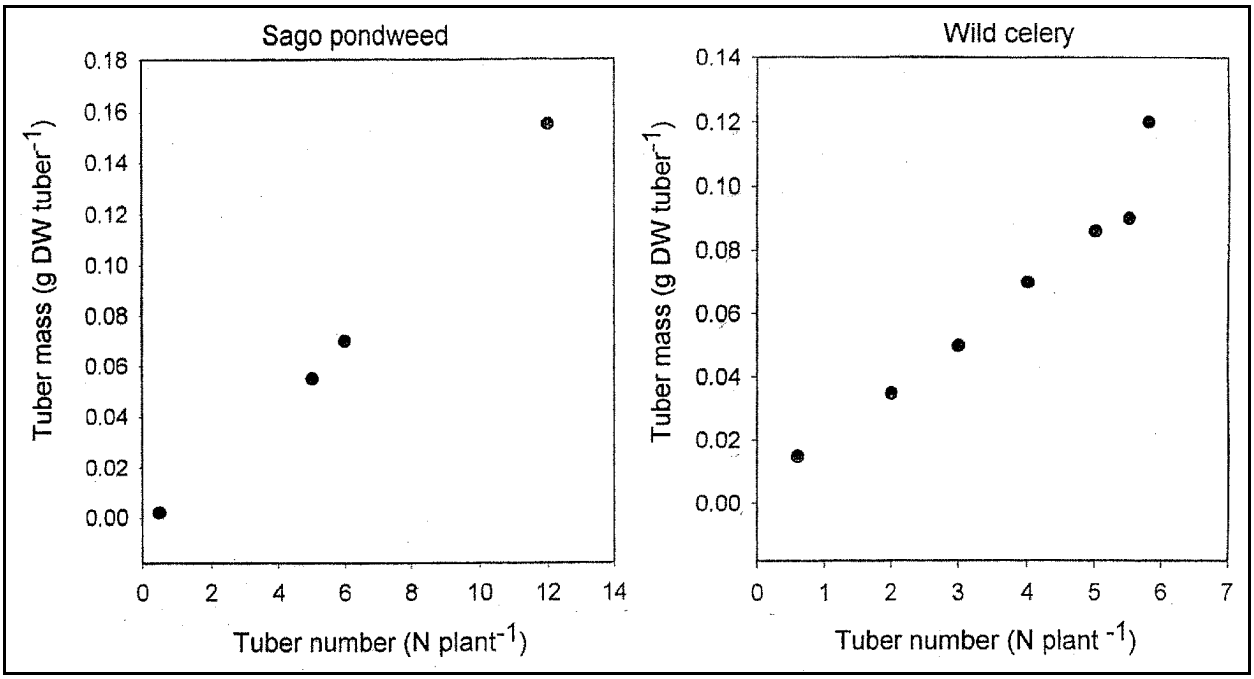

Figure 15. The relationship between tuber number concurrently initiated per plant and tuber size for sago pondweed and wild celery (Donnermeyer and Smart 1985, Spencer and Anderson 1987)

temperatures, until a realistic timing of decreasing shoot biomass occurred. Values for the relative death rate were found by applying the same differential equation that is commonly used for simple exponential growth to describe exponential decrease in biomass after flowering, with a negative specific decrease rate (Hunt 1982, Thornley and Johnson 1990b). Following this approach, relative death rates of 0.021 g DW g DW^{-1} d^{-1} for wild celery and 0.047 g DW g DW^{-1} d^{-1} for sago pondweed were calculated. The timing and values of the relative death rates for the tubers have been derived similarly from published data on tuber bank dynamics (Titus and Stephens 1983, Van Wijk 1989). Figure 16 illustrates translocation, tuber formation, and senescence in the models.

Plant growth model simulations performed for model calibration and validation

Several simulation experiments were performed to evaluate the utility of the plant growth models for this risk assessment; three examples will be discussed below. VALLA was used to simulate changes in biomass and tubers of wild celery, and POTAM was used to simulate those of sago pondweed plant communities. Parameter values used in calibration of VALLA and POTAM are listed in Tables B4 and B5. The first example consists of the results of calibration and allows for the comparison with measured biomass data. The second example illustrates model performance using the same physiological parameter

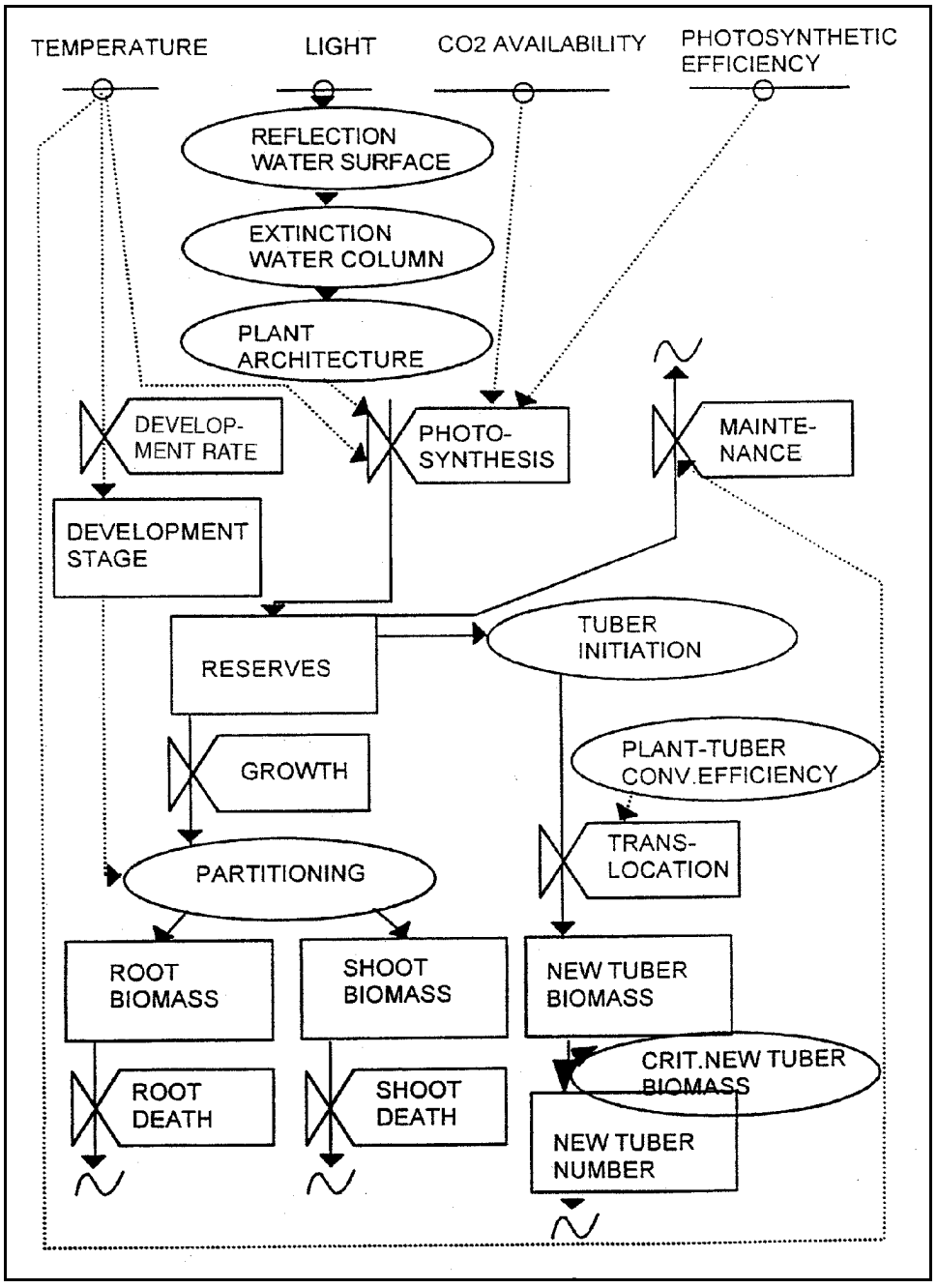

Figure 16. A relational diagram illustrating translocation, tuber formation, and senescence

values as input but with weather data from a different location (latitude). Weather data for the second example are from Minneapolis/St. Paul, Minnesota, representative for the UMR (10-year average, 1985-94). The third example illustrates the effects of water transparency values, representative for Pool 4 of the UMR (5-year average; 1991-96, growth season values only) on plant biomass and tuber formation, using the same Minneapolis/St. Paul weather data as for the second example.

Wild Celery. The simulated plant biomass of wild celery was similar to that found in Chenango Lake, New York in 1983 (Titus and Stephens 1983) (Figure 17). Peak biomass occurred at the same time and was somewhat lower in the simulation than actually measured, possibly as an artifact of the rather low frequency of field measurements. The simulated tuber number was well within the measured tuber number range.

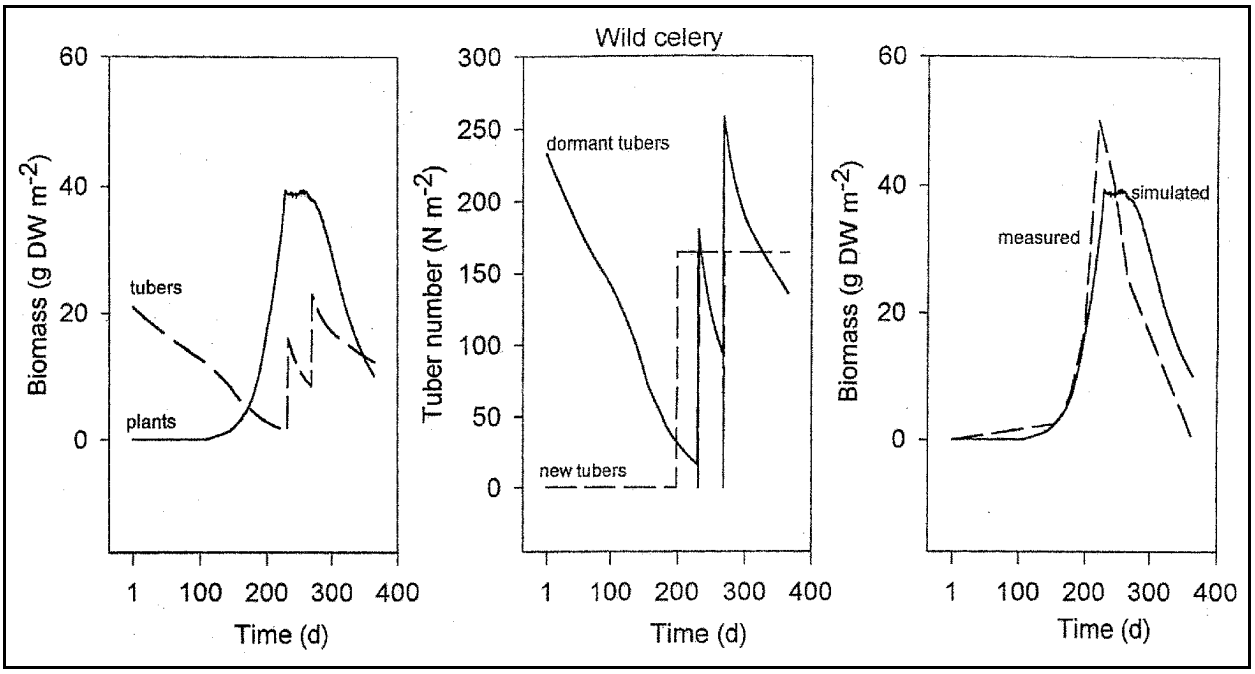

Figure 17. The simulated biomass of plants, dormant and new tuber numbers, and measured plant biomass of a wild celery community in Chenango Lake, New York. Field data from Titus and Stephens (1983); climatological data pertaining to Binghamton, New York, 1987; longitude 75°50'E, latitude 42°15'N; water depth 1.4 m; light extinction coefficient 0.43 m^{-1}

Using the same parameter values as input for a simulation of biomass dynamics in the UMR, located at a higher latitude than Chenango Lake, model simulations yielded higher plant biomass and tuber numbers (three instead of two tuber classes were completed), largely as a consequence of higher irradiance (Figure 18). Extending the duration of the simulation to two years indicated that, in such conditions, a stable population could exist, with the end-of-year tuber numbers equaling 267 m^{-2}.

A simulation of a wild celery community at a more shallow rooting depth of 1 m, but at water transparency values representative of Pool 4 of the UMR, indicated that these environmental conditions inhibit biomass and tuber production to such an extent that the population becomes extinct after one year. Extinction in this case means that the population is not capable of completing any tuber class, because the plant biomass itself is very low. However, a lower tuber density of 10 m^{-2} allowed larger individual plants to develop, due to less

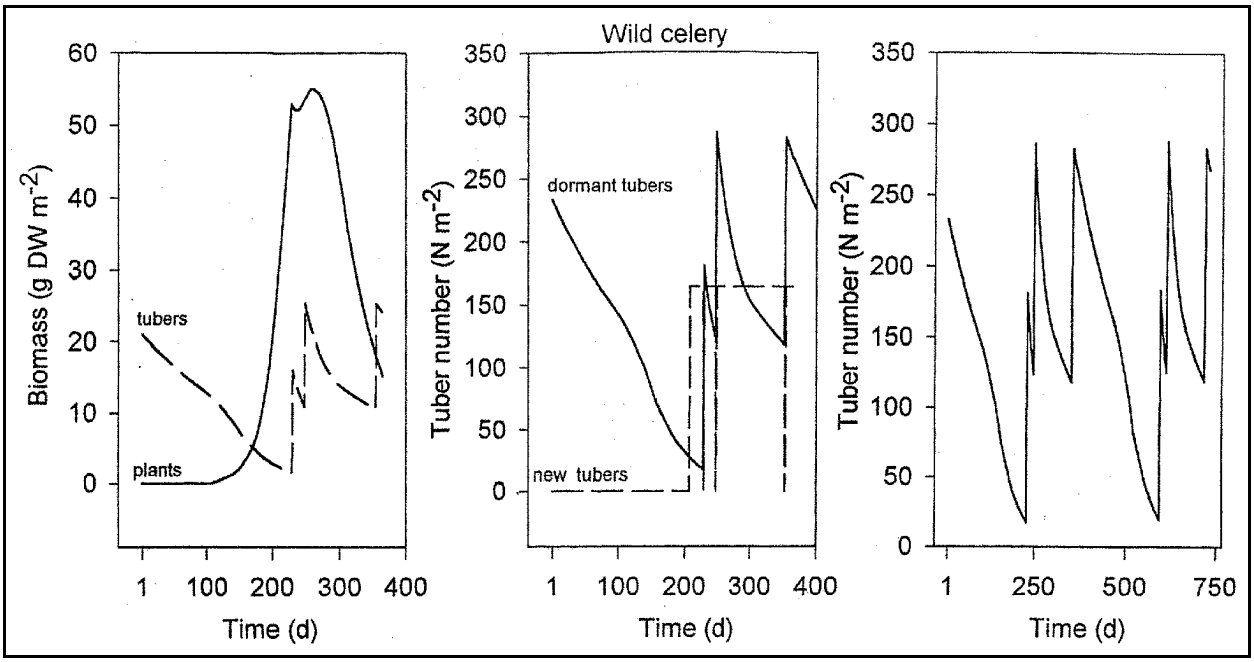

Figure 18. The simulated biomass of plants, dormant tuber numbers, and new tuber numbers of a wild celery community in the UMR. The same parameter values as those in Figure 17 are used. Climatological data pertaining to St. Paul, Minnesota, 10-year average (1985-1994); longitude 93°E, latitude 45°N; water depth 1.4 m; light extinction coefficient 0.43 m^{-1}

self-shading. The latter plants were able to complete a tuber class composed of a lower number and lighter tubers (3.3 tubers of 0.06 g DW per plant) and, in doing so, increased the tuber bank density. Although smaller tubers are less likely to give rise to viable new shoots in deep, turbid water, they may generate viable plants under temporary clear-water conditions at the same rooting depth or under the pertinent turbid water conditions at a more shallow rooting depth. Smaller tubers can, therefore, still be important for system-wide persistence (in contrast to local persistence) of a population in a given water body. At a more shallow depth of 0.5 m, substantial biomass and tuber formation proved possible, with two tuber classes being completed and an end-of-year tuber number of 134 m^{-2} (Figure 19).

Although the simulated plant biomass production was substantial at a rooting depth between 0.5 and 1.0 m, it was considerably less than reported for a depth range of 0.5 to 1.3 m with a minimum of 0.3 m in Pool 9 of the UMR (Donnermeyer and Smart 1985). At the shallow depth of 0.5 m, there may be too much uprooting by wave exposure to permit permanent plant establishment. However, the simulated biomass for the minimum rooting depth of 0.3 m was within the reported range (105 g DW m^{-2}), and five tuber classes were completed, confirming similarity between simulated and measured biomass data.

Wild celery tubers, as well as sago pondweed tubers, are an important food source for waterfowl, such as canvasback ducks (Korschgen et al. 1988), and

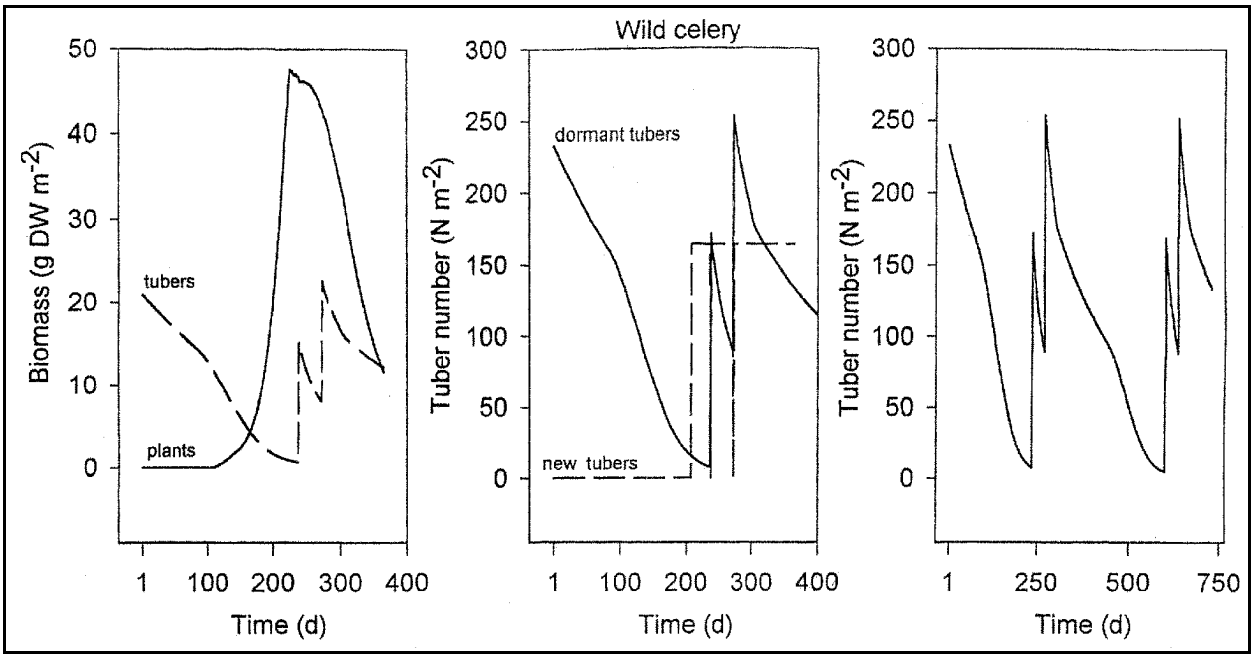

Figure 19. The simulated biomass of plants, dormant tuber numbers, and new tuber numbers of a wild celery community in UMR Pool 4. The same parameter values as those in Figure 17 are used. Climatological data pertaining to St. Paul, Minnesota, 10-year average (1985-1994); longitude 93°E, latitude 45°N; water depth 0.5 m; light extinction coefficient 2.0-3.173 m^{-1} (5-year average UMR Pool 4, 1991-1996)

herbivory may significantly reduce tuber bank density. A simulation starting from an initial, reduced, dormant tuber density of 10 tubers m^{-2} indicated that wild celery behaves similar to sago pondweed under these conditions: relatively heavier plants are formed due to decreased self-shading, and the equilibrium tuber density is gradually restored over the years.

Sago Pondweed. The simulated plant biomass of sago pondweed was similar to that found in the Zandvoort Canals, The Netherlands, in 1987 (Best 1987) (Figure 20). Peak biomass occurred somewhat later and was higher in the simulation than measured values, possibly as an artifact of the rather low frequency of field measurements. The simulated tuber number was well within the measured tuber number range; the end-of-year tuber number was 64 m^{-2}.

Using the same parameter values as input for a simulation of biomass dynamics in the UMR, located at a lower latitude than Zandvoort, yielded a somewhat higher plant biomass and far higher tuber numbers than in Zandvoort (Best 1987) (Figure 21). The higher tuber numbers were largely attributed to the higher irradiance and considerably longer window for tuber formation in the UMR. Extending the duration of the simulation to two years indicated that, in such conditions, a stable population could exist, with the end-of-year tuber numbers equaling 130 tubers m^{-2}.

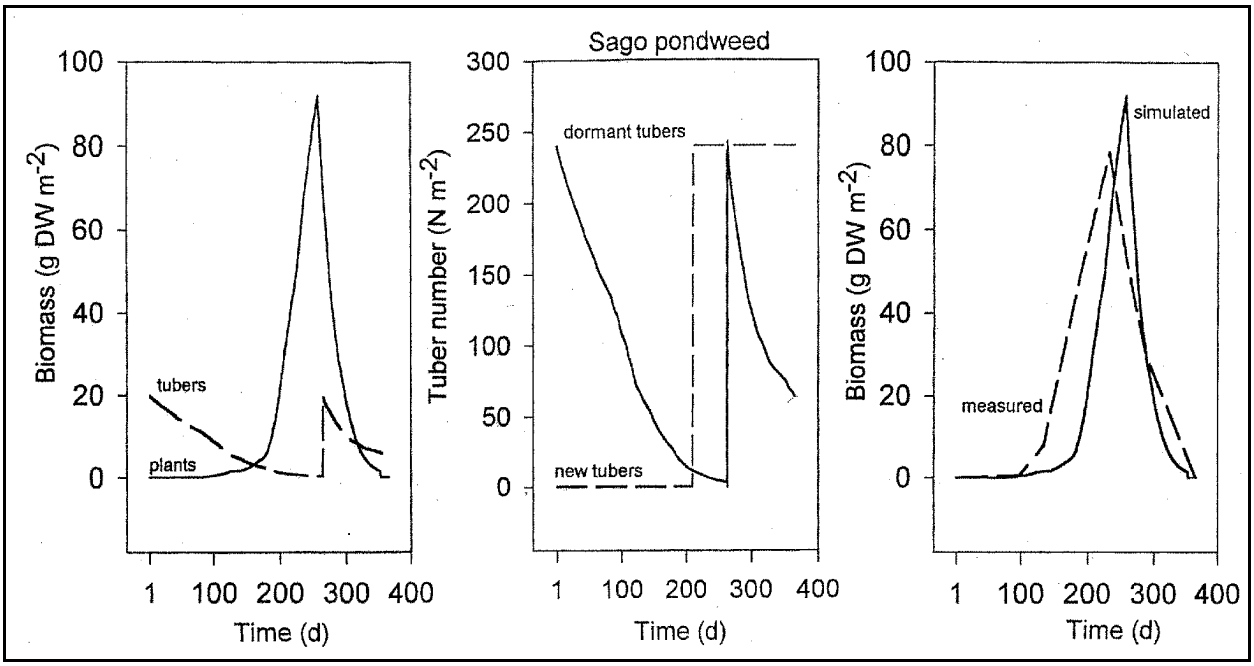

Figure 20. The simulated biomass of plants, dormant and new tuber numbers, and measured plant biomass of a sago pondweed community in Zandvoort Canals, The Netherlands. Field data from Best (1987); climatological data pertaining to De Bilt, The Netherlands, 1987; longitude 5°11'E, latitude 52°6'N; water depth 1.3 m; light extinction coefficient 1.07 m^{-1}

Simulation of a sago pondweed community at a more shallow rooting depth of 1 m, but at water transparency values representative of Pool 4 of the UMR, indicated that biomass and tuber production are inhibited under these environmental conditions, since lower values were computed (Figure 22). Only two tuber classes were completed in this case, where formerly three tuber classes were produced in the less turbid, but deeper, water. However, by extending the duration of the simulation to two years, it was observed that this plant population also was stable, with tuber numbers equaling 62 tubers at the end of the year. Sago pondweed data relevant to the UMR are not available; therefore, comparisons between simulated and measured data were not possible.

Conditions that could endanger the persistence of sago pondweed populations in the UMR were investigated by performing various simulations using POTAM. An increase in the light extinction coefficient of the water column to 3.0 m^{-1} during the whole year combined with weather data of a cold year (1992) caused a relatively small decrease in peak biomass. However, these conditions allowed only one tuber class to be completed. Nevertheless, although the end-of-year tuber numbers were relatively low (37 m^{-2}) (Table B5), the population was still viable. Sago pondweed tubers are a popular food source for waterfowl, and an already sparse population of 37 tubers can easily be cropped to 10 m^{-2} (Bick and Van Schaik 1980, Dirksen 1982). Herbivory could effectively eliminate the diminished population. However, running POTAM with an initial tuber density of 10 m^{-2} demonstrates that more biomass per plant was formed due to less

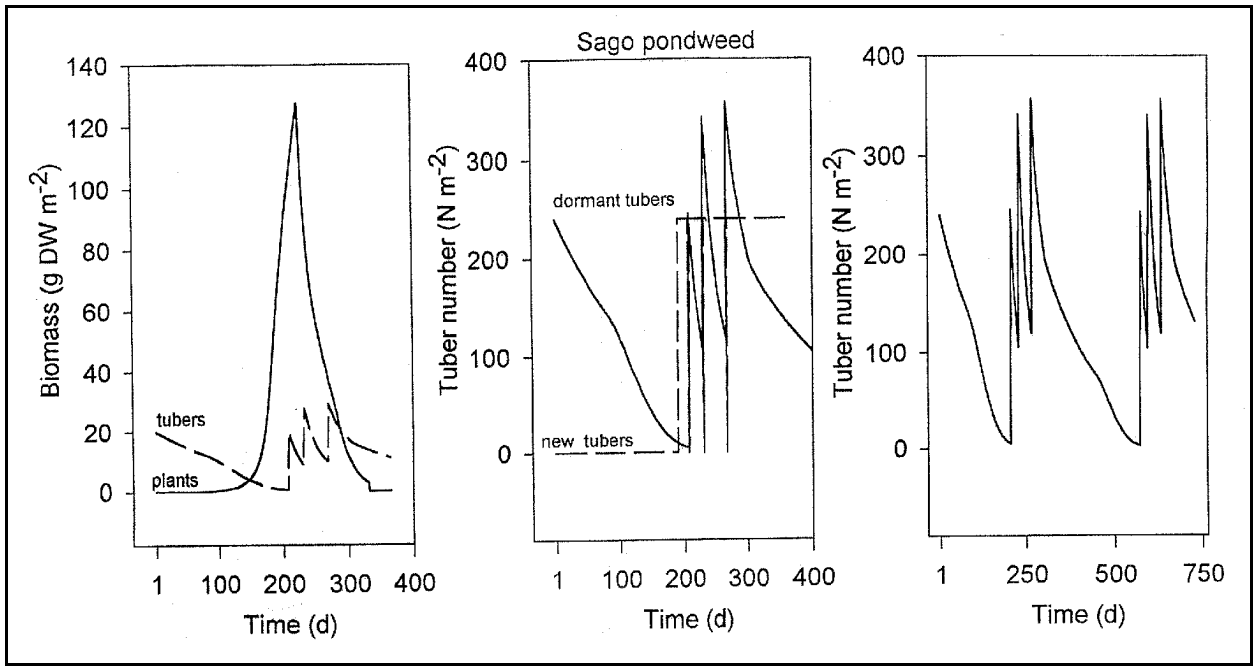

Figure 21. The simulated biomass of plants, dormant tuber numbers, and new tuber numbers of a sago pondweed community in the UMR. The same parameter values as in Figure 20 are used. Climatological data pertaining to St. Paul, Minnesota, 10-year average (1985-1994); longitude 93°E, latitude 45°N; water depth 1.3 m; light extinction coefficient 1.07 m^{-1}

self-shading, and four tuber classes were completed, restoring the tuber density to 61 m^{-2} at the end of the year.

Model Validation Simulation Results. From the simulations performed for model validation, it appears that both plant populations can persist in monotypic stands at a rooting depth of 1 m or less at current water transparency levels in the UMR. Under the turbid conditions, sago pondweed benefits from its canopy-type growth form, which maximizes light interception and carbon gain near or at the water surface. Wild celery is in a less advantageous position due to its pyramid-type growth form, which allows less light interception in the deeper water and, consequently, less carbon gain. In addition, sago pondweed shoots appear to benefit from a longer establishment period during the spring and persist for a longer time span without photosynthetic net carbon gain than wild celery. This results in stable population dynamics for sago pondweed, while wild celery experiences population fluctuations.

Increasing turbidity and herbivory will cause local decreases in tuber densities. Populations which have a low-density tuber bank have the ability to survive and return to normal tuber densities under average weather and water level conditions; this ability is more pronounced for sago pondweed than for wild celery. However, populations with a low-density tuber bank are at risk to becoming locally extinct under unfavorable weather or high water level conditions. It may be possible for locally extinct populations to be restored by

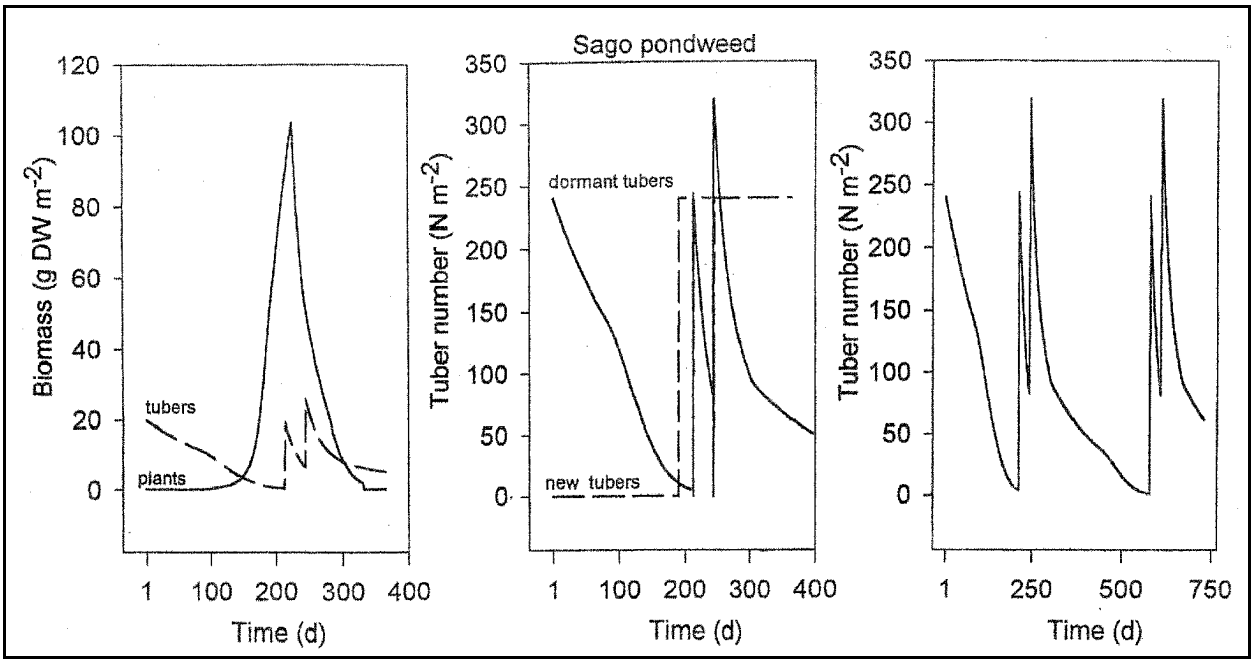

Figure 22. The simulated biomass of plants, dormant tuber numbers, and new tuber numbers of a sago pondweed community in UMR Pool 4. The same parameter values as in Figure 20 are used. Climatological data pertaining to St. Paul, Minnesota, 10-year average (1985-1994); longitude 93°E, latitude 45°N; water depth 1.0 m; light extinction coefficient 2.0-3.173 m^{-1} (5-year average UMR Pool 4, 1991-1996)

propagule imports from elsewhere, provided that the sources are nearby and that conduits between the propagule source and the site of local extinction exist. In addition, prerequisites for recolonization include (1) presence of propagules, (2) sufficient light, (3) suitable substrate, (4) tolerable current velocities and waves, (5) sufficient nutrients, and (6) minimal herbivory. Two periods appear to be critical for the persistence of local populations: (1) early spring during the initial elongation of the sprouts, and (2) the latter part of summer during tuber formation. The prerequisites for local persistence of populations with low-density tuber banks are the ability of the new shoots to reach a maximum attainable height in the water column where they can generate a positive carbon gain and the ability of full-grown plants to complete one large-size tuber class. The models can be used to calculate the timing of these sensitive periods for any combination of locations, rooting depth, and water transparency and can serve as important tools for developing water management strategies concerning submerged aquatic plant populations.

Plant growth model sensitivity analysis

A sensitivity analysis of the plant growth models indicated that the models are most sensitive to changes in maximum photosynthetic rate at light saturation (*AMX*) and photosynthetic light use efficiency (*EE*). In addition, the same analysis performed on environmental factors other than latitude indicated that light extinction within the water column is the most sensitive environmental

factor. This sensitivity of these plant growth models to values of the light extinction coefficient makes them appropriate tools to examine the potential impacts of traffic-induced increases in suspended sediment concentrations and, thus, concomitant decreases in light availability on growth and vegetative reproduction of submerged aquatic plants.

Plant growth model limitations

In the models, the parameter values for both photosynthetic rate and light use efficiency have been set and kept constant throughout the year. However, it is extremely difficult to obtain accurate estimates of both of these values as well as accurate descriptions of the environmental conditions under which they were obtained and, thus, to decide whether the published parameter values are valid for the conditions to be modeled. A discussion of the variation in compiled data and their causes and consequences is presented by Sondergaard (1988). No quantification has been published to date of the singular and combined effects of changes in carbon availability, oxygen regimes, periphyton dynamics, and water movements on the population dynamics of submerged aquatic plants. More integration of experimental and field data on photosynthetic behavior and the inclusion of equations describing the interactions of physicochemical processes with plant physiological activity are expected to improve the predictive power of the current models. Predictability of the submerged aquatic plant population behavior on a larger spatial scale would be improved by including the behavior of sexual and vegetative propagules in the current models. Linking the plant growth models to a GIS could provide information on the importance of water movements and quality to these models and, conversely, information on plant biomass (live and dead) to other models. The current versions of the submerged aquatic plant growth models simulate plant biomass, tuber density, and tuber size within published ranges at various environmental and climatological conditions and are, therefore, useful as tools for understanding submerged aquatic plant dynamics.

Summary of Ecological Impacts

The ecological impacts of concern (i.e., endpoints) in this risk assessment included (1) direct physical damage to plants, and (2) the indirect effects of increased suspended sediment on plant growth and vegetative reproduction. Physical damage to plants was assessed in relation to changes in current velocity and waves resulting from the increased frequency of vessel passage. The indirect effects were evaluated in relation to anticipated increases in sediment resuspension by an increased number of commercial vessels operating within the UMR.

The direct impacts on submerged aquatic plants were estimated by comparing the number of combinations of vessel types and pool segments (i.e., GIS "cells") <1.5 m deep that resulted in changes in current velocity or wave heights which exceeded threshold values associated with physical damage to submerged

aquatic vegetation. Risks were characterized as the percent of the total possible combinations of cells and vessel that exceeded the threshold for three discharge regimes or stage heights (5^{th}, 50^{th}, and 95^{th} percentiles) and three different vessel locations in relation to the navigation chart sailing line (left edge of the navigation channel, right edge of the navigation channel, or centered on sailing line).

The indirect effects on submerged aquatic plants were estimated using bioenergetics-based plant growth models. Several modeled impacts of increased sediment resuspension on plant growth and vegetative reproduction were used to characterize risk.

- Values of daily gross production (g $CO_2/m^2/d$) were calculated as the product of average hourly gross photosynthesis and day length. Total annual gross production was calculated as the sum of the daily values. The average daily rate of gross production was calculated for the growing season. The maximum daily gross production rate was also recorded. This measure records ecological impacts at a biological level scaled closely to source of disturbance.

- Daily values of the total biomass of living plant tissue (not including vegetative reproductive structures) were plotted for each species, pool, and traffic scenario. The average and maximum daily values of living biomass were also tabulated. This measure reflects the impacts of reduced photosynthesis on the plant's ability to produce additional, subsequent photosynthetic tissue.

- Daily values of the total (living + non-living) biomass of living plant tissue (not including vegetative reproductive structures) were plotted for each species, pool, and traffic scenario. The daily values were summed to produce an overall estimate of plant organic matter produced and accumulated under the different traffic scenarios. The average and maximum daily values of total biomass were also tabulated. This measure reflects the impacts of reduced photosynthesis on the accumulation of living and dead tissues that serve as sources of food, cover, and habitat to other aquatic organisms.

- The average and maximum number per square meter and biomass per square meter of vegetative reproductive structures (e.g., tubers) were also tabulated for each traffic scenario. These values were used to assess the impacts of increased commercial traffic on the allocation of fixed carbon to vegetative reproduction.

To characterize risk, the percent differences in the preceding measures of impact were calculated and tabulated for each of the traffic scenarios using the 1992 traffic impacts as the reference.

5 Risk Characterization

This section summarizes an initial assessment of the potential for plant breakage and reduced plant growth and vegetative reproduction for scenarios of commercial traffic increases in UMR Pools 4, 8, and 13.

Physical Damage to Submerged Aquatic Plants

The potential for physical damage to plants was assessed by comparing the values of current velocity and wave height calculated by the NAVEFF model with the screening criteria of 0.75 m/s for current velocity and 0.2 m for wave height for all 108 vessel types in all cells in Pools 4, 8, and 13 that were 1.5 m or less in depth. Cell depth is an output of the NAVEFF model and is determined by the flow conditions and bathymetry specified as input data for each pool.

The screening calculations were performed for the nine combinations of stage height and vessel location for each pool (Tables 9-11). The results demonstrate the increase in possible combinations of vessel type and cell number with increasing stage height. Due to constraints imposed by the bathymetry data on some of the pool cross sections, it was not possible to run all the vessel types using the NAVEFF model for all stage heights and sailing lines. Thus, in several instances (i.e., Pool 4, low stage; Pool 13, medium stage) the numbers in columns one and two vary in Tables 9-11. However, dividing the number of combinations of cell x vessel in the second column by 108 vessel types approximates the number of cells of 1.5-m depth for each stage height: 596 for low stage, 613 for medium, and 204 for high stage. The corresponding numbers for Pool 13 are 2,017 for low, 2,088 for medium, and 2,131 for the high stage height.

Table 9
Summary of Screening Assessment for Plant Breakage in Pool 4[1]

Stage/ Sailing Line	Number of Combinations Cells x Vessels	Number in Cells <1.5 m Deep	Number That Failed the Screen
Low Stage			
Left	1,193,134	64,012	342 (0.53)
Center	1,202,082	64,376	188 (0.29)
Right	1,195,641	64,064	224 (0.35)
Medium Stage			
Left	1,377,865	66,204	596 (0.90)
Center	1,377,865	66,204	340 (0.51)
Right	1,377,865	66,204	376 (0.57)
High Stage			
Left	1,440,613	22,032	304 (1.38)
Center	1,440,613	22,032	128 (0.58)
Right	1,440,613	22,032	164 (0.74)

[1] The number in parentheses is the percentage of cells <1.5 m deep that failed the screen.

Table 10
Summary of Screening Assessment for Plant Breakage in Pool 8[1]

Stage/ Sailing Line	Number of Combinations Cells x Vessels	Number in Cells <1.5 m Deep	Number That Failed the Screen
Low Stage			
Left	1,053,973	278,964	2,412 (0.86)
Center	1,053,973	278,964	1,500 (0.54)
Right	1,053,973	278,964	2,046 (0.73)
Medium Stage			
Left	1,070,821	381,024	3,372 (0.88)
Center	1,070,821	381,024	2,304 (0.60)
Right	1,070,821	381,024	2,772 (0.73)
High Stage			
Left	1,141,777	309,744	2,352 (0.76)
Center	1,141,777	309,744	1,338 (0.43)
Right	1,141,777	309,744	2,304 (0.74)

[1] The number in parentheses is the percentage of cells <1.5 m deep that failed the screen

Table 11
Summary of Screening Assessment for Plant Breakage in Pool 13[1]

Stage/ Sailing Line	Number of Combinations Cells x Vessels	Number in Cells <1.5 m Deep	Number That Failed the Screen
Low Stage			
Left	559,873	217,836	872 (0.400)
Center	559,873	217,836	528 (0.242)
Right	559,873	217,836	748 (0.343)
Medium Stage			
Left	625,321	225,504	808 (0.358)
Center	625,321	225,504	536 (0.238)
Right	609,661	212,328	760 (0.358)
High Stage			
Left	757,837	230,148	980 (0.426)
Center	757,837	230,148	524 (0.228)
Right	757,837	230,148	760 (0.330)

[1] The number in parentheses is the percentage of cells <1.5 m deep that failed the screen.

Of the possible number of cell x vessel combinations in Pools 4, 8, and 13, the numbers and percentages of combinations that failed either the current velocity or the wave height screening criteria were small. Less than 1.5% of the 1.5-m depth combinations failed the screen (Pool 4, high stage, left sailing line) for all combinations of stage height, vessel type, and sailing location across the three pools. For each pool, the greatest impacts resulted for vessels located at the left edge of the navigation channel, independent of pool stage height. In general, vessels operate in this portion of the navigation channel approximately 5% of the time.

The specific combinations of vessel type, sailing line, and stage height that failed the screening process could become the focus of a more detailed assessment. The cell identification number, the vessel type, and the NAVEFF model results (current velocity, wave height) for this screening exercise were recorded and saved as computer files. Analysis of these screening results indicated that the criterion that consistently failed the screening was wave height (>95% of all screening failures). The screening criterion was a wave height of 0.2 m; of the thousands of screening failures (Tables 9-11), the wave heights produced by the NAVEFF model calculations were less than 0.3 m. Thus, the wave height screening value was violated usually by small amounts. In more detailed assessments, the uncertainties associated with both the NAVEFF model computations and the screening criterion of 0.2 m should be examined to determine the probability that physical damage would be expected.

Decreased Growth and Vegetative Reproduction of Submerged Aquatic Plants

The impacts of traffic-induced sediment resuspension on plant growth and reproduction were assessed for one example cell selected from Pool 4 (115L7560), Pool 8 (145L6875), and Pool 13 (85L5300). The Pool 4 example location is 115 m left of the main sailing line at River Mile 756.0; the Pool 8 location is 145 m left of the sailing line at River Mile 687.5; and the Pool 13 cell is 85 m left of the sailing line at River Mile 530.0. Each cell is approximately 0.81 km (i.e., 0.5 mile) in length by 10 m wide and was selected because it was one that failed the physical screening for one or more vessel types, and the cell depth was ~1.5 m at high pool stage.

Light extinction coefficients

Time series of daily suspended sediment concentrations (mg/L) were constructed for each month in the May through September growing season for the 1992 baseline and the percentage increase in traffic scenarios. These concentrations were used to estimate daily values of light extinction coefficients. The suspended sediment concentrations were first converted to estimates of Secchi depth (m) using the regression equations for Pools 4, 8, and 13 (Table 4). The Secchi depths were then transformed to light extinction coefficients using the Giesen et al. (1990) equation (Figure 3). The monthly average values of the extinction coefficients are summarized for the selected cells in Tables 12-14.

The values estimated for suspended sediments associated with the 1992 baseline traffic data resulted in monthly average extinction coefficients that ranged from 3.08 to 4.24 m^{-1} in Pool 4 (2.62 to 3.00 m^{-1}); 2.96 to 4.59 m^{-1} in Pool 8 (3.30 to 3.84 m^{-1}), and 2.96 to 3.42 m^{-1} in Pool 13 (4.23 to 4.58 m^{-1}). The values in parentheses for each pool are estimated using the average monthly ambient suspended sediment concentrations (Table 5). Differences between the extinction values based on simulated 1992 traffic (Tables 12-14) and the coefficients reported in Table 5 result largely from different ambient suspended sediment concentrations reported for the particular cell within each pool in comparison to the reported monthly average value. The greatest difference was for the selected cell from Pool 13, which had an associated ambient suspended sediment concentration of 0.2 mg/L compared with values of 46-76 mg/L reported in Table 5.

Table 12
Summary of Pool 4 Monthly Average Light Extinction Coefficients (m^{-1}) Calculated for Different Traffic Increase Scenarios[1]

	Traffic Scenario				
	1992	**25%**	**50%**	**75%**	**100%**
May					
Mean	3.08	3.36	3.45	3.51	3.69
% Increase		8.98	11.93	14.03	19.64
June					
Mean	4.24	4.29	4.45	4.48	4.59
% Increase		1.40	4.93	5.73	8.39
July					
Mean	4.20	4.36	4.55	4.54	4.63
% Increase		3.75	8.37	8.15	10.40
August					
Mean	4.04	4.22	4.16	4.34	4.47
% Increase		4.49	3.05	7.56	10.72
September					
Mean	3.55	4.11	4.09	4.38	4.26
% Increase		15.76	15.09	23.12	19.86

[1] Percentage increases in average extinction coefficients compared to the 1992 reference values are also presented.

Table 13
Summary of Pool 8 Monthly Average Light Extinction Coefficients (m^{-1}) Calculated for Different Traffic Increase Scenarios[1]

	Traffic Scenario				
	1992	**25%**	**50%**	**75%**	**100%**
May					
Mean	2.96	3.16	3.49	3.59	3.87
% Increase		6.56	17.98	21.39	30.81
June					
Mean	4.59	4.78	4.96	5.12	5.36
% Increase		4.03	7.91	11.33	16.62
July					
Mean	4.43	4.67	4.79	4.98	5.11
% Increase		5.51	8.30	12.55	15.44
August					
Mean	3.71	3.90	4.22	4.48	4.49
% Increase		5.08	13.78	20.82	21.16
September					
Mean	3.63	3.93	4.00	4.17	4.38
% Increase		8.26	10.04	14.70	20.72

[1] Percentage increases in average extinction coefficients compared to the 1992 reference values are also presented.

Table 14
Summary of Pool 13 Monthly Average Light Extinction Coefficients (m^{-1}) Calculated for Different Traffic Increase Scenarios[1]

	Traffic Scenario				
	1992	**25%**	**50%**	**75%**	**100%**
May					
Mean	2.96	3.17	3.23	3.87	3.39
% Increase		6.82	9.00	30.66	14.43
June					
Mean	3.31	3.57	3.83	4.08	4.24
% Increase		7.64	15.57	22.85	27.85
July					
Mean	3.38	3.59	3.77	4.14	4.28
% Increase		6.07	11.26	22.47	26.58
August					
Mean	3.42	3.40	4.02	3.82	4.10
% Increase		-0.54	17.60	11.66	19.92
September					
Mean	3.14	3.36	3.56	3.76	3.93
% Increase		6.96	13.20	19.77	25.03

[1] Percentage increases in average extinction coefficients compared to the 1992 reference values are also presented.

The increases in monthly light extinction coefficients across traffic scenarios demonstrate that a proportional increase in traffic intensity does not translate simply to the same proportional increase in light extinction. The light extinction coefficient is an exponent, so a small increase in it actually means an exponentially greater decrease in light availability. A 100% increase in traffic intensity produced, at most, a 28% increase in the average extinction coefficient (i.e., Pool 13, June). The results also reflect the monthly varying values of baseline traffic intensity and ambient suspended sediment concentrations. In Pool 4, the greatest relative increase in light extinction occurred for the months of May and September. In Pool 8, the greatest relative increase in light extinction occurred for the months of May and August. The greatest percentage increase in light extinction occurred for the months of June and July in Pool 13; these month-to-month differences were greater compared to Pools 4 and 8.

Within each month, the relative increase in light extinction coefficients with increasing traffic intensity is approximately linear for these pools (Tables 12-14). However, the variation introduced by the random selection of interarrival times and vessel types resulted in extinction values that are not simple multiples for successive scenarios of percentage increases in navigation traffic.

The results of increased traffic on suspended sediments produced increases in light extinction coefficients on the order of 1 to 28%, depending on the combination of month, pool, and traffic scenario (e.g., Tables 12-14). However, the value of the light extinction coefficient is an exponent in the equation which describes light attenuation within the water column in the plant growth models. Therefore, the impacts of these small increases in light extinction coefficients can be magnified when used in the plant models to examine the implications of increases in suspended sediments on growth and reproduction for wild celery (i.e., VALLA) and sago pondweed (i.e., POTAM).

Plant growth and biomass

The plant growth models for wild celery and sago pondweed were implemented for the selected locations (GIS cells) in Pools 4, 8, and 13. The time series of daily light extinction coefficients developed for each location and traffic scenario replaced the nominal values for the model days that correspond to the May through September growing season. For each representative plant species, simulations were performed for the four percentage traffic increase scenarios in addition to the 1992 baseline. The simulated values of total plant biomass, plant living biomass, tuber numbers (number/m^2), and tuber biomass (g dry mass/m^2) were summarized for the traffic scenarios.

Figures 23 through 25 illustrate the temporal growth dynamics of wild celery in Pools 4, 8, and 13 for the baseline and percentage increase traffic scenarios. The results of tow-induced increased suspended sediments and corresponding reductions in light availability have demonstrated impacts on plant growth for the selected cells in these pools. The severity of the modeled impacts was greatest in Pool 13, followed by Pool 4. Minimal impacts on wild celery were

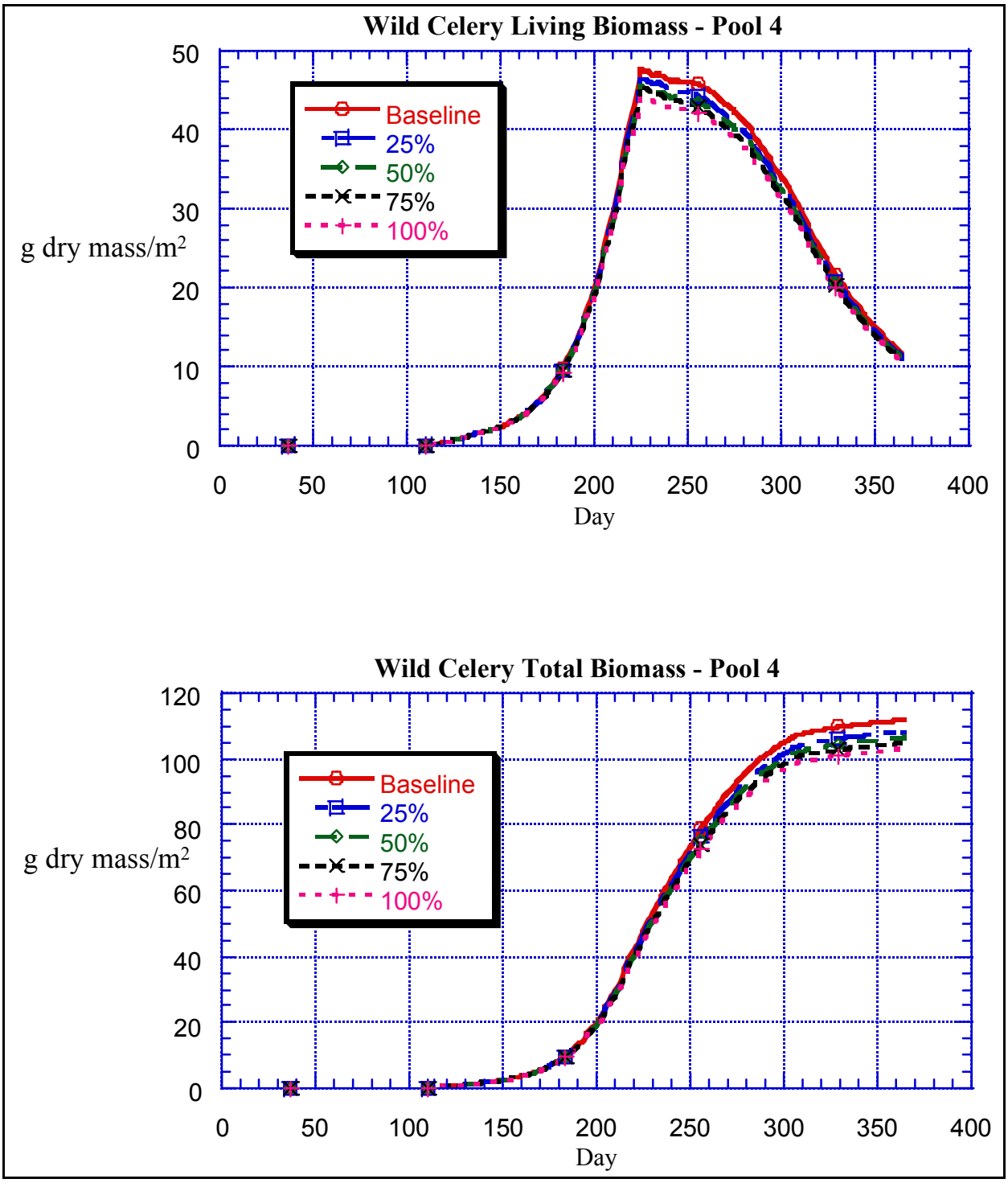

Figure 23. The growth (living biomass and total biomass) of wild celery in UMR Pool 4 for the baseline and percentage increase traffic scenarios. Climatological data pertaining to St. Paul, Minnesota, 10-year average (1985-1994) were used, water depth is 1.5 m, and Day 1 = January 1

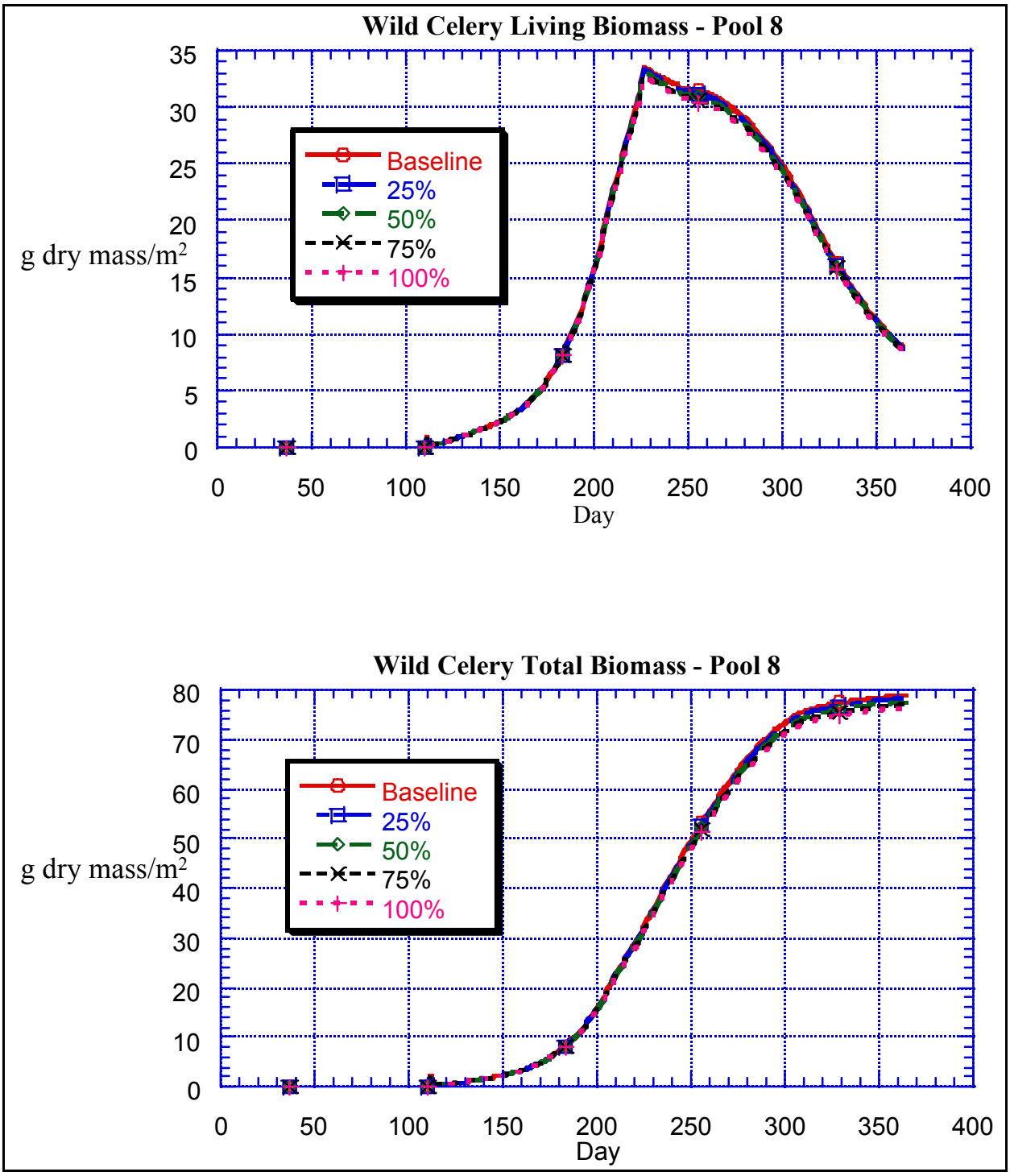

Figure 24. The growth (living biomass and total biomass) of wild celery in UMR Pool 8 for the baseline and percentage increase traffic scenarios. Climatological data pertaining to La Crosse, Wisconsin, 30-year average (1961-1990) were used, water depth is 1.5 m, and Day 1 = January 1

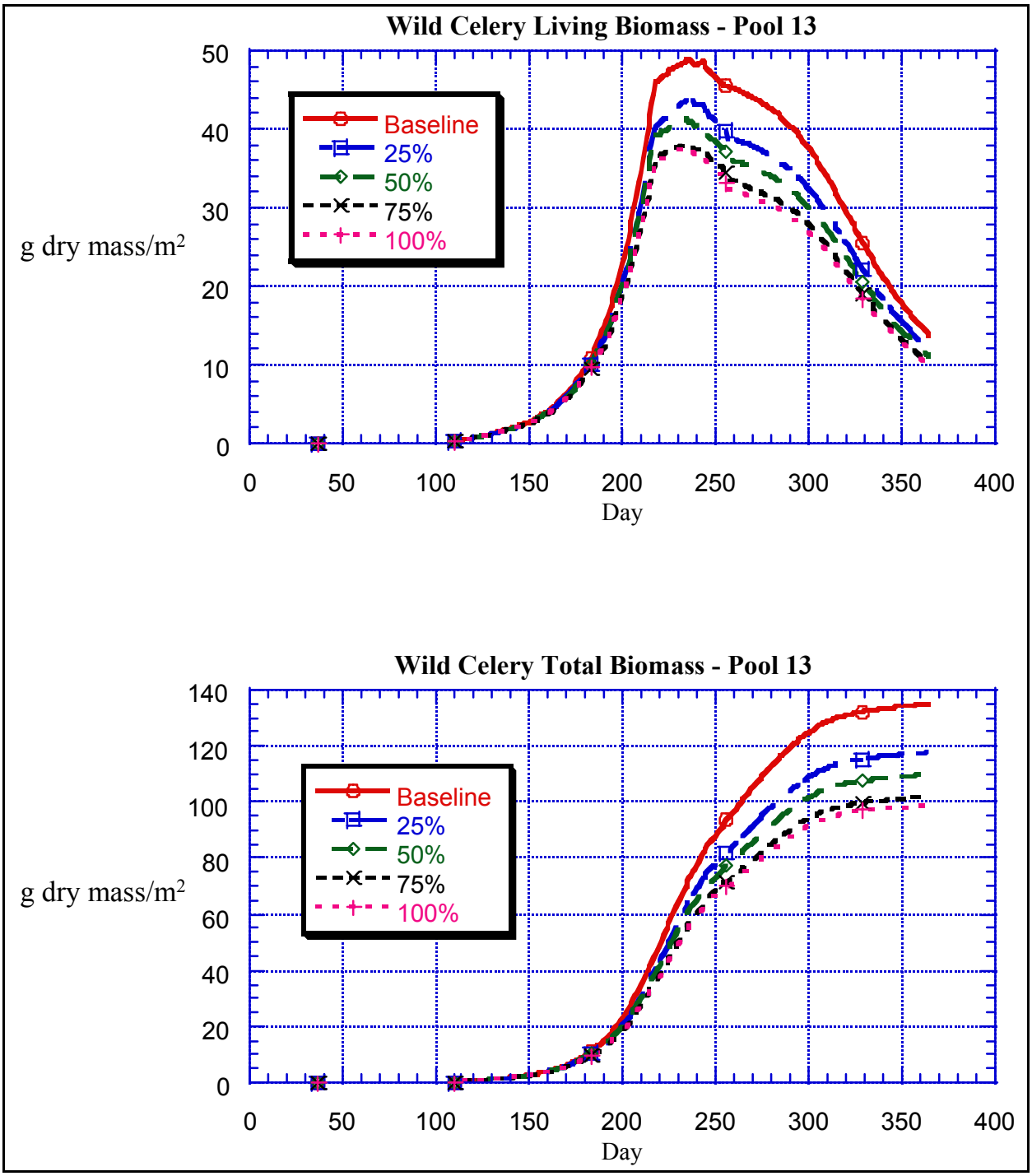

Figure 25. The growth (living biomass and total biomass) of wild celery in UMR Pool 13 for the baseline and percentage increase traffic scenarios. Climatological data pertaining to Moline, Illinois, 30-year average (1961-1990) were used, water depth is 1.5 m, and Day 1 = January 1

projected in Pool 8. The traffic-induced sediment resuspension appeared to exert its main impact during the latter part of the plant growth cycle (e.g., Figure 25).

The model results for total wild celery plant biomass (living + non-living) were summarized for the annual sum of daily values, the average daily value, and the maximum daily value (Table 15). Total annual plant biomass decreased by as much as 27% for a 100% traffic increase in Pool 13. Across the assessed scenarios, impacts ranged from 12-27% in Pool 13. Contrastingly, in Pools 4 and 8, the simulated traffic increases had less impact. Decreases in total plant biomass values ranged from approximately 1-8% compared to the 1992 baseline for Pools 4 and 8. The results indicated that a 25% increase in traffic did not translate into a corresponding 25% reduction in total biomass. However, the incremental decreases in total biomass were approximately linearly related to the increase in traffic; the incremental percentage decrease in biomass was nearly constant for each biomass measure with each 25% increase in traffic intensity (Table 15).

Table 15
Impacts on Total (Living + Dead) Biomass (g dry mass/m^2) of Wild Celery for the Percentage Increase Traffic Scenarios for the UMR-IWW System[1]

		Percent Traffic Increase			
Pool	Baseline 1992	25	50	75	100
Pool 4					
Annual Sum	14,564	14,126 (-3.0)	13,892 (-4.6)	13,706 (-5.9)	13,470 (-7.5)
Mean Biomass	39.9	38.7 (-3.0)	38.1 (-4.5)	37.6 (-5.8)	36.9 (-7.5)
Maximum Biomass	111.8	108.2 (-3.2)	106.5 (-4.7)	104.8 (-6.3)	103.1 (-7.8)
Pool 8					
Annual Sum	10,208	10,135 (-0.7)	10,039 (-1.7)	9,971 (-2.3)	9,907 (-2.9)
Mean Biomass	39.4	39.1 (-0.8)	38.8 (-1.5)	38.5 (-2.3)	38.3 (-2.8)
Maximum Biomass	79.0	78.3 (-0.9)	77.6 (-1.8)	77.0 (-2.5)	76.5 (-3.2)
Pool 13					
Annual Sum	17,371	15,228 (-12.3)	14,304 (-17.7)	13,263 (-23.6)	12,944 (-25.5)
Mean Biomass	47.6	41.7 (-12.3)	39.2 (-17.6)	36.3 (-23.7)	35.5 (-25.4)
Maximum Biomass	134.9	117.7 (-12.7)	109.8 (-18.6)	101.8 (-24.5)	98.9 (-26.7)

Values in parentheses are percent changes in production referenced to the 1992 baseline impacts.

Table 16 summarizes the corresponding projected traffic impacts on plant annual gross production, as well as on the mean and maximum values of daily plant living biomass for wild celery. The pattern of traffic impacts on gross production and living biomass essentially parallels the impacts recorded for total plant biomass. Percentage differences compared to the 1992 baseline scenario are of similar magnitude as the response of total biomass (i.e., Table 15). Again, the largest impacts were observed for the cell selected from Pool 13, and growth was reduced by ~10 to ~27% across the four increased traffic scenarios. Successively lesser impacts resulted for the simulations of traffic increases in Pools 4 and 8. Growth reductions were on the order of 0-4% in Pool 8, while corresponding impacts in Pool 4 ranged from ~3 to ~9% compared to the 1992 baseline simulations.

Table 16
Impacts on Annual Gross Production (g CO_2/m^2) and Living Biomass (g dry mass/m^2) of Wild Celery for the Percentage Increase Traffic Scenarios for the UMR-IWW System[1]

		Percent Traffic Increase			
Pool	Baseline 1992	25	50	75	100
Pool 4					
Gross Production	285.6	275.8 (-3.4)	271.3 (-5.0)	265.4 (-7.1)	260.5 (-8.8)
Mean Biomass	22.7	22.0 (-3.1)	21.7 (-4.4)	21.4 (-5.7)	21.0 (-7.5)
Maximum Biomass	47.6	46.4 (-2.5)	45.5 (-4.4)	45.4 (-4.6)	44.3 (-6.9)
Pool 8					
Gross Production	199.4	197.5 (-1.0)	195.3 (-2.1)	193.6 (-2.9)	192.0 (-3.7)
Mean Biomass	16.5	16.3 (-1.2)	16.2 (-1.8)	16.1 (-2.4)	16.0 (-3.0)
Maximum Biomass	33.5	33.4 (-0.3)	33.1 (-1.2)	32.8 (-2.1)	32.7 (-2.4)
Pool 13					
Gross Production	316.0	278.6 (-11.8)	257.6 (-18.5)	238.2 (-24.6)	230.4 (-27.0)
Mean Biomass	24.3	21.3 (-12.3)	20.1 (-17.3)	18.6 (-23.4)	18.2 (-25.1)
Maximum Biomass	49.1	44.2 (-10.0)	41.4 (-15.7)	38.0 (-22.6)	37.6 (-23.4)

[1] Values in parentheses are percent changes in production referenced to the 1992 baseline impacts.

The dynamics of sago pondweed living biomass and total biomass in Pools 4, 8, and 13 for the baseline and percentage increases in traffic are presented in Figures 26 through 28. The results indicate minimal impact of traffic on growth of sago pondweed in Pool 4 (Figure 26) and Pool 8 (Figure 27). However, modeled impacts on growth of this species were apparent for Pool 13 (Figure 28). The daily measures of total biomass (i.e., annual sum, average, maximum) demonstrated greater baseline production of sago pondweed compared to wild celery for Pools 4, 8, and 13 (Tables 15 and 17). As with wild celery, the largest impacts on sago pondweed from traffic increases were observed for Pool 13. However, the impact on sago pondweed growth was comparatively less than that for wild celery. The measures of sago pondweed total biomass were reduced from approximately 4-9% in Pool 13, compared with the 10-27% reductions simulated for wild celery in Pool 13. Modeled decreases in total sago pondweed biomass for Pools 4 and 8 were less than 3% of the 1992 baseline values across all four increases in traffic.

The impacts of simulated traffic increases on gross production and living biomass for sago pondweed are summarized in Table 18. The percentage changes in production and living biomass are approximately the same as those observed for total biomass. The greatest impacts occurred for Pool 13, with correspondingly lesser impacts in Pools 4 and 8, respectively. For all three measures summarized in Table 18 for all four traffic increase scenarios, the modeled impacts were less than 10% of the 1992 baseline values for production and living biomass.

Vegetative reproduction

The number and biomass of vegetative reproductive structures produced by the plant growth models during the growing season provides an indication of the potential impact of increased traffic on the availability of these structures to initiate plant growth in the subsequent year. Continued, significant reductions in the production of these vegetative reproductive structures might portend the disappearance of plant beds at affected locations within the UMR.

Under baseline conditions, the average number and biomass of tubers by wild celery was greatest in Pool 4, followed in order by Pools 8 and 13 (Table 19). The modeled impacts of increased traffic on the allocation of photosynthetically fixed carbon to these reproductive structures were minimal. The maximum values of tuber numbers and biomass were unchanged in Pools 8 and 13. Average number and biomass increased slightly with increased traffic in Pool 8 (Table 19). Minimal impacts were simulated in Pools 8 and 13. The greatest impacts were in Pool 4, and the projected decreases were less than 3% for average tuber number and biomass. Reductions in the maximum values of these measures ranged from 2-8% across the traffic scenarios in Pool 4.

The modeled impacts of increased commercial traffic on vegetative reproductive structures produced by sago pondweed are summarized in Table 20. No

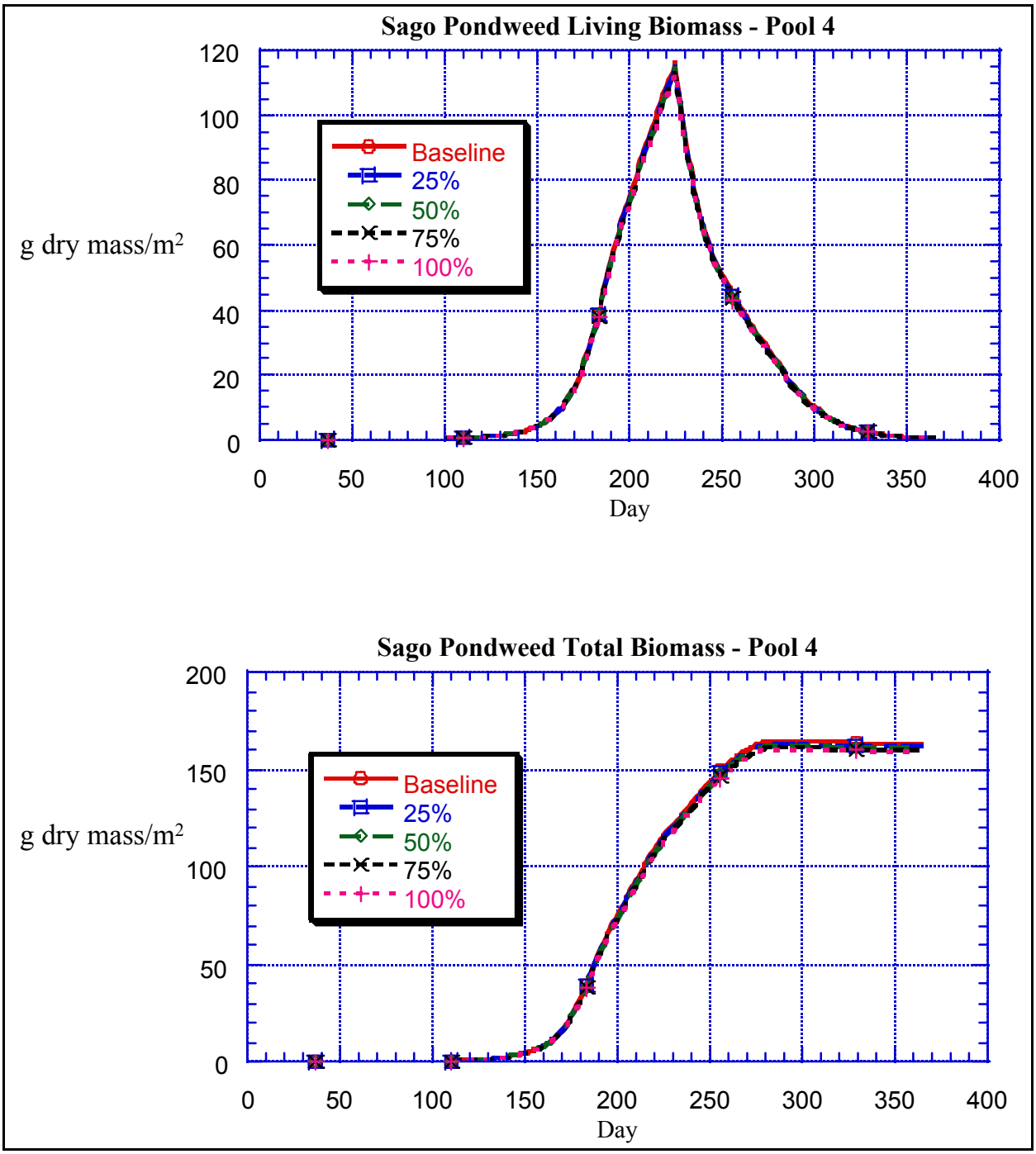

Figure 26. The growth (living biomass and total biomass) of sago pondweed in UMR Pool 4 for the baseline and percentage increase traffic scenarios. Climatological data pertaining to St. Paul, Minnesota, 10-year average (1985-1994) were used, water depth is 1.5 m, and Day 1 = January 1

changes in average or maximum numbers or biomass resulted for sago pondweed in Pool 4. In both Pools 8 and 13, the average number and biomass of

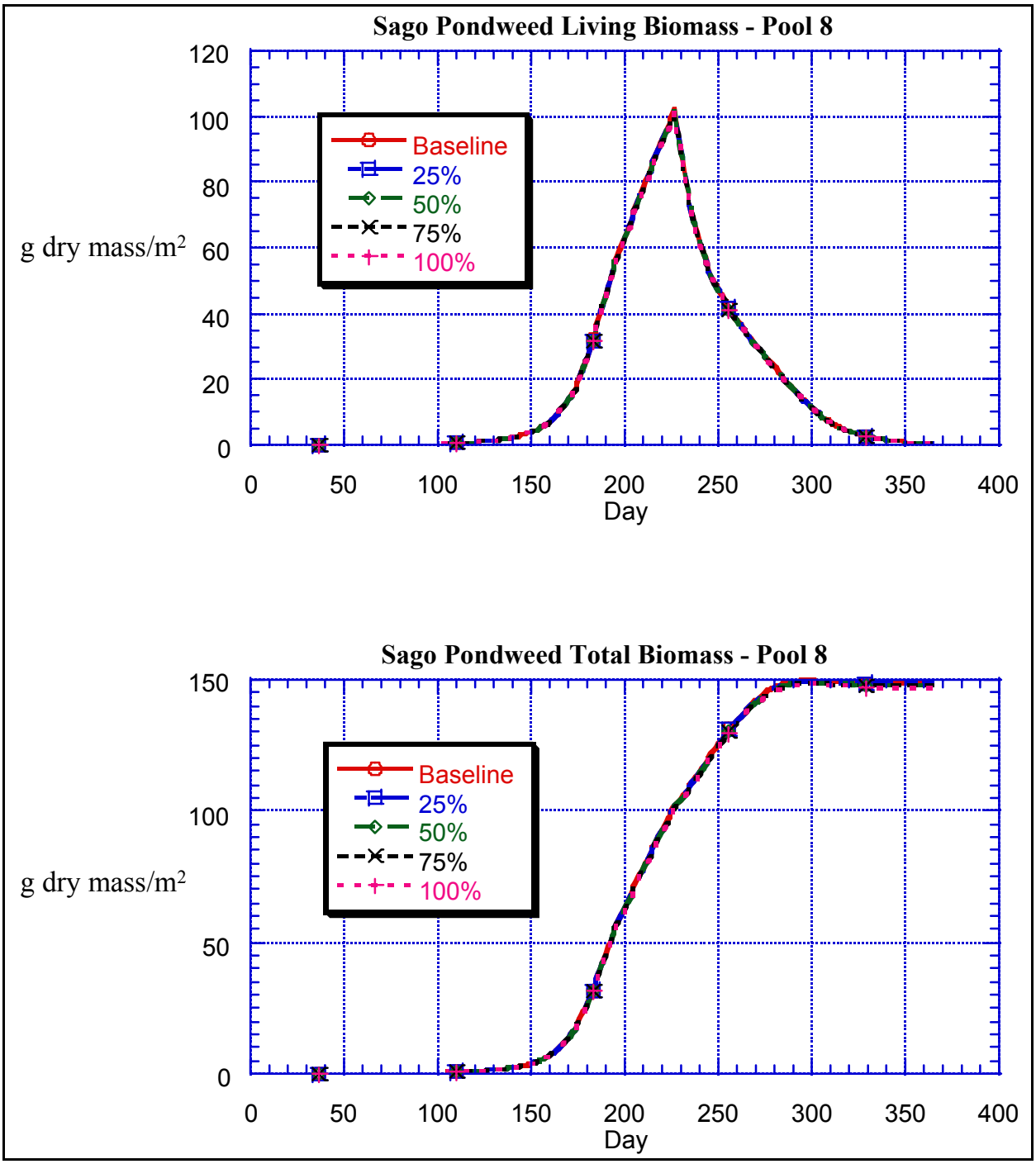

Figure 27. The growth (living biomass and total biomass) of sago pondweed in UMR Pool 8 for the baseline and percentage increase traffic scenarios. Climatological data pertaining to La Crosse, Wisconsin, 30-year average (1961-1990) were used, water depth is 1.5 m, and Day 1 = January 1.

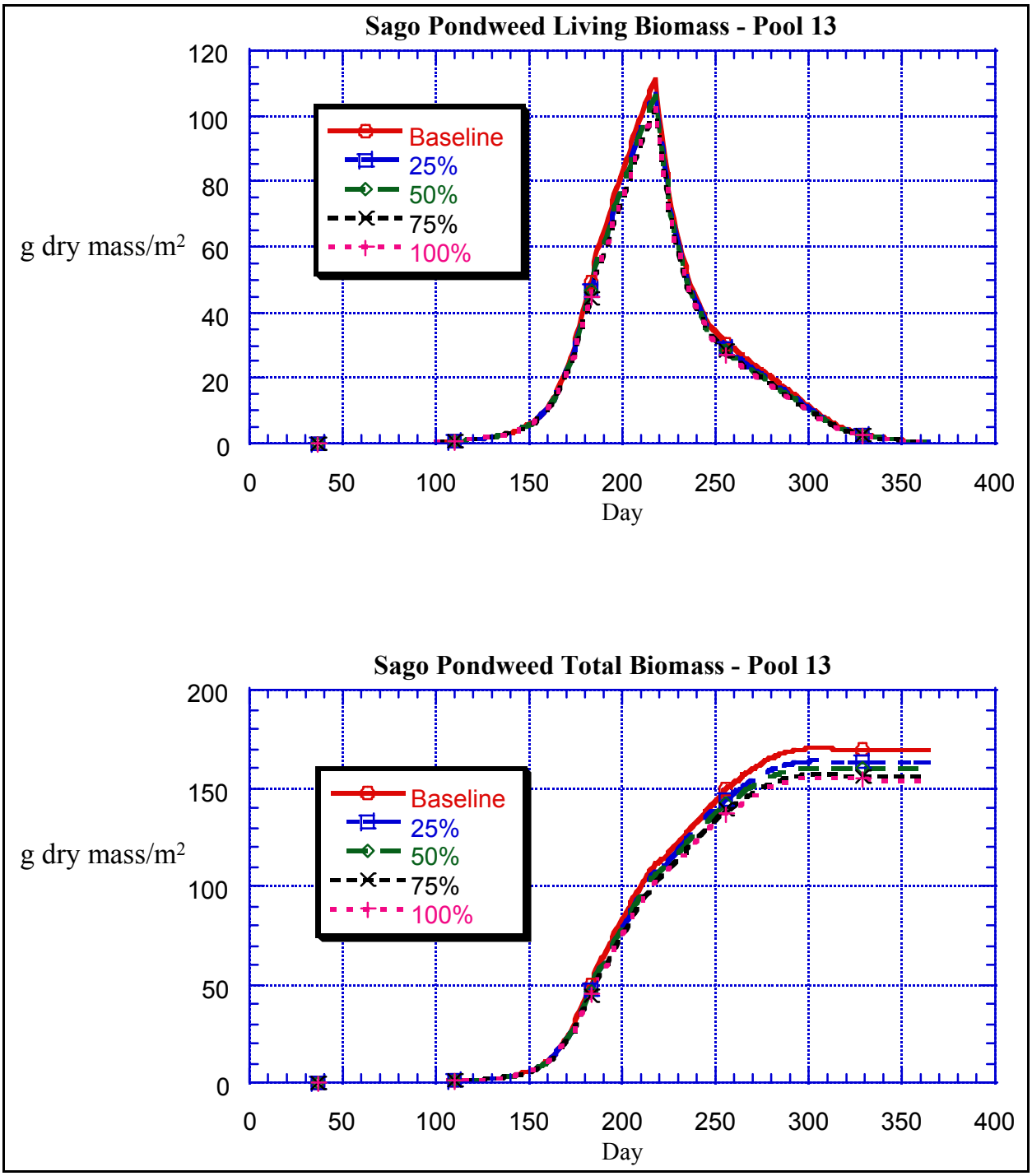

Figure 28. The growth (living biomass and total biomass) of sago pondweed in UMR Pool 13 for the baseline and percentage increase traffic scenarios. Climatological data pertaining to Moline, Illinois, 30-year average (1961-1990) were used, water depth is 1.5 m, and Day 1 = January 1

Table 17
Impacts on Total (Living + Dead) Biomass (g dry mass/m^2) of Sago Pondweed for the Percentage Increase Traffic Scenarios for the UMR-IWW System[1]

		Percent Traffic Increase			
Pool	Baseline 1992	25	50	75	100
Pool 4					
Annual Sum	25,905	25,660 (-0.9)	25,524 (-1.5)	25,378 (-2.0)	25,272 (-2.4)
Mean Biomass	71.0	70.3 (-1.0)	69.9 (-1.5)	69.5 (-2.1)	69.2 (-2.5)
Maximum Biomass	164.6	162.9 (-1.0)	162.3 (-1.4)	161.0 (-2.2)	160.5 (-2.5)
Pool 8					
Annual Sum	23,047	22,992 (-0.2)	22,925 (-0.5)	22,873 (-0.8)	22,820 (-1.0)
Mean Biomass	81.2	80.9 (-0.4)	80.7 (-0.6)	80.5 (-0.9)	80.4 (-1.0)
Maximum Biomass	149.8	149.4 (-0.3)	148.9 (-0.6)	148.6 (-0.8)	148.2 (-1.1)
Pool 13					
Annual Sum	26,910	25,922 (-3.7)	25,464 (-5.4)	24,804 (-7.8)	24,599 (-8.6)
Mean Biomass	73.7	71.0 (-3.7)	69.8 (-5.3)	67.9 (-7.9)	67.4 (-8.5)
Maximum Biomass	170.3	163.9 (-3.8)	160.4 (-5.8)	156.7 (-8.0)	154.9 (-9.0)

[1] Values in parentheses are percent changes in production referenced to the 1992 baseline impacts.

Table 18
Impacts on Annual Gross Production (g CO_2/m^2) and Living Biomass (g dry mass/m^2) of Sago Pondweed for the Percentage Increase Traffic Scenarios for the UMR-IWW System[1]

		Percent Traffic Increase			
Pool	Baseline 1992	25	50	75	100
Pool 4					
Gross Production	483.8	479.3 (-0.9)	476.8 (-1.4)	473.7 (-2.1)	471.4 (-2.6)
Mean Biomass	26.9	26.7 (-0.7)	26.5 (-1.5)	26.4 (-1.9)	26.3 (-2.2)
Maximum Biomass	116.2	115.1 (-0.9)	114.2 (-1.7)	114.2 (-1.7)	113.2 (-2.6)
Pool 8					
Gross Production	426.1	425.0 (-0.3)	423.7 (-0.6)	422.7 (-0.8)	421.5 (-1.1)
Mean Biomass	23.8	23.7 (-0.4)	23.7 (-0.4)	23.6 (-0.8)	23.6 (-0.8)
Maximum Biomass	102.9	102.0 (-0.9)	101.7 (-1.2)	101.4 (-1.5)	101.2 (-1.7)
Pool 13					
Gross Production	518.4	498.5 (-3.8)	488.8 (-5.7)	475.6 (-8.3)	470.7 (-9.2)
Mean Biomass	25.0	24.0 (-4.0)	23.7 (-5.2)	22.9 (-8.4)	22.8 (-8.8)
Maximum Biomass	111.2	107.0 (-3.8)	106.2 (-4.5)	102.6 (-7.7)	102.4 (-7.9)

[1] Values in parentheses are percent changes in production referenced to the 1992 baseline impacts.

Table 19
Impacts on Vegetative Reproduction of Wild Celery (i.e., Tubers) for the Percentage Increase Traffic Scenarios for the UMR-IWW System[1]

		Percent Traffic Increase			
Pool	Baseline 1992	25	50	75	100
Pool 4					
Average Number/m^2	129.2	128.9 (-0.2)	128.8 (-0.3)	127.7 (-1.2)	125.8 (-2.6)
Maximum Number/m^2	253.5	247.6 (-2.3)	246.6 (-2.7)	241.1 (-4.9)	234.6 (-7.5)
Average Biomass/m^2	11.5	11.5	11.5	11.4 (-0.9)	11.2 (-2.6)
Maximum Biomass/m^2	22.5	22.0 (-2.2)	21.9 (-2.7)	21.5 (-4.4)	21.0 (-6.7)
Pool 8					
Average Number/m^2	99.9	99.9	100.1 (+0.2)	100.1 (+0.2)	100.1 (+0.2)
Maximum Number/m^2	233.0	233.0	233.0	233.0	233.0
Average Biomass/m^2	8.97	8.97	8.98 (+0.1)	8.98 (+0.1)	8.98 (+0.1)
Maximum Biomass/m^2	21.0	21.0	21.0	21.0	21.0
Pool 13					
Average Number/m^2	97.5	97.5	97.3 (-0.2)	96.9 (-0.6)	96.5 (-1.0)
Maximum Number/m^2	233.0	233.0	233.0	233.0	233.0
Average Biomass/m^2	8.73	8.73	8.72 (-0.1)	8.68 (-0.6)	8.64 (-1.0)
Maximum Biomass/m^2	21.0	21.0	21.0	21.0	21.0

[1] Values in parentheses are percent changes in production referenced to the 1992 baseline impacts.

Table 20
Impacts on Vegetative Reproduction of Sago Pondweed (i.e., Tubers) for the Percentage Increase Traffic Scenarios for the UMR-IWW System[1]

		Percent Traffic Increase			
Pool	Baseline 1992	25	50	75	100
Pool 4					
Average Number/m^2	112.3	112.3	112.3	112.3	112.3
Maximum Number/m^2	330.1	330.1	330.1	330.1	330.1
Average Biomass/m^2	9.21	9.21	9.21	9.21	9.21
Maximum Biomass/m^2	26.3	26.3	26.3	26.3	26.3
Pool 8					
Average Number/m^2	114.2	114.2	114.5 (+0.3)	114.5 (+0.3)	114.5 (+0.3)
Maximum Number/m^2	319.6	319.6	317.1 (-0.8)	317.1 (-0.8)	317.1 (-0.8)
Average Biomass/m^2	9.39	9.39	9.41 (+0.2)	9.41 (+0.2)	9.41 (+0.2)
Maximum Biomass/m^2	25.7	25.7	25.5 (-0.8)	25.5 (-0.8)	25.5 (-0.8)
Pool 13					
Average Number/m^2	125.6	126.6 (+0.8)	127.9 (+1.8)	128.8 (+2.5)	129.3 (+2.9)
Maximum Number/m^2	349.6	346.6 (-0.9)	333.9 (-4.5)	330.9 (-5.3)	330.9 (-5.3)
Average Biomass/m^2	10.3	10.3	10.5 (+1.9)	10.5 (+1.9)	10.6 (+2.9)
Maximum Biomass/m^2	27.9	27.8 (-0.4)	26.9 (-3.6)	26.6 (-4.7)	26.3 (-5.7)

[1] Values in parentheses are percent changes in production referenced to the 1992 baseline impacts.

sago pondweed tubers increased slightly with increased traffic. However, the corresponding maximum values decreased by as much as 6% for the 100% traffic increase scenario in Pool 13.

Uncertainties

There are several sources of bias and imprecision associated with this initial assessment of commercial traffic on submerged aquatic vegetation in the main channel and main channel borders of the UMR-IWW System. These uncertainties are listed below.

- The physical criteria for plant breakage are based on a small number of experiments and publications. The 0.75-m/s current velocity and the 0.2-m wave heights may be pessimistic.

- The screening for physical damage does not address the potential impacts of continued and repeated exposure to current velocities and wave heights that are near, but fail to exceed, the threshold criteria for damage. It was assumed that each tow passage represents an independent event in relation to possible plant breakage.

- The plant growth models for wild celery and sago pondweed were calibrated using field data from the Netherlands and New York. It is possible that plant populations in the UMR-IWW System differ genetically from the calibration populations and/or possess adaptation mechanisms to other climates unknown to the authors of this report. These differences may cause the UMR-IWW System populations to behave differently than the calibrated model plant populations.

- Concentrations of potentially different suspended sediments were assumed to exert the same reduction in light availability. No distinction was made between suspended sands versus suspended silts in their characteristic effects on underwater light fields. However, the nearshore algorithms for sediment resuspension were developed for the fine, cohesive sediments that are characteristic of the nearshore environment in the UMR-IWW System.

- Risks to plant growth and reproduction were estimated only for one cell of ~1.5-m depth in each of Pools 4, 8, and 13. Variability in sediment resuspension by the same vessel configurations for other cells of similar depth would result in different light extinction coefficients and presumably in different modeled impacts on plant growth and reproduction.

- It was assumed that the simulated impacts on sago pondweed and wild celery growth and reproduction are characteristic responses for other submerged aquatic plant species with similar phenology, biomass, and water column distribution in the UMR-IWW System.

- The current versions of the models do not calculate seed production and plant establishment from seeds. Recent literature on submerged aquatic plant population survival under adverse conditions indicates that seeds may play an important role.

Future revisions of the described assessment approaches will address these (and others yet to be identified) sources of bias and imprecision. Where possible, the impact of the specific sources of uncertainty on the estimated risks to plant breakage, growth, and reproduction will be quantified using methods of sensitivity and uncertainty analysis.

Probabilistic Risk Assessment

The main purposes of this preliminary assessment of hypothetical traffic scenarios were to (1) examine the efficacy of the overall approach and determine the feasibility of ecological risk assessment using the methods and models described, and if the methodology appears feasible, (2) to estimate the magnitude of impact of increased traffic on two plant species for selected locations with Pools 4, 8, and 13. The risk assessment described in this report represents a preliminary analysis where risks were characterized as single-value estimates or percentage changes in plant growth and vegetative reproduction. These analyses might be expanded in spatial extent by assessing more cells per pool to identify specific locations or areas within pools that might be at risk.

The next phase in assessing traffic impacts on submerged aquatic plants will be to incorporate the current methodology into a framework that characterizes risk in probabilistic terms. More detailed, probabilistic assessments will be performed for selected locations and traffic scenarios identified by the preliminary analyses. Parameters used in the calculations (e.g., suspended sediment concentrations produced by the NAVSED model, light extinction coefficients based on the regressions equations developed by Soballe, plant growth model coefficients) that are imprecisely known will be defined as statistical distributions. Monte Carlo simulation methods will be used to propagate these uncertainties through the model calculations to produce distributions of impacts on growth and vegetative reproduction in relation to specific traffic scenarios. These distributions of results can be used to estimate the probability of different magnitudes of impact in a manner consistent with probabilistic risk estimation.

References

Bartell, S. M. (1996). "Ecological/environmental risk assessment: principles and practices," *in* Kolluru, R. V., Bartell, S. M., Pitblado, R. M., Stricoff, R. S., Editors, *Risk Assessment and Management Handbook*. McGraw-Hill, Inc., New York, NY, 10.3-10.59.

Best, E. P. H. (1981). "A preliminary model for growth of *Ceratophyllum demersum* L.," *Verhandlungen Internationale Vereinigung Fuer Theoretische Und Angewandte Limnologie* 21, 1484-1491.

Best, E. P. H. (1987). "Characteristic photosynthesis and respiration rates under laboratory conditions, and in situ biomass production of *Elodea nuttallii* and *Potamogeton pectinatus* (Unpublished)," Centre for Agrobiological Research, Wageningen, The Netherlands.

Best, E. P. H., and Boyd, W. A. (1996). "A simulation model for growth of the submersed aquatic macrophyte hydrilla (*Hydrilla verticillata* (L.F.) Royle," Technical Report A-96-8, U.S. Army Engineer Waterways Experiment Station, Vicksburg, MS. 43 p. + app.

Best, E. P. H., and Boyd, W. A. (2000a). "A simulation model for growth of the submersed aquatic macrophyte Sago pondweed (*Potamogeton pectinatus* L.) (In review)," ERDC/EL TR-00-X, U.S. Army Engineer Research and Development Center, Vicksburg, MS.

Best, E. P. H., and Boyd, W. A. (2000b). "POTAM (Version 1.0): A simulation model for growth of Sago pondweed (In review)," ERDC/EL TR-00-X, U.S. Army Engineer Research and Development Center, Vicksburg, MS.

Best, E. P. H., and Boyd, W. A. (2000c). "A simulation model for growth of the submersed aquatic macrophyte wild celery (*Vallisneria americana* Michx.) (In press)," ERDC/EL TR-00-X, U.S. Army Engineer Research and Development Center, Vicksburg, MS.

Best, E. P. H., and Boyd, W. A. (2000d). "VALLA (Version 1.0): A simulation model for growth of wild celery (In press)," ERDC/EL TR-00-X, U.S. Army Engineer Research and Development Center, Vicksburg, MS.

Best, E. P. H., and Jacobs, F. H. H. (1990). "Potential and actual production of submerged aquatic angiosperms common in temperate regions," *Proceedings EWRS 8th Symposium on Aquatic Weeds*, Upsala, Sweden, 39-47.

Bick, H., and Van Schaik, A. W. J. (1980). "Oecologische visie randmeren," Advies van de Natuurwetenschappelijke Commissie van de Natuurbeschermingsraad, 291 p. (In Dutch).

Biggs, B. J. F. (1996). "Hydraulic habitat of plants in streams," *Regulated Rivers: Research and Management* 12, 131-144.

Bowes, G., Van, T. K., Garrard, L. A., and Haller, W. T. (1977). "Adaptation to low light levels by Hydrilla," *Journal of Aquatic Plant Management* 15, 32-35.

Boyd, W. A., and Best, E. P. H. (1996). "HYDRIL (Version 1.0): A simulation model for growth of Hydrilla," Instruction Report A-96-1, U.S. Army Engineer Waterways Experiment Station, Vicksburg, MS, 30 p.

Chambers, P. A., Prepas, E. E., Hamilton, H. R., and Bothwell, M. L. (1991). "Current velocity and its effect on aquatic macrophytes in flowing waters," *Ecological Applications* 1, 249-257.

Collins, C. D., Park, R. A., and Boylen, C. W. (1985). "A mathematical model of submersed aquatic plants," Miscellaneous Paper A-85-2, U.S. Army Engineer Waterways Experiment Station, Vicksburg, MS.

Collins, C. D., and Wlosinski, J. (1989). "A macrophyte submodel for aquatic ecosystems," *Aquatic Botany* 33,191-206.

Coops, H., and Van der Velde, G. (1996). "Effects of waves on helophyte stands: mechanical characteristics of stems of *Phragmites australis* and *Scirpus lacustris,*" *Aquatic Botany* 53, 175-185.

Copeland, R. R., Abraham, D. D., Nail, G. H., Seal, R., and Brown, G. L. (1999). "Sedimentation study, numerical model investigation (Draft)," ENV Report 25, U.S. Army Engineer Waterways Experiment Station, Vicksburg, MS.

Dirksen, S. (1982). "The importance of pondweed for Bewicks swans in the Lauwersmeer," *Limosa* 55, 30-31 (In Dutch).

Donnermeyer, G. N., and Smart, M. M. (1985). "The biomass and nutritive potential of *Vallisneria americana* Michx. in Navigation Pool 9 of the Upper Mississippi River," *Aquatic Botany* 22, 33-44.

Doyle, R. D. (1999). "Effects of waves on the early growth of *Vallisneria americana*," ENV Report 12, U.S. Army Engineer Waterways Experiment Station, Vicksburg, MS.

Fremling, C. R., and Claflin, T. O. (1984). "Ecological history of the Upper Mississippi River," *in* Wiener, J. G., Anderson, R. V., and McConville, D. R., Editors, *Contaminants in the Upper Mississippi River*. Butterworth Publishers, Boston, MA.

Giesen, W. B. J. T., van Katwijk, M. M., and den Hartog, C. (1990). "Eelgrass condition and turbidity in the Dutch Wadden Sea," *Aquatic Botany* 37, 71-85.

Golterman, H. L. (1975). *Physiological Limnology. An Approach to the Physiology of Lake Ecosystems*. Elsevier Scientific Publishing Company, Amsterdam, 489 p.

Goudriaan, J. (1986). "A simple and fast numerical method for the computation of daily totals of crop photosynthesis," *Agricultural and Forestry Meteorology* 38, 251-255.

Griffin, K. L. (1994). "Caloric estimates of construction cost and their use in ecological studies," *Functional Ecology* 8, 551-562.

Haller, W. T. (1974). "Photosynthetic characteristics of the submersed aquatic plants Hydrilla, southern naiad, and Vallisneria," Ph.D. Thesis, University of Florida, Gainesville, FL. 88 p.

Holland, L. E. (1986). "Effects of barge traffic on distribution and survival of ichthyoplankton and small fishes in the Upper Mississippi River," *Transactions of the American Fisheries Society* 115, 162-165.

Holland-Bartels, L. E., Dewey, M. R., and Zigler, S. J. (1990a). "Pilot study of spatial patterns of ichthyoplankton among river reaches and habitats of the Upper Mississippi River System," U.S. Fish and Wildlife Service, La Crosse, WI.

Holland-Bartels, L. E., Littlejohn, S. K., and Huston, M. L. (1990b). *A Guide to Larval Fishes of the Upper Mississippi River*. U.S. Fish and Wildlife Service, LaCrosse, WI.

Hootsmans, M. J. M. (1991). "A growth analysis model for *Potamogeton pectinatus* L.," *in* Hootsmans, M. J. M., and Vermaat, J. E., Editors, *Macrophytes, A Key to Understanding Changes Caused by Eutrophication in Shallow Freshwater Ecosystems*. International Institute for Hydraulic and Environmental Engineering, The Netherlands, 263-310.

Hunt, R. (1982). *Plant Growth Curves*, Arnold, London.

Ikusima, I. (1970). "Ecological studies on the productivity of aquatic plant communities IV. Light condition and community photosynthetic production," *Botanical Magazine (Tokyo)* 83, 330-341.

Knight, S. E. (1992). "Cost of carnivory in the common bladderwort, *Utricularia macrorhiza*," *Oecologia* 89, 348-355.

Korschgen, C. E., George, L. S., and Green, W. L. (1988). "Feeding ecology of canvasbacks staging on Pool 7 of the Upper Mississippi River," *in* Weiler, M. W., Editor, *Waterfowl in Winter*, University of Minnesota Press, Minneapolis, MN, 237-249.

Korschgen, C. E., and Green, W. L. (1988). "American wild celery (*Vallisneria americana*): ecological considerations for restoration," Fish and Wildlife Technical Report 19, Washington, D.C., U.S. Department of the Interior, Fish and Wildlife Service.

Korschgen, C. E., Green, W. L., and Kenow, K. P. (1997). "Effects of irradiance on growth and winter bud production by *Vallisneria americana* and consequences to its abundance and distribution," *Aquatic Botany* 58, 1-9.

Laing, W. A., and Browse, J. (1985). "A dynamic model for photosynthesis by an aquatic plant, *Egeria densa*," *Plant, Cell and Environment* 8, 639-649.

Lips, F. (1985). "An investigation of growth of the aquatic macrophyte *Hydrilla verticillata* Royle under various environmental conditions," *Report Limnological Institute Nieuwersluis/Oosterzee* 1985(23), 81 p. (In Dutch).

Madsen, J. D., and Adams, M. S. (1989). "The light and temperature dependence of photosynthesis and respiration in *Potamogeton pectinatus* L.," *Aquatic Botany* 36, 23-31.

Maynord, S. (1999). "Comparison of NAVEFF model to field return velocity and drawdown data," ENV Report 14, U.S. Army Engineer Waterways Experiment Station, Vicksburg, MS.

Ondok, J. P., and Gloser, J. (1978). "Modelling of photosynthetic production in littoral helophyte stands," *in* Dykyjova, D. and Kvet, J., Editors, *Plant Photosynthetic Production. Manual of Methods*. W. Junk, The Hague, 1-48.

Ondok, J. P., Pokorny, J., and Kvet, J. (1984). "Model of diurnal changes in oxygen, carbon dioxide, and bicarbonate concentrations in a stand of *Elodea canadensis* Michx.," *Aquatic Botany* 19, 293-305.

Penning de Vries, F. W. T., and Van Laar, H. H. (1982a). "Simulation of growth processes and the model BACROS. Simulation of plant growth and crop production," Pudoc, Wageningen, 99-102.

Penning de Vries, F. W. T., and Van Laar, H. H. (1982b). "Simulation of growth processes and the model BACROS. Simulation of plant growth and crop production," Pudoc, Wageningen, 114-131.

Rutherford, J. C. (1977). "Modeling effects of aquatic plants in river," *Journal of the Environmental Engineering Division* 1003(EE4), 575-591.

Scheffer, M., Bakema, A. H., and Wortelboer, F. G. (1993). "MEGAPLANT: a simulation model of the dynamics of submerged plants," *Aquatic Botany* 45, 341-356.

Sher Kaul, S., Oertli, B., Castella, E., and Lachavanne, E. (1995). "Relationship between biomass and surface area of six submerged aquatic plant species," *Aquatic Botany* 51, 147-154.

Simons, D. B., Chen, Y. H., Li, R-M., and Ellis, S. S. (1981). "Assistance in evaluation of the existing rivers environment and assessment impacts of navigation activity on the Upper Mississippi River System," SLA Associates.

Simons, D. B., Simons, R. K., Ghaboosi, M., and Chang, Y. H. (1988). "Physical impacts of navigation on the Upper Mississippi River System," Report to the U.S. Army Corps of Engineers, St. Louis District.

Sondergaard, M. (1988). "Photosynthesis of aquatic plants under natural conditions," *in* Symoens, J. J., Editor, *Vegetation of Inland Waters*. Kluwer Academic Publishers, Dordrecht, The Netherlands, 63-113.

Spence, D. H. N. (1982). "The zonation of plants in freshwater lakes," *Advances in Ecological Research* 12, 37-125.

Spencer, D. F., and Anderson, L. W. J. (1987). "Influence of photoperiod on growth, pigment composition and vegetative propagule formation for *Potamogeton nodosus* and *Potamogeton pectinatus* L.," *Aquatic Botany* 28, 103-112.

Spitters, C. J. T. (1986). "Separating the diffuse and direct component of global radiation and its implications for modeling canopy photosynthesis. II. Calculation of canopy photosynthesis," *Agricultural and Forestry Meteorology* 38, 231-242.

Stewart, R. M., McFarland, D. G., Ward, D. L., Martin, S. K., and Barko, J. W. (1997). "Flume study investigation of the direct impacts of navigation-generated waves on submersed aquatic macrophytes in the Upper Mississippi River," Upper Mississippi River-Illinois Waterway System Navigation Study ENV Report 1, U.S. Army Engineer Waterways Experiment Station, Vicksburg, MS.

Thornley, J. H. M., and Johnson, I. R. (1990a). "Development," *in Plant and Crop Modelling. A Mathematical Approach to Plant and Crop Physiology*, Clarendon Press, Oxford, 139-144.

Thornley, J. H. M., and Johnson, I. R. (1990b). "Plant growth functions," *in Plant and Crop Modelling. A Mathematical Approach to Plant and Crop Physiology*. Clarendon Press, Oxford, 74-89.

Titus, J., and Adams, M. A. (1979a). "Coexistence and the comparative light relations of the submersed macrophytes *Myriophyllum spicatum* L. and *Vallisneria americana* Michx.," *Oecologia (Berlin)* 40, 273-286.

Titus, J. E., and Adams, M. A. (1979b). "Comparative carbohydrate storage and utilization patterns in the submersed macrophytes, *Myriophyllum spicatum* and *Vallisneria americana,*" *American Midland Naturalist* 102, 263-272.

Titus, J., Goldstein, R. A., Adams, M. A., Mankin, J. B., O'Neill, R. V., Weiler, P. R., Shugart, H. H., and Booth, R. S. (1975). "A production model for *Myriophyllum spicatum* L.," *Ecology* 56, 1129-1138.

Titus, J. E., and Stephens, M. D. (1983). "Neighbor influences and seasonal growth patterns for *Vallisneria americana* in a mesotrophic lake," *Oecologia* 56, 23-29.

U.S. Environmental Protection Agency (USEPA). (1998). "Guidelines for ecological risk assessment," Risk Assessment Forum, U.S. Environmental Protection Agency, Washington, D.C., EPA/630/R-95/002F.

Van der Bijl, L., Sand-Jensen, K., and Hjermind, A. L. (1989). "Photosynthesis and canopy structure of a submerged plant, *Potamogeton pectinatus*, in a Danish lowland stream," *Journal of Ecology* 77, 947-962.

Van der Zweerde, W. (1981). "Research of the influence of light intensity and day length on the formation of turions in the aquatic macrophyte *Hydrilla verticillata* Royle," Student Report, Centre for Agrobiological Research, Wageningen (In Dutch).

Van Dijk, G. M., Breukelaar, A. W., and Gijlstra, R. (1992). "Impact of light climate history on seasonal dynamics of a field population of *Potamogeton pectinatus* L. during a three-year period (1986-1988)," *Aquatic Botany* 43, 17-41.

Van Vierssen, W., Mathies, A., and Vermaat, J. E. (1994). "Early growth characteristics of *Potamogeton pectinatus* L.: the significance of the tuber," *in* van Vierssen, W., Hootsmans, M., and Vermaat, J., Editors, *Lake Veluwe, a Macrophyte-dominated System under Eutrophication Stress*. Kluwer Academic Publishers, Dordrecht, Boston, London, 135-144.

Van Vooren, A. (1983). "Distribution and relative abundance of Upper Mississippi River fishes," Upper Mississippi River Conservation Commission, Fish Tech. Sect., Rock Island, IL.

Van Wijk, R. J. (1989). "Ecological studies on *Potamogeton pectinatus* L. I. General characteristics, biomass production and life cycles under field conditions," *Aquatic Botany* 31, 211-258.

Weber, J. A., Tenhunen, J. D., Westrin, S. S., Yocum, C. S., and Gates, D. M. (1981). "An analytical model of photosynthetic response of aquatic plants to inorganic carbon and pH," *Ecology* 62(3), 690-705.

Westlake, D. F. (1966). "A model for quantitative studies of photosynthesis by higher plants in streams," *Air and Water Pollution International Journal* 10, 883-896.

Wetzel, R. L., and Neckles, H. A. (1986). "A model of *Zostera marina* L. photosynthesis and growth: simulated effects of selected physical-chemical variables and biological interactions," *Aquatic Botany* 26, 307-323.

Wortelboer, F. G. (1990). "A model on the competition between two macrophyte species in acidifying shallow soft-water lakes in the Netherlands," *Hydrobiol. Bulletin* 24(1), 91-107.

Wright, R. M., and McDonnell, A. J. (1986). "Macrophyte growth in shallow streams: biomass model," *Journal of Environmental Engineering* 112(5), 967-984.

Appendix A
Submerged Aquatic Plant Coverage Maps for UMR Pools 4, 8, and 13

POOL 4 VEGETATION / BATHYMETRY

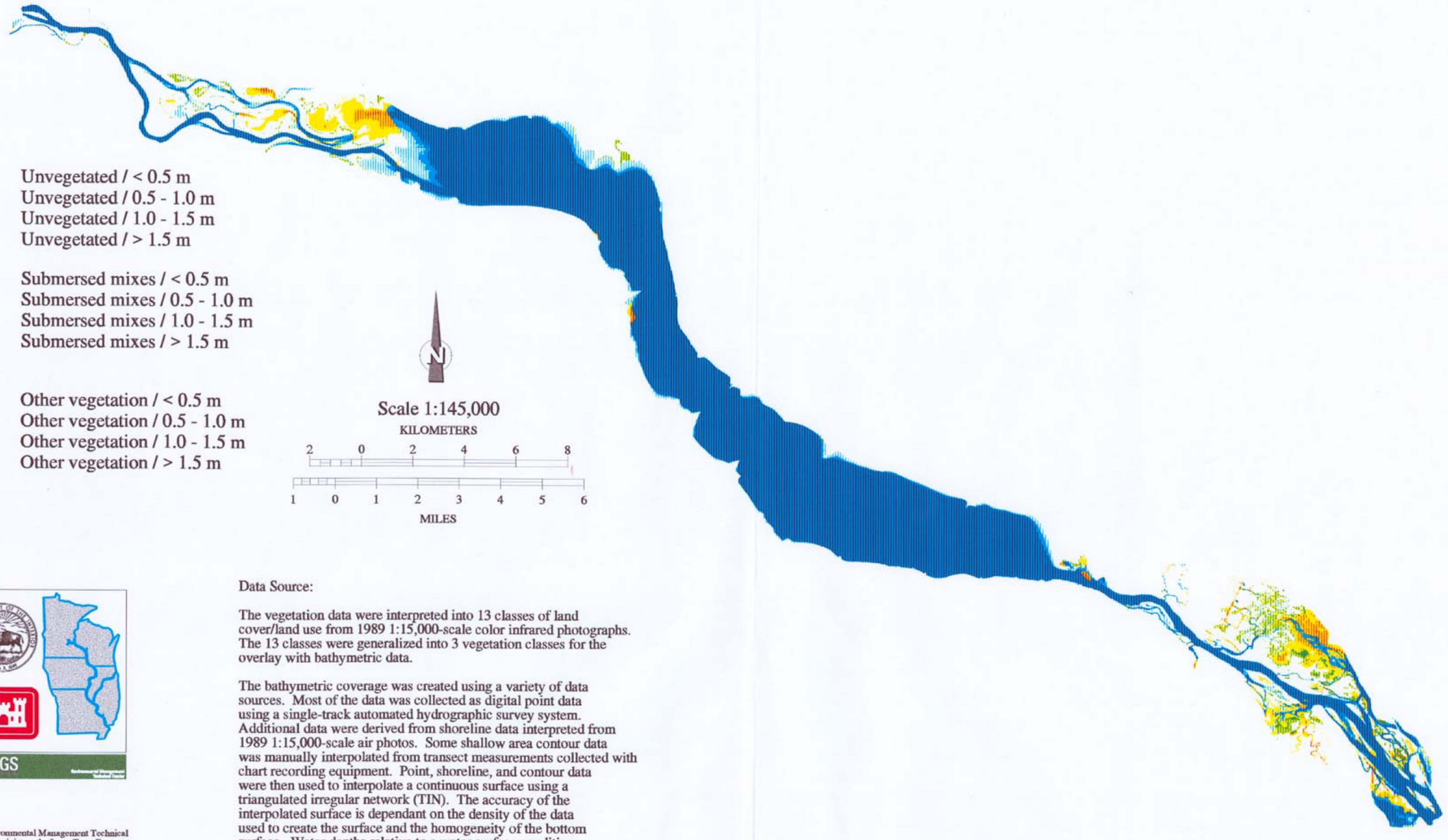

Unvegetated / < 0.5 m
Unvegetated / 0.5 - 1.0 m
Unvegetated / 1.0 - 1.5 m
Unvegetated / > 1.5 m

Submersed mixes / < 0.5 m
Submersed mixes / 0.5 - 1.0 m
Submersed mixes / 1.0 - 1.5 m
Submersed mixes / > 1.5 m

Other vegetation / < 0.5 m
Other vegetation / 0.5 - 1.0 m
Other vegetation / 1.0 - 1.5 m
Other vegetation / > 1.5 m

N

Scale 1:145,000

KILOMETERS
2 0 2 4 6 8

1 0 1 2 3 4 5 6
MILES

USGS

EMTC:
The Environmental Management Technical Center administers the Long Term Resource Monitoring Program for the Upper Mississippi River System, performing ecological monitoring and research on the river system.

Data Source:

The vegetation data were interpreted into 13 classes of land cover/land use from 1989 1:15,000-scale color infrared photographs. The 13 classes were generalized into 3 vegetation classes for the overlay with bathymetric data.

The bathymetric coverage was created using a variety of data sources. Most of the data was collected as digital point data using a single-track automated hydrographic survey system. Additional data were derived from shoreline data interpreted from 1989 1:15,000-scale air photos. Some shallow area contour data was manually interpolated from transect measurements collected with chart recording equipment. Point, shoreline, and contour data were then used to interpolate a continuous surface using a triangulated irregular network (TIN). The accuracy of the interpolated surface is dependant on the density of the data used to create the surface and the homogeneity of the bottom surface. Water depths relative to a water surface condition exceeded 90% of the time was used for the overlay with vegetation data.

POOL 8 VEGETATION / BATHYMETRY

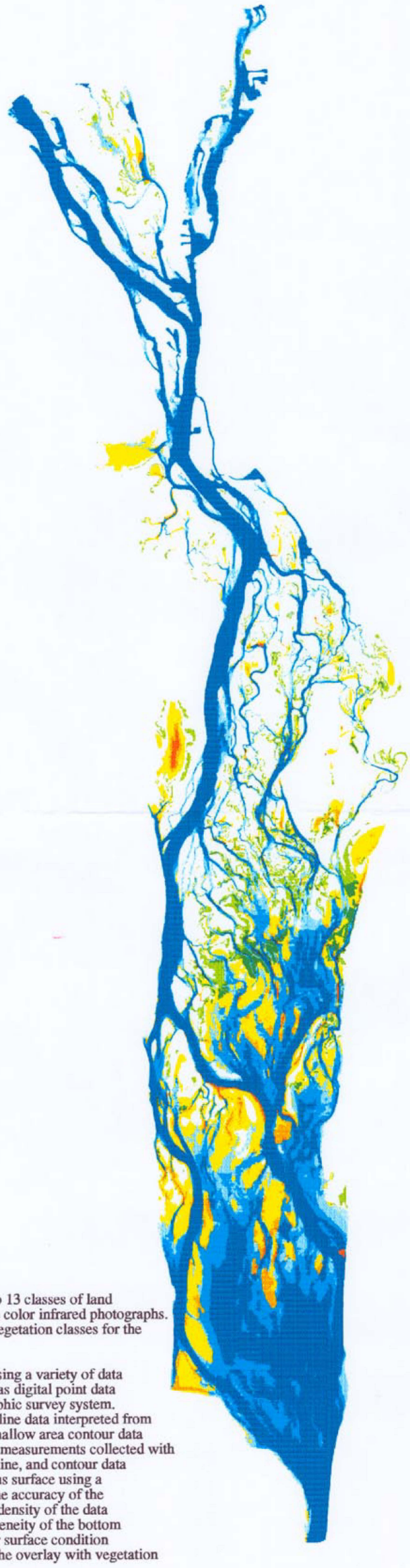

Unvegetated / < 0.5 m
Unvegetated / 0.5 - 1.0 m
Unvegetated / 1.0 - 1.5 m
Unvegetated / > 1.5 m

Submersed mixes / < 0.5 m
Submersed mixes / 0.5 - 1.0 m
Submersed mixes / 1.0 - 1.5 m
Submersed mixes / > 1.5 m

Other vegetation / < 0.5 m
Other vegetation / 0.5 - 1.0 m
Other vegetation / 1.0 - 1.5 m
Other vegetation / > 1.5 m

N

Scale 1:89,000

KILOMETERS

1 0 1 2 3 4 5 6 7 8

1 0 1 2 3 4 5

MILES

USGS

EMTC:
The Environmental Management Technical Center administers the Long Term Resource Monitoring Program for the Upper Mississippi River System, performing ecological monitoring and research on the river system.

Data Source:

The vegetation data were interpreted into 13 classes of land cover/land use from 1989 1:15,000-scale color infrared photographs. The 13 classes were generalized into 3 vegetation classes for the overlay with bathymetric data.

The bathymetric coverage was created using a variety of data sources. Most of the data was collected as digital point data using a single-track automated hydrographic survey system. Additional data were derived from shoreline data interpreted from 1989 1:15,000-scale air photos. Some shallow area contour data was manually interpolated from transect measurements collected with chart recording equipment. Point, shoreline, and contour data were then used to interpolate a continuous surface using a triangulated irregular network (TIN). The accuracy of the interpolated surface is dependant on the density of the data used to create the surface and the homogeneity of the bottom surface. Water depths relative to a water surface condition exceeded 90% of the time was used for the overlay with vegetation data.

POOL 13 VEGETATION / BATHYMETRY

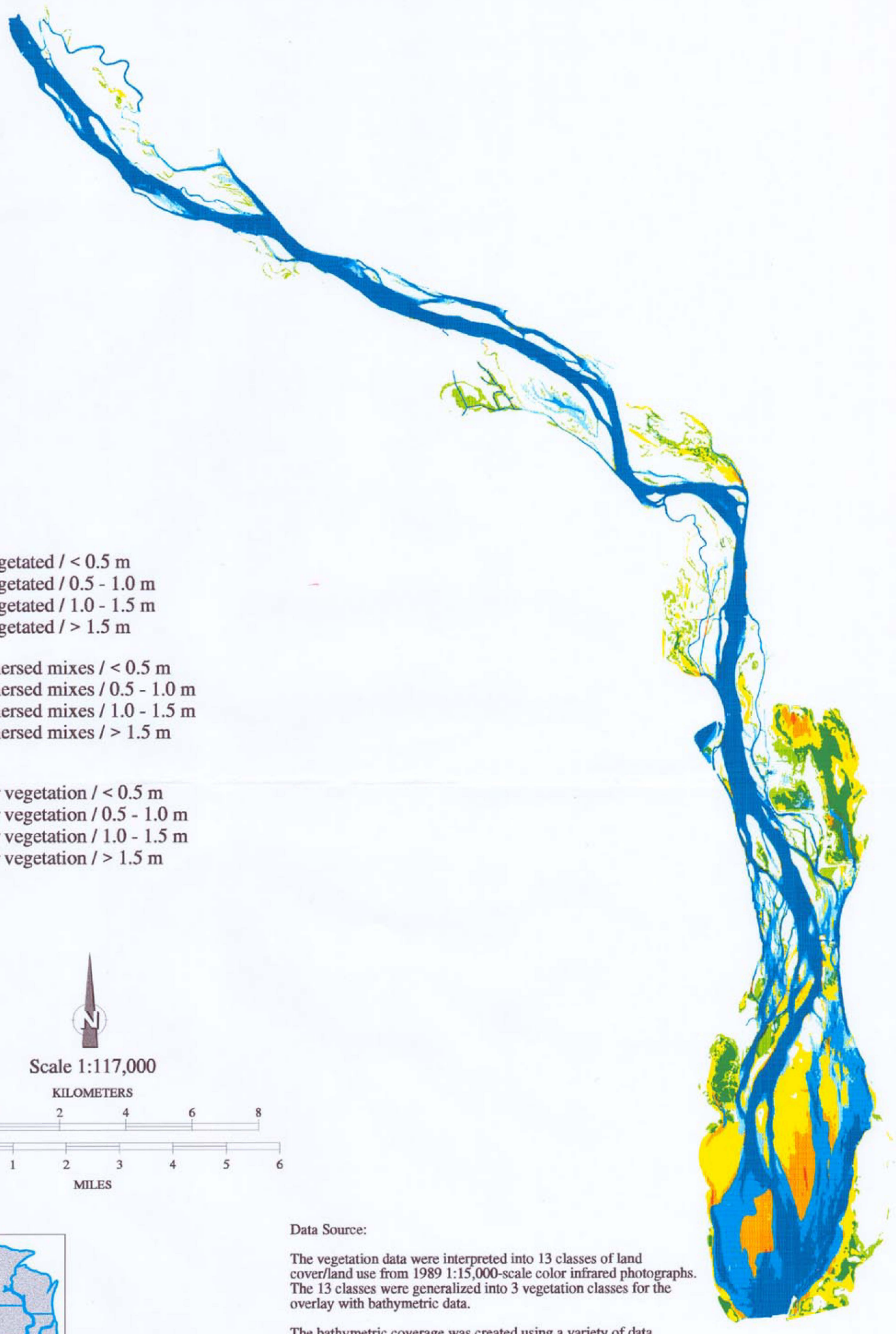

Unvegetated / < 0.5 m
Unvegetated / 0.5 - 1.0 m
Unvegetated / 1.0 - 1.5 m
Unvegetated / > 1.5 m

Submersed mixes / < 0.5 m
Submersed mixes / 0.5 - 1.0 m
Submersed mixes / 1.0 - 1.5 m
Submersed mixes / > 1.5 m

Other vegetation / < 0.5 m
Other vegetation / 0.5 - 1.0 m
Other vegetation / 1.0 - 1.5 m
Other vegetation / > 1.5 m

N

Scale 1:117,000

KILOMETERS

2 0 2 4 6 8

1 0 1 2 3 4 5 6

MILES

USGS

EMTC:
The Environmental Management Technical Center administers the Long Term Resource Monitoring Program for the Upper Mississippi River System, performing ecological monitoring and research on the river system.

Data Source:

The vegetation data were interpreted into 13 classes of land cover/land use from 1989 1:15,000-scale color infrared photographs. The 13 classes were generalized into 3 vegetation classes for the overlay with bathymetric data.

The bathymetric coverage was created using a variety of data sources. Most of the data was collected as digital point data using a single-track automated hydrographic survey system. Additional data were derived from shoreline data interpreted from 1989 1:15,000-scale air photos. Some shallow area contour data was manually interpolated from transect measurements collected with chart recording equipment. Point, shoreline, and contour data were then used to interpolate a continuous surface using a triangulated irregular network (TIN). The accuracy of the interpolated surface is dependant on the density of the data used to create the surface and the homogeneity of the bottom surface. Water depths relative to a water surface condition exceeded 90% of the time was used for the overlay with vegetation data.

Appendix B
Plant Growth Model Parameters

Table B1
The Output Variable Listing for VALLA (for Wild Celery) and POTAM (for Sago Pondweed)

Abbreviation	Explanation	Dimension
DAVTMP	Daily average temperature	°C
DAYL	Day length	h
DDTMP	Daily average daytime temperature	°C
DTEFF	Daily effective temperature	°C
DTGA	Daily total gross CO_2 assimilation of the plant	$gCO_2.m^{-2}.d^{-1}$
DVS	Development phase of the plant	-
FGROS	Instantaneous CO_2 assimilation rate of the plant	$gCO_2.m^{-2}.h^{-1}$
GPHOT	Daily total gross CH_2O assimilation rate of the community	$gCH_2O.m^{-2}.d^{-1}$
IRS	Total irradiance just under the water surface	$J.m^{-2}.s^{-1}$
MAINT	Maintenance respiration rate of the plant	$gCH_2O.m^{-2}.d^{-1}$
NDTUB	Dormant tuber number	dormant tubers.m^{-2}
NNTUB	New tuber number	new tubers.m^{-2}
NTM	Tuber density measured (field site)	tubers.m^{-2}
NTUBD	Dead tuber number	dead tubers.m^{-2}
REMOB	Remobilization rate of carbohydrates	$gDW.m^{-2}.d^{-1}$
TEFF	Factor accounting for effect of temperature on maintenance respiration	-
TGW	Total live plant dry weight (excluding tubers)	$gDW.m^{-2}$
TGWM	Total live plant dry weight measured (field site)	$gDW.m^{-2}$
TRANS	Translocation rate of carbohydrates	$gCH_2O.m^{-2}.d^{-1}$
TREMOB	Total remobilization	$gDW.m^{-2}$
TW	Total live + dead plant dry weight (excluding tubers)	$gDW.m^{-2}$
TWGTUB	Total dry weight of germinating tubers	$gDW.m^{-2}$
WTMP	Daily water temperature	°C
TWLVG	Total dry weight of live leaves	$gDW.m^{-2}$
TWNTUB	Total dry weight of new tubers	$gDW.m^{-2}$
TWRTD	Total dry weight of dead roots	$gDW.m^{-2}$

(Continued)

Table B1 (Concluded)

Abbreviation	Explanation	Dimension
TWRTG	Total dry weight of live stems	$gDW.m^{-2}$
TWSTD	Total dry weight of dead stems	$gDW.m^{-2}$
TWSTG	Total dry weight of live stems	$gDW.m^{-2}$
TWTUB	Total dry weight of dormant tubers	$gDW.m^{-2}$
TWTUBD	Total dry weight of dead tubers	$gDW.m^{-2}$

Table B2
Relationship Between Development Phase (DVS) of Wild Celery, Day of Year, and 3 °C Day-degree Sum [Development Rate as a Function of Temperature (DVRVT) = 0.015; DVRRT = 0.040]

Developmental Phase Description	DVS Value	Day Number	3 °C Day-degree Sum
First Julian day number → tuber sprouting and initiation elongation	0 -> 0.291	0 -> 105	1 -> 270
Tuber sprouting and initial elongation → leaf expansion	0.292 -> 0.875	106 -> 180	271 ->1215
Leaf expansion → floral initiation and anthesis	0.876 - >1.000	181 - >191	1216 -> 1415
Floral initiation and anthesis--> induction of tuber formation, tuber formation and senescence	1.001 -> 2.000	192 -> 227	1416-> 2072
Tuber formation and senescence → senesced	2.001 -> 4.008	228 -> 365	2073 -> 3167
Senesced	4.008	365	3167

Note: Calibration was on field data from 1978 from Chenango Lake, NY (longitude 75 ° 50'W, latitude 42 ° 15'N; Titus and Stephens 1983) and climatological data were from 1978 from Binghamton (air temperatures) and Ithaca (irradiance), NY.

Table B3
Relationship Between Development Phase (DVS) of Sago Pondweed, Day of Year, and 3 °C Day-degree Sum (DVRVT = 0.015; DVRRT = 0.040)

Developmental Phase Description	DVS Value	Day Number	3 °C Day-degree Sum
First Julian day number → tuber sprouting and initiation elongation	0 -> 0.210	0 -> 77	1 -> 193
Tuber sprouting and initial elongation → leaf expansion	0.211 -> 0.929	78 -> 187	194 -> 1301
Leaf expansion → floral initiation and anthesis	0.930 - >1.000	188 - >195	1302 -> 1434
Floral initiation and anthesis--> induction of tuber formation, tuber formation and senescence	1.001 -> 2.000	196 -> 233	1435 -> 2077
Tuber formation and senescence → senesced	2.001 -> 4.033	234 -> 365	2078 -> 3193
Senesced	4.033	365	3193

Note: Calibration was on field data from 1987 from Zandvoort (longitude 5 ° 38'E, latitude 51 ° 54'N; Best 1987) and climatological data were from 1987 from De Bilt, The Netherlands.

Table B4
Parameter Values for VALLA (Values Listed Are Those Used for Calibration, and Ranges Are in Parentheses)

Parameter	Abbreviation	Value	Reference
Morphology, Development and Phenological Cycle			
First Julian day number	DAYEM	1	
Base temperature for juvenile plant growth	TBASE	3 ^{o}C	calibrated
Development rate as function of temperature	DVRVT* DVRRT	0.015 0.040	calibrated
Fraction of total dry matter increase allocated to leaves	FLVT	0.718	1, 2
Fraction of total dry matter increase allocated to stems	FSTT	0.159	1, 2
Fraction of total dry matter increase allocated to roots	FRTT	0.123	1, 2
Plant density	NPL	30. m^{-2}	1
Wintering and Sprouting of the Tubers			
Dormant tuber density	NDTUB	233. m^{-2}	3 (4)
Initial dry weight of a tuber	INTUB	0.090 g DW. $tuber^{-1}$ (0.002 - 0.120)	3, 4
Relative death rate of tubers (on number basis)	RDTU	0.018 d^{-1} (0.015 - 0.021)	5
Growth of the Sprouts to the Water Surface			
Relation coefficient tuber weight-stem length	RCSHST	12 m. g DW^{-1}	6, 7
Relative conversion rate of tuber into plant material	ROC	0.0576 g CH_2O. g DW^{-1} d^{-1}	6
Critical shoot weight per depth layer	CRIFAC	0.0091 g DW. 0.1 m plant $layer^{-1}$ (0.0091 - 0.041)	3, 4
Survival period for sprouts with negative net photosynthesis	SURPER	23 d	8,9

(Continued)

Table B4 (Continued)

Parameter	Abbreviation	Value	Reference
Light, Photosynthesis, Maintenance, Growth and Assimilate Partitioning			
Potential CO_2 assimilation rate at light saturation for shoot tips	AMX	0.0165 g CO_2. g DW^{-1} h^{-1}	10
Conversion factor for translocated dry matter into CH_2O	CVT	1.05	11
Water depth	DEPTH	1 m	user def.
Initial light use efficiency for shoot tips	EE	0.000011 g CO_2 J^{-1}	11
Reduction factor to relate AMX to water pH	REDAM	1	
Thickness per plant layer	TL	0.1 m	12
Daytime temperature effect on AMX as function of DVS	AMTMPT*	0 -1	10
Reflection coefficient of irradiance at water surface	RC	0.06	13
Plant species specific light extinction coefficient	K	0.0235 m^2 g DW^{-1}	10
Water type specific light extinction coefficient	L	0.43 - 0.80 m^{-1}	1
Reduction factor for AMX to account for senescence plant parts over vertical vegetation axis	REDF	1.0	user def.
Dry matter allocation to each plant layer	DMPC*	0-1	10
Daily water temperature (field site)	WTMPT	-, ^oC	user def.
Lag period chosen to relate water temp. to air temp., in case water temp. has not been measured	DELAY	1 d	user def.
Total live dry weight measured (field site)	TGWMT	-, g DM m^{-2}	user def.

(Continued)

Table B4 (Concluded)

Parameter	Abbreviation	Value	Reference
Induction and Formation of Tubers			
Translocation (part of net photosynthetic rate)	RTR	0.247	5
Critical tuber weight	TWCTUB	14.85 g DW m^{-2}	1, 3, 5
Tuber number concurrently initiated per plant	NINTUB	5.5 $plant^{-1}$ (0.002 - 15)	4, 1
Tuber density measured (field site)	NTMT	55-233 $.m^{-2}$	4
Senescence			
Relative death rate of leaves (on DW basis; Q10 =2)	RDRT	0.021 d^{-1}	1
Relative death rate of stems and roots (on DW basis; Q10=2)	RDST	0.021 d^{-1}	1
Harvesting			
Harvesting	HAR	0 (0 or 1)	user def.
Harvesting day number	HARDAY	304 (1 - 365)	user def.
Harvesting depth (measured from water surface; 1-5 m)	HARDEP	0.1m<DEPTH	user def.

1. Titus & Stephens 1983; 2. Haller 1974; 3. Korschgen & Green 1988; 4. Korschgen et al. 1997; 5. Donnermeyer & Smart 1985; 6. Bowes et al. 1977; 7. Van der Zweerde 1981; 8. Titus & Adams 1979b; 9. Best 1987; 10. Titus & Adams 1979a; 11. Penning de Vries & Van Laar 1982a, 1982b; 12. Titus et al. 1975; 13. Golterman 1975.
* Calibration function.

Table B5
Parameter Values for POTAM (Values Listed Are Those Used for Calibration, and Ranges Are in Parentheses)

Parameter	Abbreviation	Value	Reference
Morphology, Development and Phenological Cycle			
First Julian day number	DAYEM	1	
Base temperature for juvenile plant growth	TBASE	3 ^{o}C	calibrated
Development rate as function of temperature	DVRVT* DVRRT	0.015 0.040	calibrated
Fraction of total dry matter increase allocated to leaves	FLVT	0.731	1
Fraction of total dry matter increase allocated to stems	FSTT	0.183	1
Fraction of total dry matter increase allocated to roots	FRTT	0.086	1
Plant Density			
Plant density	NPL	30. m^{-2}	2
Wintering and Sprouting of the Tubers			
Dormant tuber density	NDTUB	240. m^{-2}	1, 2
Initial dry weight of a tuber	INTUB	0.083 g DW. $tuber^{-1}$ (0.022 - 0.155)	1 (3, 4)
Relative death rate of tubers (on number basis)	RDTU	0.026 d^{-1}	3
Growth of the Sprouts to the Water Surface			
Relation coefficient tuber weight-stem length	RCSHST	12 m. g DW^{-1}	5, 6
Relative conversion rate of tuber into plant material	ROC	0.0576 g CH_2O. g DW^{-1} d^{-1}	5
Critical shoot weight per depth layer	CRIFAC	0.0076 g DW. 0.1 m $plant\ layer^{-1}$	1, 5
Survival period for sprouts with negative net photosynthesis	SURPER	27 d	1

(Continued)

Table B5 (Continued)

Parameter	Abbreviation	Value	Reference
Light, Photosynthesis, Maintenance, Growth and Assimilate Partitioning			
Potential CO_2 assimilation rate at light saturation for shoot tips	AMX	0.019 g CO_2. g DW^{-1} h^{-1}	7
Conversion factor for translocated dry matter into CH_2O	CVT	1.05	8
Water depth	DEPTH	1.3 m	user def.
Initial light use efficiency for shoot tips	EE	0.000011 g CO_2 J^{-1}	8
Reduction factor to relate AMX to water pH	REDAM	1	1
Thickness per plant layer	TL	0.1 m	9
Daytime temperature effect on AMX as function of DVS	AMTMPT*	0-1	1
Reflection coefficient irradiance at water surface	RC	0.06	10
Plant species specific light extinction coefficient	K	0.095m^2 g DW^{-1}	1
Water type specific light extinction coefficient	L	1.09 m^{-1}	1
Reduction factor for AMX to account for senescence plant parts over vertical vegetation axis	REDFT	1.0	user def.
Dry matter allocation to each plant layer	DMPC*	0 -1	1
Daily water temperature (field site)	WTMPT	-, ^oC	user def.
Total live dry weight measured (field site)	TGWMT	-, g DM m^{-2}	user def.
Induction and Formation of Tubers			
Translocation (part of net photosynthetic rate)	RTR	0.19	1, 11
Critical tuber weight	TWCTUB	7.92 g DW m^{-2}	1,2,3,4,5
Tuber number concurrently initiated per plant	NINTUB	8 $plant^{-1}$ (7-12)	1 (4, 5)

(Continued)

Table B5 (Concluded)

Parameter	Abbreviation	Value	Reference
Induction and Formation of Tubers			
Tuber density measured (field site)	NTMT	400 -440 $.m^{-2}$	3
Senescence			
Relative death rate of leaves (on DW basis; Q10 =2)	RDRT	0.047 d^{-1}	1
Relative death rate of stems and roots (on DW basis; Q10 =2)	RDST	0.047 d^{-1}	1
Harvesting			
Harvesting	HAR	0 (0 or 1)	user def.
Harvesting day number	HARDAY	304 (1 - 365)	user def.
Harvesting depth (measured from water surface; 1-5 m)	HARDEP	0.1m<DEPTH	user def.

1. Best 1987; 2. Sher Kaul et al. 1995; 3. Van Wijk 1989; 4. Spencer & Anderson 1987; 5. Bowes et al. 1977; 6. Van der Zweerde 1981; 7. Van der Bijl et al. 1989; 8. Penning de Vries & Van Laar 1982a, 1982b; 9. Titus et al. 1975; 10. Golterman 1975;11. Wetzel & Neckles 1986.
* Calibration function.

REPORT DOCUMENTATION PAGE

Form Approved
OMB No. 0704-0188

1. AGENCY USE ONLY *(Leave blank)*	2. REPORT DATE	3. REPORT TYPE AND DATES COVERED
	September 2000	Interim report

4. TITLE AND SUBTITLE
Ecological Risk Assessment of the Effects of Incremental Increase of Commercial Navigation Traffic on Submerged Aquatic Plants in the Main Channel and Main Channel Borders

5. FUNDING NUMBERS

6. AUTHOR(S)
Steven M. Bartell, Kym Rouse Campbell, Elly P. H. Best, William A. Boyd

7. PERFORMING ORGANIZATION NAME(S) AND ADDRESS(ES)
The Cadmus Group, Inc., 136 Mitchell Road, Oak Ridge, TN 37830;
Environmental Laboratory, U.S. Army Engineer Research and Development Center, 3909 Halls Ferry Road, Vicksburg, MS 39180-6199

8. PERFORMING ORGANIZATION REPORT NUMBER

9. SPONSORING/MONITORING AGENCY NAME(S) AND ADDRESS(ES)
See reverse.

10. SPONSORING/MONITORING AGENCY REPORT NUMBER
ENV Report 17

11. SUPPLEMENTARY NOTES

12a. DISTRIBUTION/AVAILABILITY STATEMENT
Approved for public release; distribution is unlimited.

12b. DISTRIBUTION CODE

13. ABSTRACT ***(Maximum 200 words)***

This study presents an initial assessment of the potential ecological risks by commercial navigation traffic on submerged aquatic plants that grow in the main channel and the channel borders of the Upper Mississippi River-Illinois Waterway (UMR-IWW) System. The assessment addresses the possibility of plant breakage resulting from increases in current velocity or the momentum imparted by wake waves associated with the passing of commercial vessels. This part of the assessment is based on results of an experimental study on plants to various currents in flumes. The assessment also examines the possibility that commercial-vessel-induced increases in suspended sediments might diminish available underwater light enough to impair photosynthesis, growth, and vegetative reproduction of submerged aquatic plants. This part of the assessment is based on results of simulation models on growth of submerged aquatic plants. The species selected to represent contrasting characteristic life forms of the submerged aquatic vegetation in the UMR-IWW are American wild celery, a noncanopy former, and sago pondweed, a canopy former.

(Continued)

14. SUBJECT TERMS
See reverse.

15. NUMBER OF PAGES
109

16. PRICE CODE

17. SECURITY CLASSIFICATION OF REPORT	18. SECURITY CLASSIFICATION OF THIS PAGE	19. SECURITY CLASSIFICATION OF ABSTRACT	20. LIMITATION OF ABSTRACT
UNCLASSIFIED	UNCLASSIFIED		

9. (Concluded).

U.S. Army Engineer District, Rock Island, Clock Tower Building, P.O. Box 2004, Rock Island, IL 61204-2004;
U.S. Army Engineer District, St. Louis, 1222 Spruce Street, St. Louis, MO 63103-2833;
U.S. Army Engineer District, St. Paul, 190 5th Street East, St. Paul, MN 55101-1638

13. (Concluded).

The risk assessment methodology described in this report is being developed to assess the potential ecological impacts associated with the anticipated growth of commercial traffic navigating the UMR-IWW System for the period 2000-2050. In the absence of actual traffic projections, the present assessments evaluate risks posed by hypothetical 25, 50, 75, and 100% increases in traffic intensity compared to traffic intensity determined from the 1992 lockage records.

The assessment indicates that impacts of direct physical forces on aquatic vegetation up to a rooting depth of 1.5 m can be expected in less that 1.5% of the possible combinations of vessel type, location in relation to sailing line, and pool stage height. More than 95% of the impacts most likely stem from secondary wave heights exceeding the 0.2-m criterion. The assessment also indicates that across the scenarios the decreases in wild celery peak biomass are expected to be highest in UMR-Pool 13 (up to 12%) and lower in the Pools 4 and 8 (1-4%). The expected impacts on the average tuber (vegetative propagule) biomass are low, i.e. a decrease of maximally 3%. Expected impacts on sago pondweed peak biomass and tubers are less than on wild celery.

The current, initial ecological risk assessment methodology will be incorporated into a framework that characterizes risk in probabilistic terms in a following phase.

14. (Concluded).

Commerical navigation traffic
Ecological risk assessment
Feasibility study
Growth
Hydrodynamics
Planning
Potamogeton pectinatus
Simulation model
Submerged aquatic plants
Turbidity
Upper Mississippi River-Illinois Waterway System
Vallisneria americana